Numerical Simulation on Local-Contact Microwave-Heating Injector(LMI) System

DISSERTATION

Numerical Simulation on Local-contact Microwave-heating Injector (LMI) System

(局所接触型マイクロ波加熱式噴射装置の数値シミュレーション)

Graduate School of
Natural Science & Technology
Kanazawa University

Division of Innovative Technology and Science

Student ID No. : 1123122217
Name : Lukas Kano Mangalla
Chief Advisor : Hiroshi Enomoto
Date of Submission : January 8th , 2015

ABSTRACT

Heating fuel is one of the most critical issue related to an improvement on fuel atomization and evaporation. The current study focus on the electromagnetic energy heating inside injector to heat the fuel flow and this system is called “Local-contact Microwave-heating Injector” (LMI). This scheme is expected to improve evaporation of fuel spray for enhancing combustion performance and reducing exhaust emissions of the internal combustion engine.

Spray characteristics of ethanol injected from LMI injector was experimentally investigated using High Speed Camera, CMOS camera and Laser Dispersion of Spray Analyzer (LDSA). It was found that local heating of fuel has the significant impact on droplet diameter of ethanol fuel. Droplets size (SMD) were reduced around 50% when the temperature increased around boiling point of the fuel. Spray visualization analysis also showed the significant improvement on liquid particle size and ligament components of the heated spray. This heating scheme also enhances the droplet velocity during injection and become one of the advantageous of the LMI system on improving spray performances. However, microwave heating process inside the specific zone of LMI system is still unknown. Therefore, simulation study is proposed to predict phenomena related to microwave heating process on this system that are difficult to evaluate in experimental study.

Combination phenomena of electromagnetism, heat transfer and fluid dynamics were simulated using COMSOL Multiphysics. Domain simulation was discretized in to small elements size and solved the transient equations applied using Backward Differentiation Formulation (BDF) solver. The results show that radiation heating of electromagnetic has significant impacts on temperature distribution of the fuel. Temperature of ethanol was rapidly increased after imposing electromagnetic wave. This result is agree with the direct measurement in previous studies. Electromagnetic field intensity is sensitive to the geometry and shape of heating area and influences the temperature distribution. A little changed on the inner conductor diameter has significant effect on the behavior of electric field and leads to change the electric polarization and temperature distribution. Advance design on LMI system especially inside the heating area is expected for further development and optimization of the heating system.

Key words: Microwave heating, ethanol, heating zone, LMI system and dielectric properties.

DECLARATION

"I hereby declare that this thesis submission is my own work and that, to the best of my knowledge and belief, it contains no material previously published or written by another person nor material which to a substantial extent has been accepted for the award of any other degree or diploma of the university or other institute of higher learning, except where due acknowledgment has been made in the text".

(Lukas Kano Mangalla)

ACKNOWLEDGMENTS

I would like to express my great thanks and gratitude to my Professor, Hiroshi Enomoto, for his guidance, encouragement, and advice throughout the course of my studies. During the program, he gave me a lot of valuable knowledge and enthusiasm to lead this research done well and independently. His encouragement and support lead me to participate in international conference and wrote several journal papers. I sincerely appreciate him and I was very fortunate to have him as my adviser.

I am particularly thanks and appreciate to Noburu Hieda and colleague at Combustion Laboratory staff, School of Natural Science and Technology of Kanazawa University, Japan, for their advice and support during evaluation and simulation of Local-contact Microwave-heating Injector and whole system.

Thanks and appreciates to all staff of the School of Natural Science and Technology of Kanazawa University for all support and encouragement during my study.

Special thanks to Ishumi Kohei, Nozue and Kosuke Nishioka for their contributions and assistance during the preliminary studies on the LMI system. I would like to thank Shogo Kunioka and all my Laboratory members for their help and assistance in various phases during my studies.

I express my sincere gratitude to my government DIKTI that provides scholarship for my study, and Haluoleo University Indonesia, for the encouragement and support.

Finally, I would like to express my thanks to my wife, Hermita Yurinda Mangnga, and my daughters, Dewi Titania Randa and Kei Eliora Mangalla, for their patience, love, and understanding during my studies.

Lukas Kano Mangalla

Table of Content

List of Figures

List of Tables

Chapter 1

Introduction

1.1. Background.

A large number of internal combustion (IC) engines are recently utilized as power source for transportation and industrial applications. IC engines mainly use fossil fuel because of high energy density, relatively low cost, and transportable fuel. However, combustion of fossil fuels can generate several pollutant emissions that are extremely undesirable for the environment and for humanity, therefore regulated. Exhaust emissions from the engine consist of CO_2 which is highly contributed to global warming. US environmental Protection Agency (EPA) reported that more than 90% of greenhouse gas emissions come from the combustion of fossil fuel [1]. In the future, exhaust emissions from transportation sector become significantly increased because passenger car will be markedly growing. According to Word Energy Outlook [2], vehicle passenger will be increased doubled to around 1.7 billion in 2035. Consequently the fuel consumption become increased. On the other hand, the availability of fossil fuels are very limited, hence, the development on clean technology and efficient combustion of automotive industry is strongly required [3].

Recently many countries turn their attention over the alternative fuel especially bio-energy fuel such as ethanol. Bio-ethanol fuel is a form of quasi-renewable energy that can be produced from agricultural feedstocks such as sugar cane, potato, cassava and corn. Recent development is cellulosic ethanol that can be produced from a diverse array of feedstocks such as wood pulp from trees or any plant matter. It is well known that ethanol is promising alternative fuel for gasoline in order to reduce emission and dependency on petroleum fuel [4]. This fuel has high octane rating and high oxygen content which can possibly run engine with less knocking, high performances and low emissions [5-6]. However, Ethanol fuel has lower energy density (LHV = 26.8MJ/kg) compared with gasoline (LHV = 44.6 MJ/kg) and high viscosity as well as high latent heat vaporization [7]. These properties can possibly generate some problem when it is introducing into combustion chamber [8-11].

Ethanol-gasoline blended fuel for gasoline have been studied intensively to find out the best performance efficiency and the emissions reduction. Mostly of the studies recommended 5-10 % of ethanol in blended fuel [12-15]. Therefore, in some countries like UK, China, India, etc., gasoline already contains 5% bio-Ethanol (E5) or 10% in others country (e.g. Germany), without modification of the engine [10]. The use of the existing proportion of ethanol in gasoline has been established to significantly reduce the level of emissions particulate in the atmosphere. Cleaner burning of this fuel leads the pressure to increase ethanol content in much higher proportions (E85 or E100). However, at high Ethanol content blended, several issues may arise mainly at cold-start engine conditions due to lack of fuel volatility [16]. The lower volumetric energy density of ethanol can pose further challenges for the engine calibrator in terms of controlling the injector pulse width.

Temperature of the fuel should be increased to accelerated evaporation and mixing with oxygen inside combustion chamber. Evaporation of fuel is important in determining burning characteristics such as ignition delay, flame stability and completeness of burning. The droplet forming by atomization simultaneously evaporate and accelerate in combustion chamber to give good combustible mixture between fuel and air. Several studies in [17-19] proposed technical solutions on improving evaporation fuel by heating evaporation chamber or directly heated fuel flow inside injector. The new feasible method for increasing temperature of fuel flow inside injector is using microwave heating. Microwave heating received considerable attention from researchers for a wide range of applications due to offering some advantageous such as rapid heating and uniform heating [20-22]. Microwave heating is mainly occurred due to polarization and ionic vibration inside the material and generate volumetric heat [23-24].

Current study uses microwave heating system to generate heat for fuel flow inside injector. This system aim to add energy equivalent to the fuel flow inside injector and this called “Local-contact Microwave-heating Injector (LMI) system” [25-27]. In this system, heating area was created inside head injector and connected to magnetron of microwave heating. Heat is generated inside heating area due to the interaction between electromagnetic wave and dielectric properties of fuel. Fuel flow experienced heating in that area before injected and it is expected to increase temperature immediately during heating. This advantageous can offer the potential used of bio-ethanol fuel which usually has some problems at cold start conditions.

This study aims to develop of LMI system performances through numerical simulation analysis. Several complex phenomena related to the heating generating system inside heating area are still unknown. This simulation also aim to improve performance of LMI system in general. Moreover, because of the physical difficulties on measuring the fuel temperature

distribution inside the small area, then this simulation is expected to approach the problem by solution of partial differential equation of several physics interaction in LMI system.

1.2. Objectives

The primary focus of this study is to simulate heating generation system inside heating area of LMI and evaluate the effect of heating fuel on the spray characteristics. The specific objective for achieving the main goal are:

1. Simulation study to investigate the heating generation inside the heating area of LMI system. Uniform temperature generated by microwave heating is expected for enhancing evaporation of injected fuel.
2. To analyze the temperature effect on the spray characteristic of injected fuel. Images analysis on spray was also conducted to investigate the heating effect on the spray structure and the droplets distribution.

1.3. Scope of study

LMI system was develop a new method of heating fuel flow inside the injector. This system was designed for lower operating pressure at 0.3MPa, an approach condition operation of gasoline PFI engine. Microwave heating was operated at constant frequency of 2450MHz. Material fuel used in this study is Ethanol (95.5%) that produced by Kanto Chemical Company in Japan. For the desire temperature of fuel injected, the electric power input of 60Watt was applied. Furthermore, Injection and heating timing of the system were controlled. Spray characteristics of injected fuel were observed and analyzed. Temperature of fuel injected was also measured at tip of injector.

Numerical simulation of the heating characteristics inside the heating area was developed and validated with the experimental data. A coupled model between electromagnetic field, heat and mass transfer, and fluid flow was simulated in COMSOL Multiphysics to determine heating characteristic of microwave energy system within the material. The effect of convective heating system on the flow of ethanol inside heating area was also simulated in COMSOL and ANSYS Fluent. The result of this simulation then compare with the microwave heating system simulation and experimental data.

This study also consider the performance of the system in terms of spray characteristics of fuel injected from the device. Direct measurement and imaging system were conducted and analyzed. Spray characteristics such as droplet size, spray angle, spray component and particle distribution were the main parameter in this analysis.

1.4. Organization of Dissertation

The structure of this dissertation is mainly consist of my research during study in Kanazawa University in Japan. The three main part of this dissertation consist of numerical simulation on the heating area of LMI system, an imaging analysis of spray fuel from LMI system and spray characteristic of LMI system fueled with ethanol fuel. This dissertation consist of the following parts.

- Chapter 1 consist of introduction, numerical simulation, objective, scope and organization of dissertation.
- Chapter 2 consist of Literature review of heating system and basic theory of electromagnetic wave.
- Chapter 3 consists of simulation study of electromagnetism, heat transfer and fluid dynamic. Convective heating was also described. Two different model of inner cable shape, square and round shapes, were also compared.
- Chapter 4 consist of the analysis of spray performance of Local-contact Microwave-heating Injector (LMI) system. Spray characteristics of SMD and droplet velocity were analyzed and discussed.
- Chapter 5 Consist of spray characteristic of Local-contact Microwave-heating Injector fueled with ethanol.
- Chapter 6 consist of summary and recommendation for future development.
- The appendices contain an additional information relating to various part of the dissertation.

Chapter 2

Literature review

2.1. Review of literatures

Microwave heating is widely used at domestic and industrial applications such as food processing industrial, chemical and material processing, and many other industrial processes. In contrast to conventional heating, microwave heating generated volumetric heating inside the material. Microwave heating process also reduces time heating and more effective used for several application. In this heating process, the wave of electromagnetic field polarizes the dipole molecular in dielectric materials and creates heat by to rotation of the molecules at high frequency [23].

Heating fuel inside injector using microwave heating is the main consideration of this study. Microwave heating applied in this system aims to add some energy equivalent to the ethanol flow in order to improve the atomization and evaporation of the injected fuel. This system is called Local-contact Microwave-heating Injector (LMI). An in-house injector development was used to heat fuel flow using radiation of electromagnetic wave energy. A heating area created inside head injector was connected to magnetron of microwave heating using coaxial dielectric material of PTFE (Teflon). Electromagnetic energy is propagated into material through this coaxial cable and generates volumetrically heat distribution due to molecular friction mechanism. Polarization of electromagnetic wave in this system can increase fuel temperature rapidly after imposing power into the microwave generator. Heating process in this system aims to improve fuel evaporation and reduce droplet size of fuel spray during injection [27].

In the recent years, several study conducted to evaluate the effect of dielectric properties, size and shape of material on temperature characteristic of heated material. One problem related to this heating system is also lack of the uniformity of temperature distribution inside material. Complex phenomena of scattering and reflecting as well as the absorption of electromagnetic wave could be main sources of the problem [28-29]. This phenomenon can also be generated by several factors such as dielectric loss, penetration depth, thickness, shape

and size of the product [30-31]. Hossan and Dutta [32] investigated the effect of dielectric properties, physical structure and incident wave frequency on the temperature distribution and concluded that slight changed in length of the object can significant change in temperature.

Controlling heating process to obtain the desire temperature distribution inside material is still remains challenging task in microwave heating application. Several physical phenomena cannot be observed through the experimental study. Due to the complexity process, numerical simulation has been widely utilized to study microwave heating process and their interaction with material properties [33-35]. Computer simulation can assist to optimize design of the object to improve quality and temperature distribution.

2.2.Microwave heating

2.2.1. Microwave heating applications

Microwave heating occurs in dielectric material because of the polarization of water molecule with electromagnetic radiation. Electromagnetic radiation transfer energy to the vacuum or no medium by the oscillation of electric field and magnetic field. In the vacuum space, the electromagnetic wave moves at constant speed of $3x10^8$m/s. Microwaves are electromagnetic waves at frequency ranging from 300 MHz to 300 GHz with wave length between 1m and 1mm. Recently microwaves are widely used in some areas such as communication (Satellite, radio, TV and wireless cable system), radar for navigation and

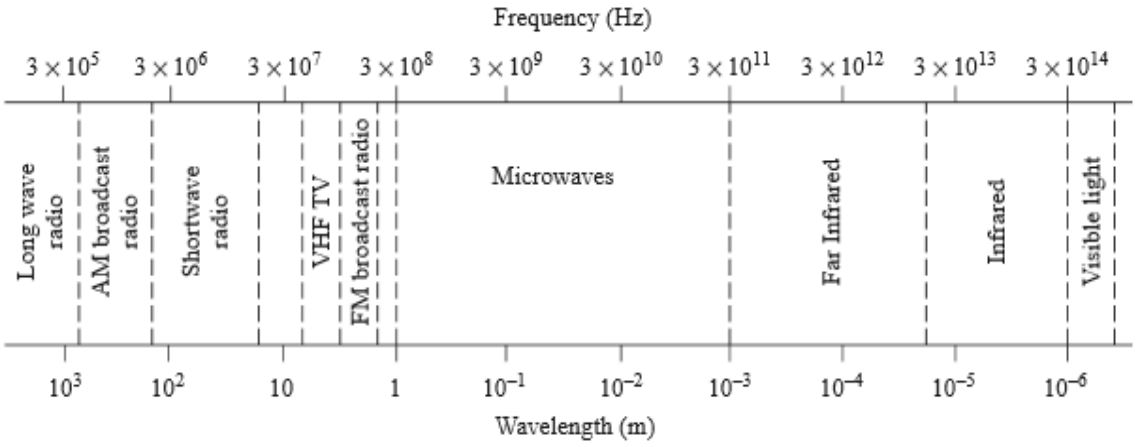

Figure 2.1. Electromagnetic spectrum (Source: D.M. Pozar: Microwave Engineering [36])

Industrial, scientific and medical applications etc. [37]. Microwave heating is the heating process using electromagnetic wave radiation inside the materials and it is widely used in domestic and industrial application as a source of thermal energy. Compared with conventional

heating methods, the advantages of microwave heating include time and energy saving, rapid heating rates, selective heating, considerably reduced processing time and temperature, unique microstructure and properties, improved product yield, environmental friendliness, and so on [38]. The different characteristic of microwave heating over the conventional heating is volumetric heat generation, a special heating behavior of microwave, dealing with the ionic motion and dielectric of the material heated. Moisture content inside material behave as a polar component that vibrates in molecular level at microwave frequency. Ionic vibration and dipole polarization due to the electromagnetic wave create heat and enhance internal energy of material heated. It has been established that microwave heating can significantly reduce the heating time and the energy cost. In microwave heating, the heating performance depends on the interaction between the dielectric properties of materials and the microwave frequencies.

2.2.2. Microwave heating characteristics

Recently, microwave heating become popular used in many area such as industry and household applications. The main used of microwave heating is warmed food in microwave oven. In this device the microwave is radiated, transmitted and reflected inside the metal box of to generated heat inside object heated (such as food, cake, etc.). Compare with conventional heating, microwave heating have some advantageous such as rapid heating, high thermal efficiency heating, direct and uniform heating.

Microwave generated heating rapidly in object due to oscillation of electric and magnetic field that generated heat inside material. This mechanism is different with conventional heating which transfers heating by conduction. Microwave heating does not need time to penetrate heat (heat conduction) into object heated because the heating generated inside the material.

Microwave oven convert parts of electrical input into microwave energy. High thermal energy of microwave heating is due to minimum losses of energy into ambient air or furnace. Heat directly generated inside material so high efficiency can be obtained.

Uniform heating in microwave can be achieved since the heat comes at the same time in all part of heated object. This phenomenon can generate uniform heating even in the relative complex material. Microwave heating also has high speed response because of the electromagnetic wave propagate very fast into material to generated heat.

2.2.3. Standing wave.

Outline of standing wave can be seen in Figure 2. If the reflected wave moves in the opposite direction of the incident wave with same amplitude and frequency the standing wave

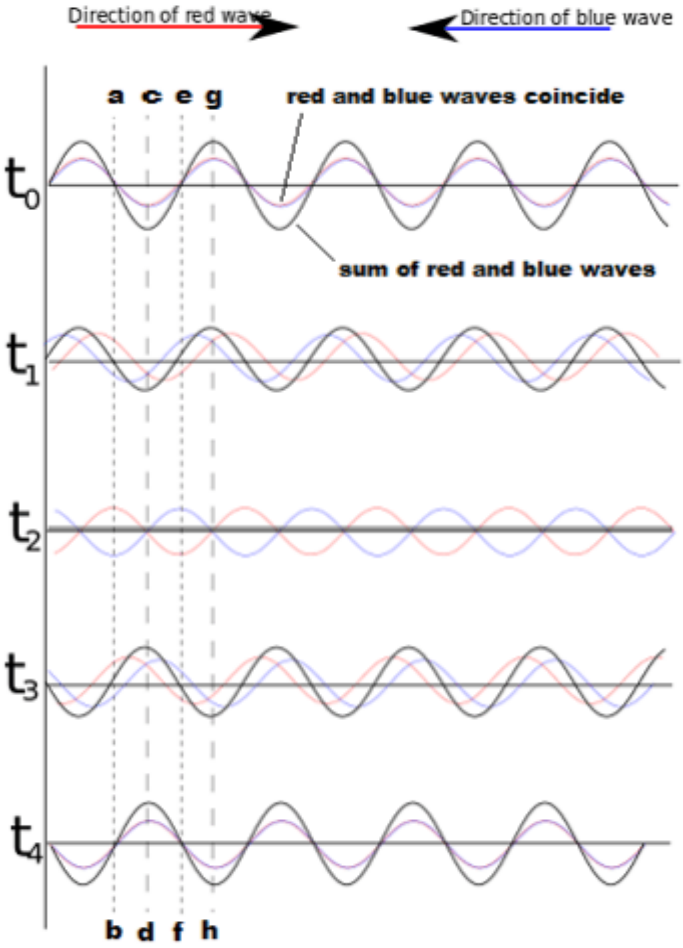

is occurred. It result from the superposition of two traveling waves moving in opposite directions and become coincide in one line. Standing waves produce for a particular physical system at its resonance conditions. Resonance occurs when a system oscillates at the natural frequency of the system. Standing wave resonances occur when the wavelengths of the exciting frequencies match those allowed by the physical boundary conditions of the system. In a string fixed at both ends must have nodes at each end and such a string has resonant frequencies for the length of the string to be $\lambda/2$, λ, $3\lambda/2$, etc., where λ is the wavelength. Only certain frequencies of oscillation can produce standing waves. These frequencies will satisfy the relation of $f = \upsilon/\lambda$, where υ is the velocity of waves in the medium and λ is the wavelength which satisfies the boundary conditions.

In figure 2, fixed boundaries will be nodes and free ends will be antinodes. Node and antinode are separated by λ/2. The equation of a standing wave can be formed by adding the displacement of the two waves of equal amplitude, period and wavelength which are traveling in opposite directions.

The equation of wave traveling in the positive x direction can be written as:

$$y_1 = A\cos 2\pi\left[\frac{t}{T} - \frac{x}{\lambda}\right] \tag{1}$$

and the equation of wave traveling in the negative x directions can be expressed as:

$$y_2 = A\cos 2\pi\left[\frac{t}{T} + \frac{x}{\lambda}\right] \tag{2}$$

Adding these two equations gives the resultant of standing wave equation as follow:

$$y_1 + y_2 = A\left\{\cos 2\pi\left[\frac{t}{T} - \frac{x}{\lambda}\right] + \cos 2\pi\left[\frac{t}{T} + \frac{x}{\lambda}\right]\right\} \tag{3}$$

This equation of a cosine wave whose amplitude varies in time. It is the equation of the standing wave.

2.2.4. Basic theory of microwave heating.

Microwave field is the electromagnetic wave at specific operational frequency. For domestic microwave heating, it is usually operated at frequency of 2.45GH. The fundamental governing equation for electromagnetic field was established by James Clerk Maxwell in 1873, and it was simply called Maxwell's equations. The four common Maxwell's equations in differential form are described as follow [39]:

$$\nabla \times E = -\frac{\partial B}{\partial t} \tag{4}$$

$$\nabla \times H = J + \frac{\partial D}{\partial t} \tag{5}$$

$$\nabla \bullet D = \rho \tag{6}$$

$$\nabla \bullet B = 0 \tag{7}$$

Where E is the electric field (V/m), B is the magnetic flux density (Wb/m2), H is the magnetic field (Wb), J is the current density (A/m2), D is electric displacement (C/m^2), and ρ is the electric charge density (C/m^3).

The four equations above describe the behavior and interaction between electric and magnetic field. Maxwell also proved that speed of electromagnetic wave in vacuum is same as

the speed of light which travel at 3000,000 km/s. Therefore, the light is also electromagnetic wave. The equation (4) describes that the electromagnetic force around a closed path is equal to the time derivative of the magnetic displacement through any surface bounded by the path. In the equation (5), the magnetic force around a closed path is equal to the conduction current plus the time derivative of the electric displacement through any surface bounded the path. Equation (6) describes that the total electric displacement through the surface enclosing the volume is equal to the total charge within the volume. And the equation (7) shows that the magnetic flux density out of the closed surface is zero.

There are three correlations that concerning the characteristics of the medium which the electric and magnetic fields exist.

$$D = \varepsilon E \tag{8}$$

$$B = \mu H \tag{9}$$

$$J = \sigma E \tag{10}$$

Where ε, μ and σ are the permittivity, permeability and electric conductivity of the medium. For the specific case of electromagnetic phenomena in free space, the equations (4)-(7) become:

$$\nabla \times E = -\frac{\partial B}{\partial t} \tag{11}$$

$$\nabla \times H = \frac{\partial D}{\partial t} \tag{12}$$

$$\nabla \bullet D = 0 \tag{13}$$

$$\nabla \bullet B = 0 \tag{14}$$

Differentiate equation (12) with respect to time then we can write:

$$\frac{\partial \nabla \times H}{\partial t} = \nabla \times \frac{\partial H}{\partial t} \tag{15}$$

Also, since ε and μ are independent of time

$$\frac{\partial D}{\partial t} = \varepsilon \frac{\partial E}{\partial t} \tag{16}$$

$$\frac{\partial B}{\partial t} = \varepsilon \frac{\partial H}{\partial t} \tag{17}$$

So that

$$\nabla \times \frac{\partial H}{\partial t} = \varepsilon \frac{\partial^2 E}{\partial^2 t} \tag{18}$$

From equation (11) and (17) the following equation can be obtain:

$$\nabla \times \nabla \times E = -\mu \nabla \times \frac{\partial H}{\partial t} \tag{19}$$

If we substitute equation (18) into (19) to get

$$\nabla \times \nabla \times E = -\mu\varepsilon \times \frac{\partial^2 E}{\partial^2 t} \tag{20}$$

Equation (17) can be written in the new form:

$$\nabla \times \nabla \times E = \nabla \nabla \cdot E - \nabla^2 E = -\mu\varepsilon \times \frac{\partial^2 E}{\partial^2 t} \tag{21}$$

The expression $\nabla \cdot E = \frac{1}{\varepsilon} \nabla \cdot D = 0$

Therefore equation (21) becomes:

$$\nabla^2 E = \mu\varepsilon \times \frac{\partial^2 E}{\partial^2 t} \tag{22}$$

With same procedures

$$\nabla^2 H = \mu\varepsilon \times \frac{\partial^2 H}{\partial^2 t} \tag{23}$$

In the uniform plane wave propagation the wave equation can be simplified where the E and H are independent of the two dimensions, y and z.

The equation (22) become:

$$\frac{\partial^2 E}{\partial x^2} = \mu\varepsilon \times \frac{\partial^2 E}{\partial^2 t} \tag{24}$$

The plane wave equation can be written in terms of the components of E as follow:

$$\frac{\partial^2 E_x}{\partial x^2} = \mu\varepsilon \times \frac{\partial^2 E_x}{\partial^2 t} \tag{25.a}$$

$$\frac{\partial^2 E_y}{\partial x^2} = \mu\varepsilon \times \frac{\partial^2 E_y}{\partial^2 t} \tag{25.b}$$

$$\frac{\partial^2 E_z}{\partial x^2} = \mu\varepsilon \times \frac{\partial^2 E_z}{\partial^2 t} \tag{25.c}$$

In the region of no charge density:

$$\frac{\partial E_x}{\partial x} + \frac{\partial E_y}{\partial y} + \frac{\partial E_z}{\partial z} = 0 \tag{26}$$

If the wave propagates in the z direction the field components of E_x and E_y vary sinusoidally in time and space [52].

$$E_x = E_o \sin[\omega t - \beta z] \tag{27}$$

$$H_x = \frac{E_o}{Z_0} \sin[\omega t - \beta z] \tag{28}$$

E_o is amplitude factor and

$$Z_0 = \sqrt{\frac{\mu_0}{\varepsilon_0}} \quad \text{is characteristic impedance} \tag{29}$$

$$\beta = \frac{2\pi}{\lambda_0} \quad \text{is propagation constant} \tag{30}$$

Temperature distribution within the system governed by microwave heating can be expressed as the following equation [40]:

$$\rho C_p \frac{dT}{dt} = \nabla \bullet (k \nabla T) + Q \tag{31}$$

The efficiency of dielectric heating also depend on the dimension of irradiated material. Characteristic distance called penetration depth is defined as the depth at which the power density decreased to 37% of its initial value at the surface [40]. Penetration depth (d_p) of microwave energy into the material is calculated based on the power density falling into the sample surface [41].

$$d_p = \frac{\lambda_0}{2\pi\sqrt{2\varepsilon'}} \left[\sqrt{1 + \tan^2 \delta} - 1\right]^{\frac{-1}{2}} \tag{32}$$

Where λ_0 is wavelength of microwave at 2450MHz, ε' is dielectric constant, and $\tan\delta$ is a dissipation of electromagnetic energy. For a good conductor the depth of penetration is simplified to the following equation [42]:

$$d_p = \sqrt{\frac{2}{\omega\mu\varepsilon}} \tag{33}$$

2.2.5. Permittivity and Permeability.

Permittivity and permeability are the material properties that related to the interaction between microwaves and materials heated. Permittivity (ε) represents the ability of a material to absorb microwave, and can be defined as follows:

$$\varepsilon = \varepsilon_0 \varepsilon_r \tag{34}$$

Where ε_0 is the permittivity of free space (8.854x10-12 F/m), ε_r is relative permittivity of material that consist of the real part ($\varepsilon_r^{'}$) and imaginary part ($\varepsilon_r^{''}$):

$$\varepsilon_r = \varepsilon_r^{'} - j\varepsilon_r^{''} \tag{35}$$

Where j is the imaginary unit

The real part of complex relative permittivity is a measure of the ability of the dielectrics to store electrical energy, while the imaginary part of complex relative permittivity represents the loss of electrical energy in dielectrics. The energy lost from the electric field to the dielectric is eventually converted into thermal energy or heat. For nonmetallic magnetic materials, such as ethanol, the absorption of microwaves depends on both the permittivity ε and permeability (μ). The permeability is defined by the following equation:

$$\mu = \mu_0 \mu_r \tag{36}$$

where μ_0 is the permeability of free space (4Πx 10-7 H/m) and μr is the complex relative permeability, which is used to describe the relation between the magnetic flux density and the magnetic field intensity. The complex relative permeability is also consisted of two components: the real part of complex relative permeability ($\mu r'$), and the imaginary part of complex relative permeability ($\mu r''$). The real part of complex relative permeability represents the ability of the dielectrics to store magnetic energy, while the imaginary part of complex relative permeability indicates the loss of magnetic field energy. For the magnetic materials, the imaginary part of complex relative permeability heavily influences the heating rate under microwave irradiation.

The ratio of the imaginary to real parts of the permittivity and permeability is defined as the loss tangent $(\tan\delta)$ which is commonly used to indicate the efficiency of conversion of microwave energy into thermal energy within the dielectrics material. For nonmagnetic materials, the dielectric loss tangent is defined as follow:

$$\tan\delta = \frac{\varepsilon_r^{''}}{\varepsilon_r^{'}} \tag{37}$$

Where $\varepsilon_r^{'}$ is relative permittivity of material (real part) and $\varepsilon_r^{''}$ is imaginary part of relative permittivity.

2.2.6. Incident and Reflection wave power.

The wave propagating into the system is called incident wave. When a plane of electromagnetic wave is incident on a planar boundary between two homogeneous media, the scattered waves are also plane waves. One of these waves is radiated back into opposite direction of incident wave into the space, and this wave is known as reflected wave. The simplest case of wave reflection is when a uniform plane wave is incident normally on the planar interface between a perfect dielectric material and a perfect conductor.

The incident wave induces current and charges only on the surface of the perfect conductor material such as aluminum, copper, etc. Since inside the conductor there is no field, the scattered field from this wall is same in amplitude as the incident wave field but in the opposite direction.

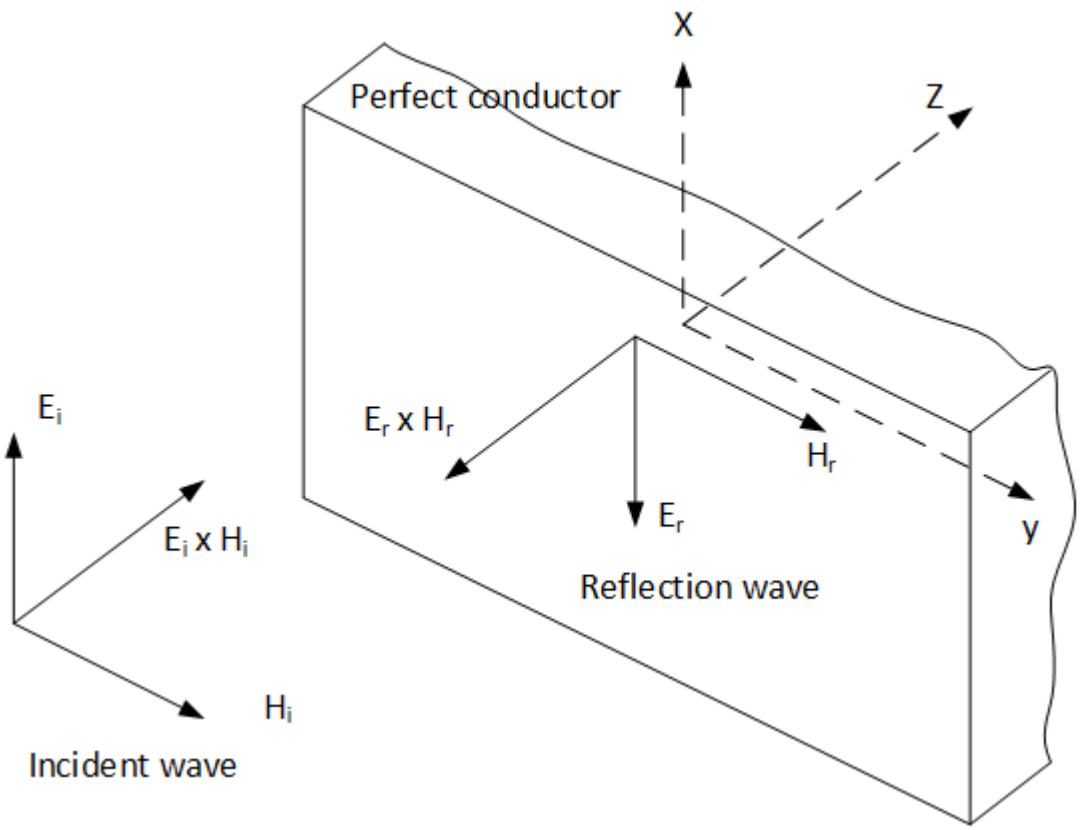

Figure 2.3. Incident and reflection wave (Source: D.M. Pozar: Microwave Engineering [36])

In the phasor form the incident of electromagnetic wave (electric and magnetic field) propagating in the z direction can be written as follow :

Electric field :

$$E_i(z) = Ee^{-j\beta z}u_x \tag{38}$$

Magnetic field

$$H_i(z) = He^{-j\beta z}u_y \tag{39}$$

The intrinsic impedance of the medium can be expressed as:

$$\eta = E/H = \sqrt{\frac{\mu}{\varepsilon}} \tag{40}$$

The reflected wave is the can be written in the form'

Electric field :

$$E_r(z) = -Ee^{+j\beta z}u_x \tag{41}$$

Magnetic field :

$$H_r(z) = He^{+j\beta z}u_y \tag{42}$$

The total field of electric and magnetic field can be obtained as a superposition of the incident and reflected waves:

$$E_{tot}(z) = Ei(z) + Er(z) = E(e^{-j\beta z} - e^{+j\beta z})u_x = -2jE\sin\beta z u_x \tag{43}$$

$$H_{tot}(z) = H_i(z) + H_r(z) = H(e^{-j\beta z} + e^{+j\beta z})u_y = 2H\cos\beta z u_y \tag{44}$$

The instantaneous value of the two vector can be expressed as:

$$E_{tot}(z.t) = 2E\sqrt{2}\sin\beta z\cos^*\omega t - \pi/2)u_x = 2E\sqrt{2}\sin\beta z\sin\omega t u_x \tag{45}$$

$$H_{tot}(z.t) = 2H\sqrt{2}\cos\beta z\cos\omega t u_y \tag{46}$$

2.2.7. Power absorption

In the microwave heating the energy is transferred to the material through the interaction of electromagnetic field at the molecular level. For nonmagnetic material, the dielectric properties determine the electromagnetic field in the material. The resistance of the induced motions of free or bound charges and rotation of the dipoles during the interaction of microwaves with the dielectric material due to inertial, elastic, and frictional forces causes losses resulting in volumetric heating. According to this mechanism, the power absorbed per unit volume *P* is expressed as

$$P = \sigma |E|^2 = 2\pi f \varepsilon_0 \varepsilon_r' \tan\delta |E|^2 \quad (47)$$

Where E is the electric field, σ is the total effective conductivity, and f is the microwave frequency. Equation (above) indicates that the power absorbed in materials strongly depends on the electromagnetic field and frequency (E and f) and the dielectric properties of loss factor ($\varepsilon r''$).

2.3.LMI system

A special injector which allow electromagnetically heated fuel is designed for low pressure injection fuel such development for Gasoline PFI engine operation. The target of this operation system is traditional port fuel injector engine operated for 300cc displacement at cold start problem. This device is developed to enhance atomization and evaporation of fuel during injected into combustion chamber. The injector has one nozzle hole with diameter of 0.3mm. This system uses microwave heating to increase the temperature of fuel before injected. Heating area was developed inside the tip of injector of around 200mm^3 volume. This area was connected to the magnetron of microwave heating throughout the coaxial cable at frequency of 2450MHz (Figure 2.5).

Fuel flow inside the area is heated by electromagnetic radiation before injected. Heating generation aims to increase the fuel temperature to around boiling point for easily evaporating during injected in to cylinder. Heating area was designed to allow the fuel flow experienced heating before injected. Heating generation from electromagnetic energy is expected to add energy equivalent to the ethanol flow for improving atomization and evaporation. Physical and chemical characteristic of ethanol fuel such as density, viscosity, and surface tension play an important role on the spray characteristics and atomization quality. As the temperature increase surface tension become lower and easy to atomize to become small droplet size.

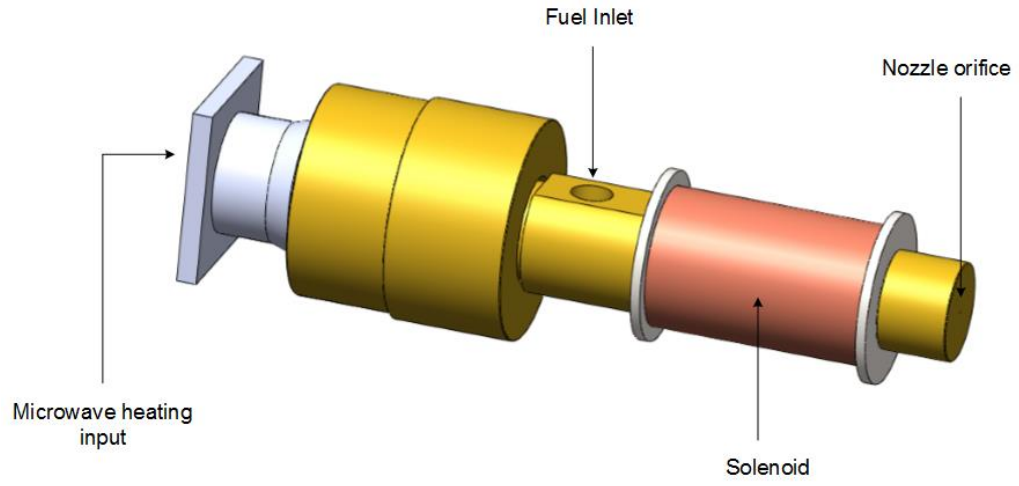

Figure. 2.4. Layout of LMI system

2.3.1. LMI components

The main part of LMI system consist of heating area, coaxial cable, inner cable and metal material wall surrounding the heating area. The surrounding parts of heating area consist of driven part, injector body and solenoid material that mainly metal material. Metal material mostly can be reflected electric and magnetic field, hence the interaction of electromagnetic energy wave and dielectric material of heated object can be optimized. Heat is generated from electric field and magnetic field distribution inside heating area. Coaxial cable of LMI functions as the electromagnetic guide from magnetron device to the heating area. Coaxial cable is the dielectric material that can propagate radiation of electromagnetic energy inside this material. In this system the material of coaxial cable is Teflon (PTFE) material.

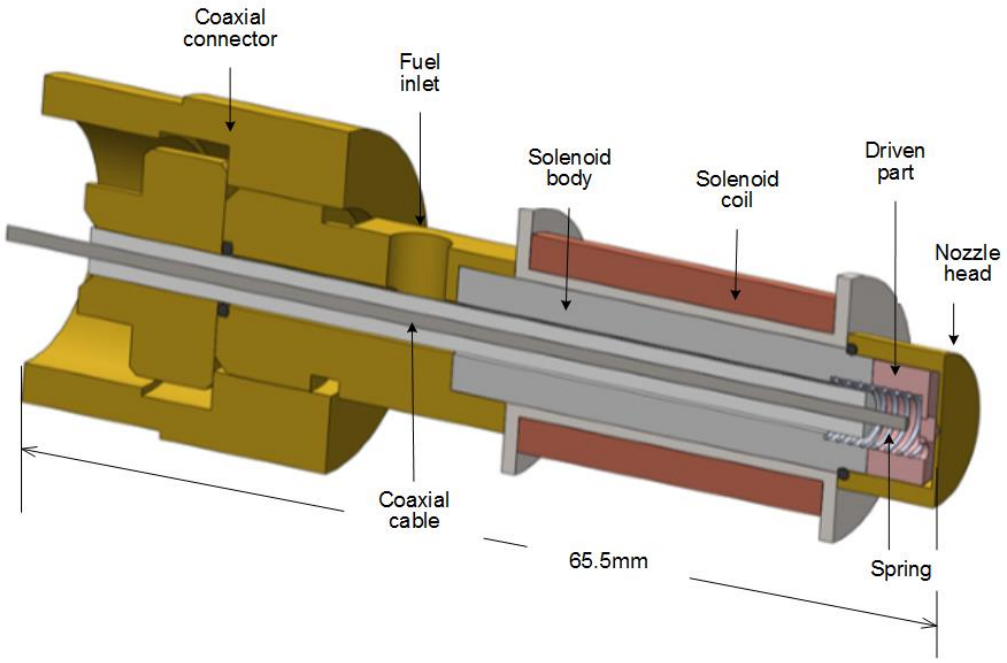

Figure. 2.5. Schematic LMI components

2.3.2. Heating area of LMI system

Heating area in Figure 2.5 is created inside the tip of injector of LMI to generate heat from microwave heating system as a result of interaction between electromagnetic radiation

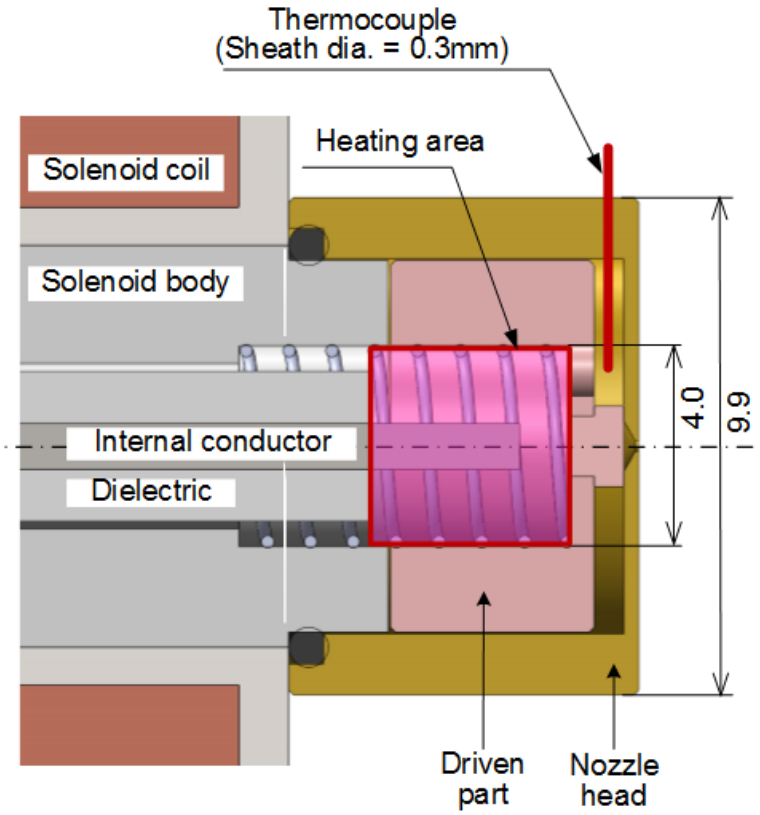

Figure. 2.6. Detail view of LMI head

and the dielectric properties of ethanol. This area has the length of around 4.0mm and radius of around 2.6mm. This zone is connected with magnetron throughout the coaxial cable (dielectric material) with frequency constant at 2.45GHz, same frequency used at domestic microwave oven. Fuel flow inside this zone will experience heat due to the friction and polarization of electromagnetic wave in the material.

2.3.3. Coaxial cable

Coaxial cable in Figure 2.6 is one of the most important component of LMI system. In this cable the electromagnetic energy radiation will propagate into the heating area. Electric and magnetic field will move and oscillate perpendicular to this coaxial cable. The outside and inside of coaxial material consist of metallic material that can reflected electric and magnetic field during propagation inside the material.

Inside the dielectric material is the internal conductor cable. This material is the electric conductor that can reflected the electric field and magnetic during propagation. Transfer of electromagnetic wave in this material is affected by the size of this cable. This inner and outer size are indicated of the cutoff wave length where the wave length cannot propagate. The cutoff wave length inside the coaxial cable can be obtained based on the following equations:

$$\lambda_c = \frac{\pi}{4}(d_i + d_o) \tag{48}$$

Where d_i is inner diameter and d_o is outer diameter of coaxial cable.

Coaxial cable in this following figure has inner diameter of 1.6mm and outer diameter of 5.0 mm. Using equation (39) it can be found that cutoff wave length inside the cable is 5.181mm. The important thing regarding the outer and the inner surface is the reflection of wave. For easy application it can be done by coating the surface with the perfect conductor that can reflected electric and magnetic wave during moving perpendicular to the directions of wavelength.

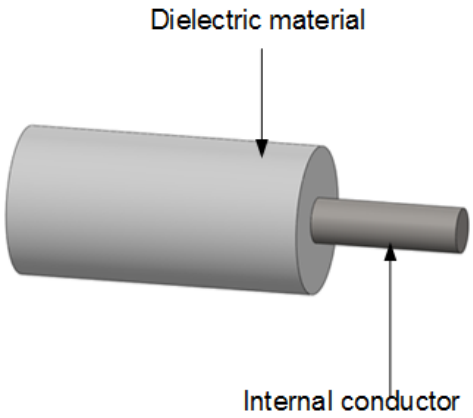

Figure 2.7 Structure of coaxial cable

2.4. Numerical simulation

Recently numerical simulation is used widely in many field of study and applications. Simulation study offers some advantageous compare with experimental study due to its faster, accuracy, and cheaper. Computer simulation also can provide detail and complete information of several variable expected. In computer simulation we can predict some phenomena that difficult to access in experimental because of several reason like small dimension, complex geometry, high temperature etc. However, the results of simulation usually need to validate with experimental data.

Numerical simulation method has been develop to solve electromagnetic equation over time. In LMI system interaction between electromagnetic wave and dielectric properties of ethanol fuel is happened in the heating area. Temperature distribution of fuel during heating is important for enhancing evaporation and combustion in the engine. However it is difficult to directly measure temperature distribution inside the area, hence numerical simulation is performed.

In this simulation study, coupled interaction between electromagnetic wave, heat transfer and fluid flow is simulated. Domain simulation consist of ethanol fuel and solid material of wall and dielectric material of Teflon. Electromagnetic wave propagated in dielectric material will be controlled to provide the appropriate temperature of the fuel. During microwave heating, some of electromagnetic energy radiation will be absorbed by the fuel and the rest will be reflected by metallic wall material surrounded the heating zone. Interaction between electromagnetic wave and dielectric material occurs inside the heating area and generates heating over the entire fuel flow inside the system. Temperature distribution generated inside heating zone of LMI system is the main consideration of this simulation.

Chapter 3

Numerical Modeling of Heating Zone in Local-contact Microwave-heating Injector (LMI) System.

3.1. Abstract

Numerical analysis was performed to investigate heating characteristics of ethanol flow inside heating zone of Local-contact Microwave-heating Injector (LMI) system. In this study, COMSOL Multiphysics was used to simulate microwave heating radiation inside heating zone of LMI system. This simulation process solved transient equations of electromagnetic wave, heat transfer and fluid dynamics of the phenomena inside heating zone. Two models geometry of the inner conductor, square and round model, were developed and simulated simultaneously using same boundary conditions. Each model was also varied at three different inner diameter (1.6mm, 1.8mm and 2.0mm) to evaluate the effect of geometry and shape of heating zone on the temperature field distribution inside heating region. Results of the simulation study were analyzed and validated with the experimental data. The result shows some advantageous predictions of microwave heating in LMI system and the flexibility of the model that allow for optimization design of heating zone inside LMI system.

Key Words*:* Microwave heating, convective heating, electromagnetic wave, and LMI system.

3.2. Introduction

Improvement on performances and emissions reduction of internal combustion (IC) engine is recently developed for the environment reason as well as the energy resources problem. By these reasons, research and development on alternative fuels become essential. Bio-component fuels become widely attracted attention as an alternative fuel for IC engine in many countries. Ethanol is the most promising alternative fuel for gasoline. It has high octane number, oxygenated fuel and heat evaporation which lead to better engine knock resistance as well as greater thermal efficiency [1]. However, several physical or chemical properties of the fuel are quite different from based fuel, and can generate some problems mainly for high ethanol blended fuel.

Injection development is needed for improving mixing and combustion rate particularly when using bio-component fuel in IC engine. Ethanol, with high latent heat of vaporization, needs an external energy supply for enhancing break-up and accelerating vaporization during injected into combustion chamber. The effect of bio-fuel heating on the injection performances is essential part especially for port-fuel injection application with low operating pressure. Heated fuel is expected for enhancing engine efficiency and exhaust emissions reduction.

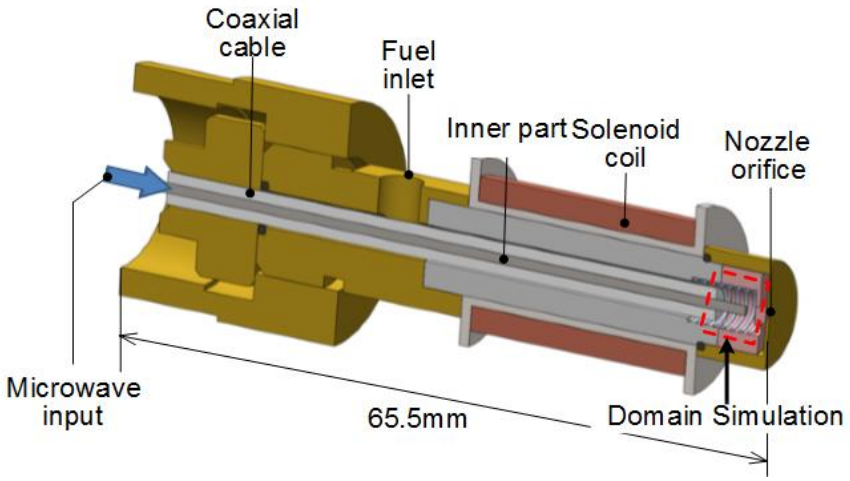

Figure 3. 1 Schematic structure of LMI system.

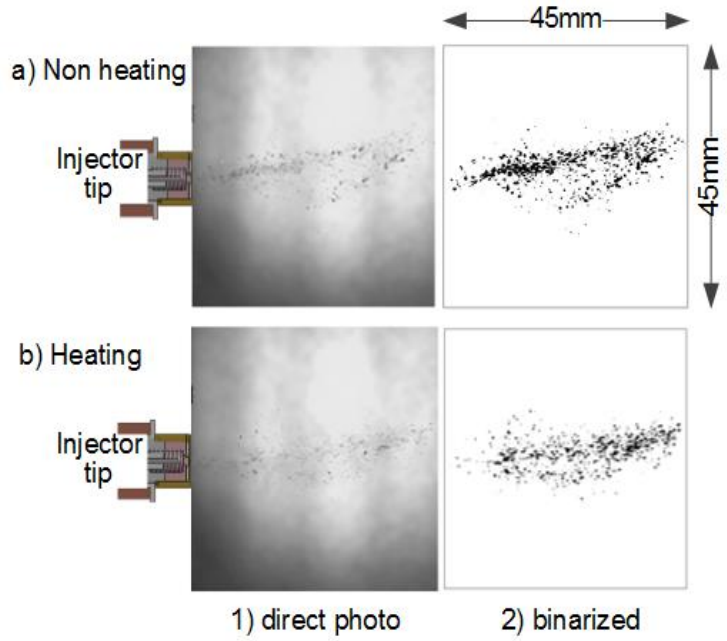

Several studies proposed technical solutions of heating evaporation chamber or directly heated fuel flow using electric heating [2-5]. Gumus [2] heated the engine block using thermal storage system and showed the reduction of CO and HC emissions to 64% and 15% respectively. Kabasin, et.al., [4]conducted experiment by heated fuel in injector using electric heating and concluded that ethanol cold star performance became similar as gasoline. They demonstrated that the emissions of HC and CO reduced 40% but NOx emission a little bit increased. Aleiferis and Van-Romunde, [5]conducted experiment to investigate spray characteristics of several bio-component fuels by heating fuel in injector and explained that spray formation was sensitive to fuel temperature. Droplets diameter were decreased as the temperature increased.

The new promising way of heating fuel inside injector is using microwave heating and this system called Local-contact Microwave-heating Injector (LMI). Microwave heating applied in this system aims to add some energy equivalent to the ethanol flow in order to improve the atomization and evaporation of the injected fuel [6]. The schematic design of LMI system can be seen in Figure 3. 1. In this system the heating zone was created inside injector head (Fig. 3. 2) and connected to the magnetron at constant frequency of 2.45GHz. An optical investigations of fuel sprayed from LMI system shows the significant improvement on spray formation of the fuel heated by microwave heating compare with the non-heating fuel as in

Figure 3. 3. Sauter Mean Diameter (SMD) of heated fuel, the droplet size was significantly reduced compare with non-heated fuel [7]. It was revealed in the previews study [7] that droplet size can reduce from 80μm of non-heating fuel to around 45 μm of heating fuel.

Heating zone is one of the most important part of LMI on the fuel spray characteristics. Rapid heating in this area is expected for ethanol flow for improving physical and chemical properties during injection. In general, volumetric heating for material subjected to microwave heating can generate rapid heating. However, temperature distribution of heated material can be affected by the dielectric properties as well as shape and geometry [8-9]. Ayappa et al., [10] suggested to avoid the corner and edge to reduce local heating of the sample. Funawatashi and Suzuki [11] analyzed the effect of size and geometry of food heated by microwave heating and identified that the non-uniform distribution of heating based on the size of the object. In smaller size of the object, interaction between transmission and reflection wave take placed, and for bigger size rapid decay of incident wave caused the non-uniform heating.

In LMI system, however, the effect of the shape, volume and geometry on the heating characteristics of the fuel flow is unknown. Therefore, the description of the complex relationship among these factors should be considered. Moreover these factors are physically generated some difficulties on controlling the parameters inside heating zone, hence, numerical modeling is proposed. Simulation study on the microwave heating phenomena inside the area was the main concerned. Two differences shape of inner part tip were evaluated. This simulation also performed convective heating in the heating zone to compare with the temperature profiles of ethanol flow during microwave heating generation system.

3.3. Numerical simulations

A 3-D geometry of heating area inside LMI system was created and simulated using COMSOL Multiphysics. Model geometry was a representation of the geometrical features of the utilized model of heating zone in the system. Two different schemes of heating process that consist of microwave heating scheme and convective heating scheme were simulated. In Microwave heating scheme, the governing equations of electromagnetism, heat transfer and fluid flow were solved using Radio Frequency (RF) module coupled with CFD module. In convective heating scheme, heat transfer and momentum equation were solved in the Heat transfer module. This study was conducted to investigate the distinction characteristic of microwave heating and convective heating. Results of simulation were validated with the measurement data.

The two schemes heating using in this study have each advantageous as describe below: For microwave heating scheme, heat is generated from the interaction between electromagnetic wave and the dielectric properties of material. Heat generation occurred in short time, internal heating, high efficiency and rapid processing. Propagation of microwave depends on the dielectric properties of material heated to generate volumetric heating.

However, for convective heating scheme, heat generates from external heating. Heat transfer is mainly depend on diffusion or conduction and convection heating in material. Rate of heat transfer is depend on physical and chemical properties of material such as heat capacity, thermal conductivity, coefficient convection, temperature, velocity, etc.

3.4.Governing equations

In microwave heating simulation, three physics phenomena of electromagnetism, heat transfer and fluid flow are coupled and solved in the same time. Flow of ethanol will be radiated by electromagnetic energy heat inside heating area. In this system, the heat transfer between fluid flow of ethanol and wall of solid material must be also considered. Electromagnetic field applied to the system is calculated based on the Maxwell's equation and the following equation is suggested [12].

$$\nabla \times \frac{1}{\mu_r}(\nabla \times E) - k_0^2(\varepsilon_r - \frac{j\sigma}{\omega\varepsilon_0})E = 0 \tag{1}$$

Where E is the electric field, ε_0 is electric permittivity of free space. ε_r is the relative permittivity, μ_r is the dielectric relative permeability, σ is the electric conductivity, ω is the angular frequency and k_o is the wave factor of the free space.

Volumetric energy heat generated (Q) by microwave heating can be calculated from the following equation:

$$Q = \omega\varepsilon_0\varepsilon'' |E|^2 \tag{2}$$

Where ε_0 is the permittivity of free space and ε'' is the dielectric loss in the material, and Q is the heat generation in the system.

The transient temperature behavior in the heated material is obtained by solving the following energy equation. Heat generation due to absorption of microwave energy inside the system can be expressed as [8].

$$\rho c_p \frac{\partial T}{\partial t} + \rho c_p u \cdot \nabla T = \nabla \cdot (k\nabla T) + Q \tag{3}$$

Where c_p is the specific heat, u is the vector velocity, T is the temperature, k is thermal conductivity. The first and the second left side equation represents the internal energy heat and kinetic energy of the system, respectively, while in the right side shows the conduction heat and energy heat generation.

In the Fluid Dynamic module, the Navier-Stoke equation of fluid flow should be considered. Conservation equations of mass, momentum and energy equation of fluid flow were solved with time dependent state in the form:

- Conservation of mass:

$$\frac{\partial \rho}{\partial t} + \nabla \cdot (\rho u) = 0 \tag{4}$$

- Momentum equation:

$$\rho \frac{\partial u}{\partial t} + \rho (u \cdot \nabla) u = \nabla \cdot \left[-pI + \mu(\nabla u + (\nabla u)^T) - \frac{2}{3}\mu(\nabla \cdot u) I \right] + F \tag{5}$$

- Energy equations

$$\rho c_p \frac{\partial T}{\partial t} + \rho c_p u \cdot \nabla T = \nabla \cdot (k \nabla T) + Q + W_p \tag{6}$$

Where p is the pressure of fluid flow, μ is the viscosity of fluid flow, I is the unit tensor on the fluid flow, F is the external momentum forces. c_p is the heat capacity of material, T is temperature, Q is heat generation and W_p is the external energy generated inside the system. In this microwave heating scheme, all equation solved in time dependent or transient state.

3.4.1. Initial conditions

In the initial of process of this study, the temperature of fuel is assumed in the thermal equilibrium with the surrounding temperature at 293.15K. This initial temperature conditions are applied for both of microwave heating scheme and convective heating scheme. Electrical power propagated into the system was set constant value of 60Watt and frequency of electromagnetic is 2450MHz.

3.4.2. Boundary conditions

Boundary condition for microwave heating system consists of reflected and transmission of electromagnetic wave. Port boundary is the inlet of power dissipated into the system. In this boundary the dissipated power of 60Watt was set at coaxial port inlet. Walls of the heating zone consist of metallic materials (copper and aluminum), thus, they can be assumed as perfect conductor (impedance) which mean that electromagnetic field inside the material must be zero.

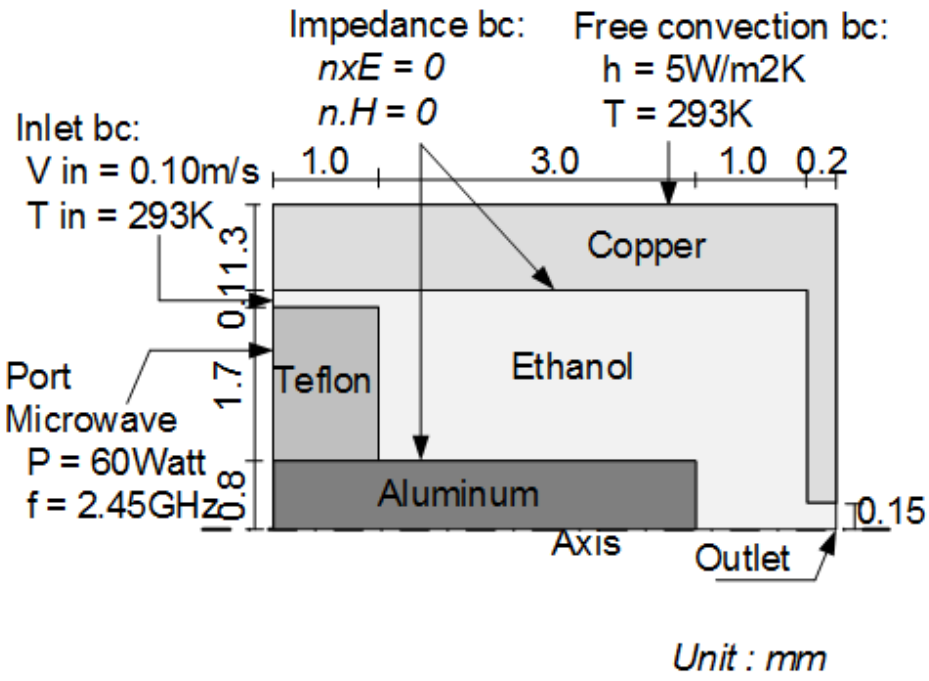

Figure 3. 3 Schematic of geometry and boundary conditions

All electromagnetics wave will be reflected from the surface of the material and this allow to have interaction of microwave energy only inside the heating area.

In this system, it is assumed that the wall is perfect electric conductor of copper and aluminum, hence the electromagnetic wave cannot penetrate inside the wall. Impedance wall boundary condition was applied in the simulation by the following condition equations [16].

$$n \times E = 0 \text{ and } n \cdot H = 0 \quad (7)$$

Ethanol fuel is modelled in microwave heating as the fluid flow and having dielectric properties as follow: electrical conductivity 1.35e-09 S/m, relative permeability 1.67, and relative permittivity (real part 24.3 and imaginary part 22.866) [17-18]. Teflon, a dielectric material, is used as the electromagnetic wave guide from magnetron to the heating zone. Teflon properties consist of electric conductivity of 1.0e-32, dielectric permittivity of 2.1 and relative permeability of 1.0 [19].

Electromagnetic wave equation was solved in the simulation at constant frequency of 2.45GHz. The electric power used in inlet port boundary is 60Watt. This power is same as applied in the experimental study.

Inside the wall of fluid flow the following boundary condition is applied. The velocity vector of fluid flow at the wall is zero:

$$\nabla u = 0 \quad (8)$$

In inlet boundary condition the velocity of fuel is set to 0.1m/s based on the measurement data on experimental study on LMI system.

In the outlet of flow, the pressure boundary condition was applied with the following expression:

$$\Delta p = 0 \tag{9}$$

In the outside of the wall, the convective cooling wall was applied with assume that all outside wall are in contact with the ambient temperature. The following equation was applied in the boundary:

$$-k\frac{\partial T}{\partial n} = h(T - Ta) \tag{10}$$

Where the *k* is thermal conductivity of wall, *h* is the convective heat transfer coefficient and *Ta* is the temperature of ambient air.

3.4.3. Solution

The system of non-linear partial differential equation was solved by finite element model developed under commercial software of COMSOL Multiphysiscs. Microwave heating coupled with fluid dynamics was solves using Multifrontal massively parallel sparse direct solver (MUMPS) to calculate heat generation inside ethanol flow. Partial differential equation developed in the system was solved using implicit method of Backward Differentiation Formula (BDF) in time dependent solver. This solver is interested since it solves the information or solution from previous step to calculate the next step. This method might need a little longer time in solving problem but proposes stability and robust solution with high accuracy of simulation result.

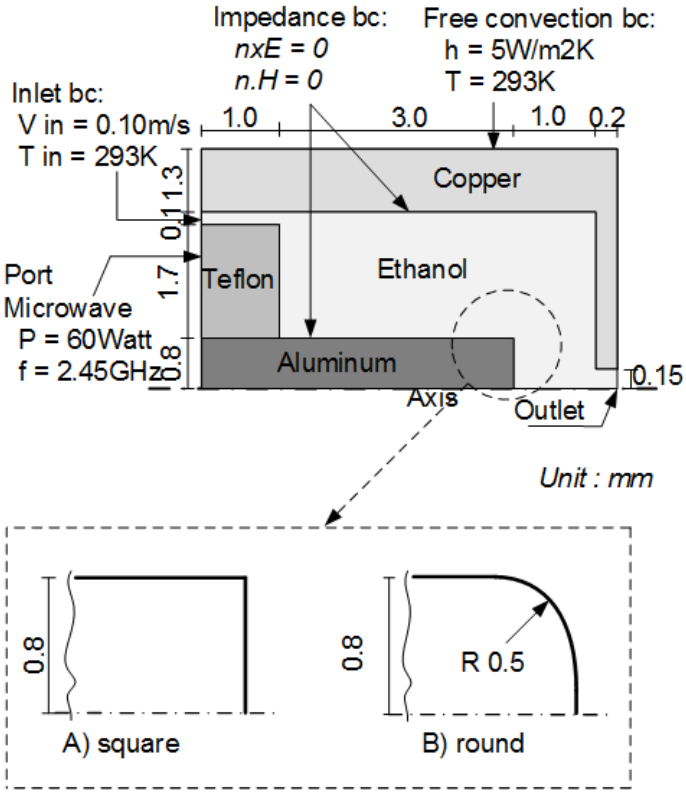

Figure 3.4. Two different model simulated

One of disadvantageous of microwave heating is the non-uniform temperature of heated object. This phenomenon is usually happened with higher temperature along the corner or edges of material. This is due to difficult in control the electromagnetic distribution inside the object or because of the geometry, size and volume of object [8-10]. In order to understand the microwave heating characteristic inside heating zone of LMI system, two models of heating area were compared as can be seen in Figure 3.5 below. Initial condition and boundary condition applied in this model were same as applied the previous study at microwave heating scheme. The main different is the shape of inner cable that can be affect the heating generation inside the zone. The tip of inner cable was modified into the round shape with radius of 0.5mm. This modified can change the geometry and lead to change the volumetric absorption of electromagnetic wave inside ethanol. The purpose of this changed is to achieve better uniform temperature distribution inside heating area and expected to improve spray characteristic of fuel during injection.

Instead of tip modification, in this study the diameter of the inner conductor also considered. Three different size of inner conductor diameter were simulated, 1.2mm, 1.8mm and 2.0mm. These modified size will affect on the changing size of coaxial cable that covered

the inner cable material. Consequently the volume of fluid experienced heat in heating zone will be different and the area of electromagnetic input will also change. The smaller the inner part, the larger the volume of fluid. The changing the volume inside this area may affect the heating generating inside the system. The phenomena inside the differences of volume will be the part of this analysis.

In order to easily construct the geometry of the system, several shapes and sizes of domain simulation were created in Solidworks software, and imported into COMSOL Multiphysics for the simulation process. Effect of these models will be the main consideration of this study. Initial and boundary conditions applied in this simulation were same as the previous scheme (Microwave heating scheme).

Table 3.1. Mesh types and CFL condition

Type	Threshold mesh size (Average)	Total mesh	CFL
Normal	0.150 mm	82852	0.0094
Fine	0.140 mm	133799	0.0101
Finer	0.105 mm	243117	0.0134

Table 3. 2. Properties of simulation study.

Description	Value
Fuel	Ethanol
Fuel temperature	293.15K
Fuel pressure	0.3MPa
Velocity inlet	0.1m/s
Microwave power	60W
Frequency	2.45GHz
Heating time	20ms over 40ms

3. 5. Meshing

3D Geometry of domain simulation was discretized into tetrahedral mesh and solved in time dependent state. Mesh resolution and quality are important aspect to be considered to solve the differential equations of electromagnetism, heat and mass transfer. For microwave heating scheme where Maxwell's equation is solving, the time is discretized into small size mesh to provide an efficient iteration scheme [13]. Mesh size can also influence the convergence solution of simulation as well as the accuracy of results simulation.

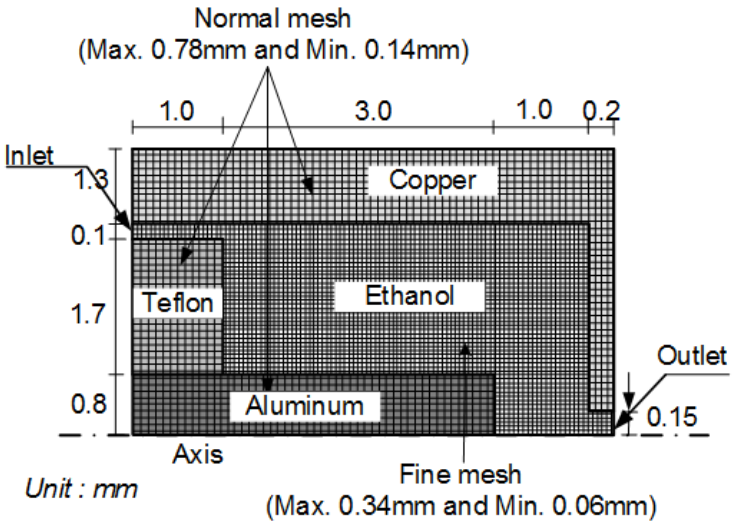

Figure 3.5 Schematic of mesh structure in the domain.

The maximum cell size in the dielectric material is important for solution of the problem in simulation and it can be evaluated based on the following equation [14]:

$$Cellsize(\Delta x) \le \frac{c}{10 f \sqrt{\varepsilon_r}} \tag{11}$$

Frequency of microwave system is 2.45GHz and relative permittivity of ethanol is 24.3. By this equation the mesh size for ethanol material should be less than 2.48mm. This size is bigger enough than the size of domain simulation that has length of 5.2mm and diameter 7.8mm respectively. The ethanol which is the subject of heated object has length of 4.0mm and maximum diameter 2.6mm respectively in the domain simulation. Furthermore, in this simulation 3D geometry was considered with using tetrahedral mesh that more flexible than other mesh types such as hexahedron or cube mesh type [Su and Wang 2003].

Figure 3.8 shows the mesh size evaluation effect on the temperature profile in ethanol. Normal and fine mesh have almost same result and finer mesh has a little bit higher but time and memory consumed. For reasonable simulation result, the fine mesh structure was used for

fluid phase with maximum and minimum size of 0.338mm and 0.0637mm respectively whereas for solid phase normal mesh structure was selected with maximum and minimum size of 0.78mm and 0.14mm respectively. Total of mesh generated in the domain of 5.2mm length and 3.9mm radius was 133,799 element meshes. These mesh structures provided finer mesh enough for solving partial differential equations of electromagnetic wave, heat transfer and fluid dynamics.

Concerning the propagation of electromagnetic, the time step must be chosen properly to satisfy the courant CFL conditions of simulation as follow [15]:

$$CFL \leq \frac{\upsilon \Delta t}{\Delta x} \leq 1 \tag{12}$$

With υ is the propagation of electromagnetic in material and can be evaluated from expression below [13].

$$\upsilon = \frac{1}{\sqrt{\varepsilon_0 \mu_0}} \frac{1}{\sqrt{\varepsilon_r \mu_r}} \tag{13}$$

Using this equation for properties of ethanol with relative permittivity of 24.4 and relative permeability of 1.67, the propagation of electromagnetic in ethanol is 0.47×10^8 m/s. This velocity is large different compare with velocity of ethanol flow inside heating area (0.1m/s). The average time step length (Δt) for electromagnetic analysis in the ethanol is around 0.03 picosecond. The solution of this calculation is theoretically stable enough since the CFL condition derived from the mesh size is less than 1 as in Table 3.1. The averages mesh used in table 1 was derived from the maximum and minimum size mesh type selected in this study.

3.6.Results and analysis

3.6.1. Geometry effect on heating generation

The effect of geometry and shape of the inner part material on temperature distribution of the microwave heating was also studied. Simulation was performed at same parameters of initial conditions and boundary in the two different models. It is the evident that the trend of temperature distribution can be affected by the shape of material heated even for small changes of shape or geometry.

In general, high frequency of electric field stimulates the polarization of water molecule inside the electric material. This polarization produces power dissipation or power absorption in the material. Distribution of electric field and power dissipated because of the heating absorption of the system can be seen in Figure 3.14. Heating distribution is mainly affected by the interaction between electric field and dielectric properties of the fuel. In the square model the electric field was generated maximum in the corner of inner tip and caused the maximum power absorption on this area. However in the round model it move to the front of the tip of inner part and generated maximum heat along the rounded tip of the part. Electric field can be reached maximum of 9.54e4V/m and 7.72e4V/m for round and square model respectively.

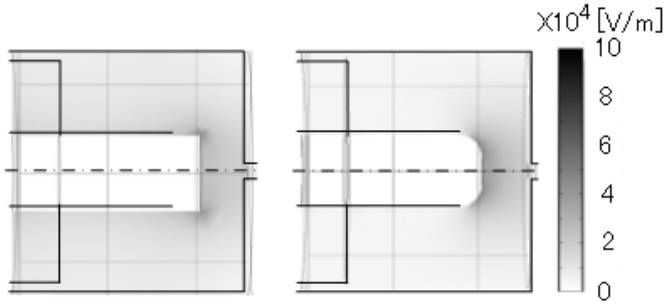

A. Electric field

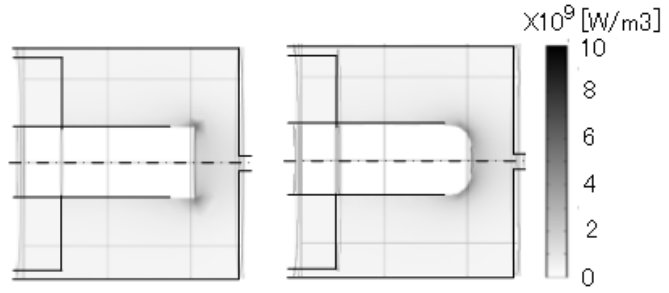

B. Power dissipation

Figure 3.6. Electric field and power dissipated distribution during imposing electromagnetic wave power (50msec)

Power dissipated is the power losses into the system from the incident power propagated along the system. Heat generated in the system is coming from the ionic vibration at high frequency of water component inside the ethanol. Dielectric properties and electric field distribution are important in power dissipated especially in the high frequency of incoming wave. During the time the electric field and power dissipated are fluctuated and a little higher in the tip of inner conductor. Power dissipated into ethanol can be reached maximum about 14e0W/m3 and 9.30e9 for round and square model respectively during imposing microwave heating.

The distinction of temperature field distribution of the two different shapes are illustrated in Figure 3. 7. In the square tip case, the maximum temperature generates at the corner of the inner conductor, however, in the round tip case, it moves to the middle of the tip of inner conductor that very close to the injector orifice. This changing can be happened due to distribution of electromagnetic wave inside the object heated. It is also can be affected by the concentration or flux intensity of electric field generated at the corner due to the wave length oscillation of electromagnetic wave. In 100msec of heating time the temperature can reach around 400K for the square model and 393K for the round model, however, the distribution was not uniform and maximum can be reached at the tip of inner conductor where the power dissipated was optimum.

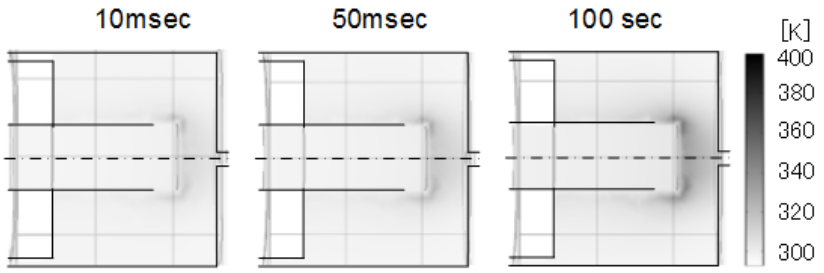

A. Square model

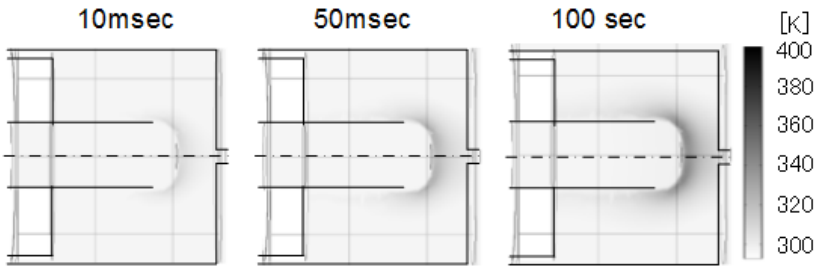

B. Round model

Figure 3. 7 Temperature distribution of two differences model simulated during several time after imposing power into the system.

In the tip of injector the temperature of fuel was evaluated and compared with the result of experimental measurement. Both simulation and experiment are in fairly good agreement of temperature at the tip injector during injection time. Small difference is several point can be due to the properties of simulation and geometry that simplified from the complex geometry of real LMI injector. Figure 3.8 shows the time history of temperature distribution characteristic of heated fuel at the tip of injector. The two model compared shows that temperature at the tip injector is almost same even though they are different in around the tip of inner cable. This phenomena can be affected by the different volume of fuel heated after cut in the tip of inner cable and affect the temperature field distribution. Even the maximum temperature moved to the tip closed to the orifice injector in round tip (modified), the temperature in inlet is almost same as in the square tip (original). It is likely that geometry of rounded tip can show the desire temperature distribution and offering the potential development of LMI system.

In the next figures we can see the effect of different inner part diameter on the temperature generated inside heating area. The changing of the geometry or size of the inner conductor can change the volume of fluid flow inside the system. It is also affect the changing of size of the coaxial cable used for propagating the electromagnetic wave. As the inner cable decreased, the normal surface area of coaxial cable become larger and leads to change the behavior of electromagnetic propagating perpendicular into normal area of coaxial cable. Figure 3.9 illustrates the electric field and temperature field distribution at the specific line. It was evaluated along the heating zone (4.0mm) and above 0.2mm from the inner conductor surface. Generally, it can be seen that the diameter of inner part is also very important on the temperature field distribution of the system. The smaller the inner diameter, the higher the

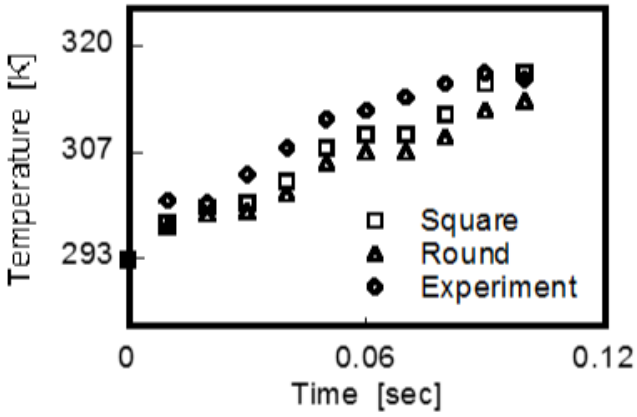

Figure 3.8. Temperature of fuel at the tip injector

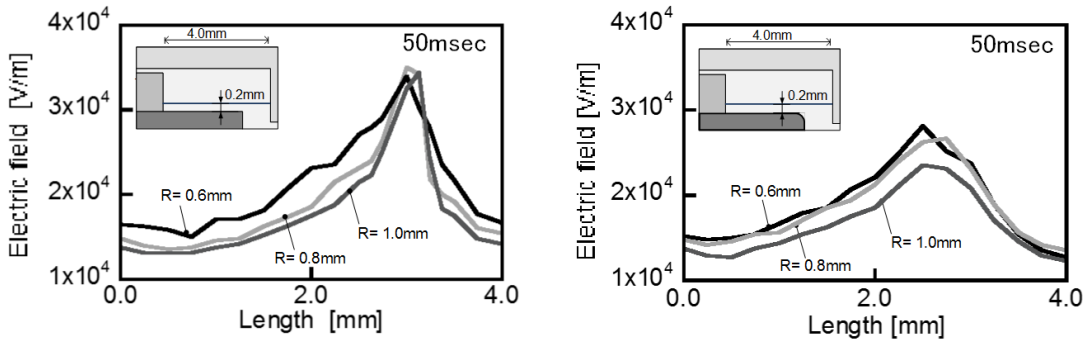

A. Electric field distribution

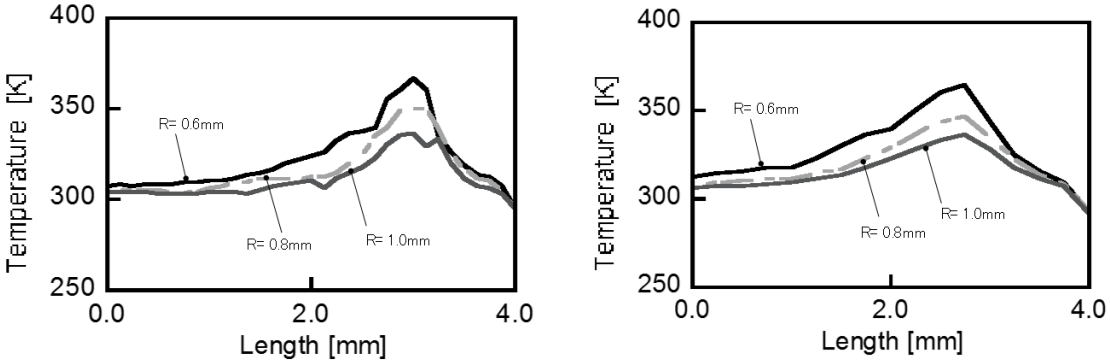

B. Temperature field distribution (100msec)

Figure.3.9. Electric and Temperature field distribution of different model and diameter of inner conductor

temperature can be generated inside heating zone. In the bigger distance between the conductors (for smaller inner diameter) the amplitude of electromagnetic wave become bigger and hence the temperature of the fuel increases. Along this line the electric field distribution was vary in each diameter and tend to increase by the increase the distance between the inner and outer conductor. As the high elelctric field generated, the temperature of the fuel can be significantly increased. For the square model the maximum Temperature field is 367K, 350K and 339K for the inner conductor radius of 0.6mm, 0.8mm and 1.0mm respectively. Whereas in the round model the maximum temperature field is 365K, 347K and 337K for the inner conductor radius of 0.6mm, 0.8mm and 1.0mm respectively.

3.5.2. Incident and reflection energy.

Power incident and power reflection are another phenomena that can affect the heating process inside the LMI system. Energy heat propagated in the system by microwave radiation will be absorbed by ethanol and another will be reflected out the system. Absorption of ethanol depends on the characteristic impedance or load impedance (Z_R) that can be calculated from expression:

$$Z_R = \sqrt{\frac{\mu}{\varepsilon}} \tag{14}$$

Where μ is permeability of ethanol [H/m] and ϵ is dielectric constant or permittivity of ethanol [F/m]. Dielectric permittivity can be calculated from the relative permittivity of dielectric material (ethanol) ϵ_r and dielectric permittivity of vacuum medium (ϵ_o =8.854x 10^{-12} F/m). Permeability if ethanol can be calculated from relative permeability ($\mu_{r)}$ and dielectric permeability of vacuum ($\mu_0 = 1.257x10^{-6}$).

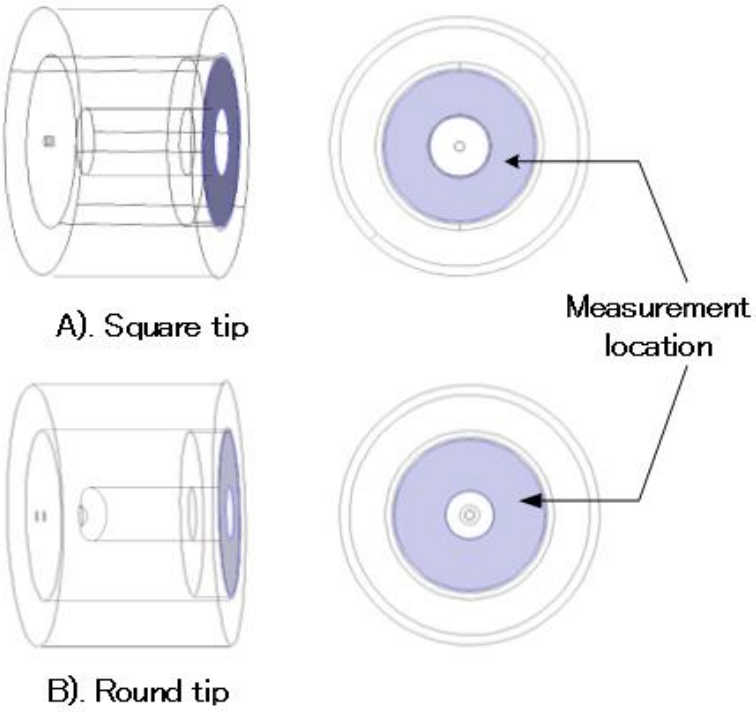

Figure 3.10. Reflective power measurement location at two different model.

Figure 3.10 shows the location measurement of the reflected power in the port of coaxial cable. The measurement system was based on the power flow reflected over the integration of normal area of coaxial cable where the electromagnetic wave propagated.

Figure 3.11 show the input power controlling in the system with power 60Watt is applied. Figure 3.23 show the result of reflection wave power measured in three different of inner part diameter (1.2mm, 1.6mm and 2.0mm respectively) at two model simulated. The reflected wave power were oscillated in the entire area of coaxial cable but this characteristics are a little vary in different area of coaxial cable during the time flow. It can be seen that the average of reflected wave power in square model is a little lower than that in the round model at same diameter and this value will increase in the bigger size of inner diameter. In square model, the maximum power reflected for inner diameter 1.2mm, 1.6mm and 2.0mm is 29.95W, 29.88W and 30.06W respectively. In round model, the maximum power reflected for inner diameter of 1.2mm, 1.6mm and 2.0mm is 30.38W, 30.40W and 30.62W respectively.

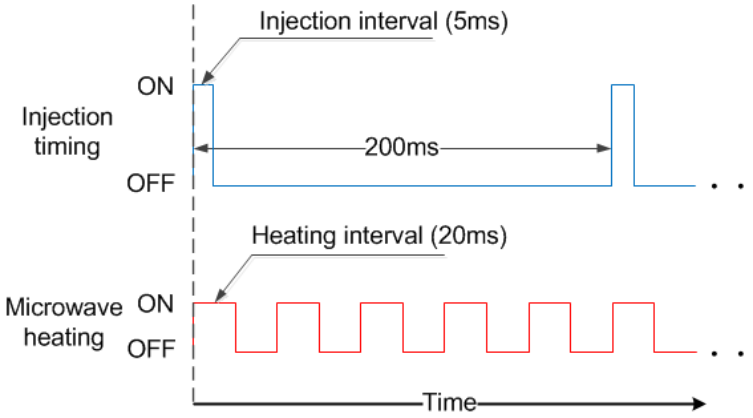

Figure 3.22. Power input and injection control in the system

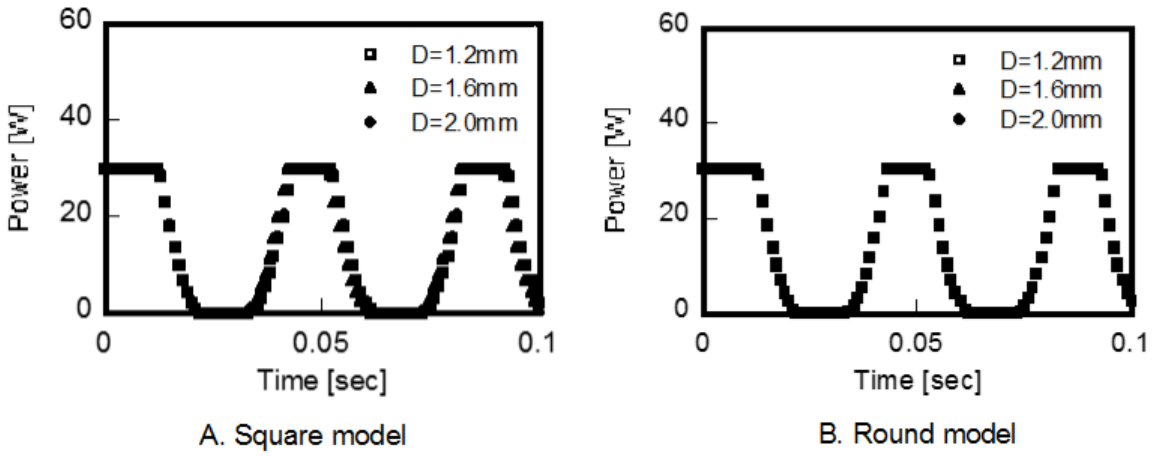

Figure 3.11 Reflected power measured in in port of two model compared.

In this simulation, ratio between reflected power and incident power was evaluated for each model. It is derived from the S-parameter (S11) that represent the power input and output into the system and can be written as follow:

$$S11 = \sqrt{\frac{Power\ reflected\ on\ port}{Power\ incident\ on\ port}} \tag{15}$$

Power flowing out (S_A) on the port of electromagnetic wave is calculated from the time average of pointing vector on the port.

$$S_A = \frac{1}{2}\mathrm{Re}(E \times H) = \frac{1}{2Z_R}\left|n \cdot E\right|^2 \tag{16}$$

Where E is electric field, H is magnetic field, and Z_R is characteristic impedance of the dielectric material. In the model square, the ratio $(S11)^2$ on this port is 0.4527, 0.4439, and 0.4339 for inner part diameter of 1.2mm, 1.6mm and 2.0mm respectively. While in model round this ratio is 0.4617, 0.4549 and 0.4492 for inner part diameter of 1.2mm, 1,6mm and 2.0mm respectively. Reflecting power can affect the behavior of the incident wave absorbed by the system. As the reflected power increased, the absorption wave power will reduce and the temperature can become lower inside the object.

In comparison the procedure in simulation study and experimental investigation it might a little different in several analysis and assumption between simulation and experimental data.

Table 3.3. Comparison of condition simulation and experiment

Simulation study	Experiment study
- Injection duration is constant	- Injection duration 5msec over 200msec
- Heating time varies same as experiment	- Heating time 20msec over 40msec
- Ethanol (Data base COMSOL)	- Ethanol 99.5%
- Time flow of simulation was 0.1sec	- Time flow was evaluated at 2.5 sec

The different in simulation and experimental is due to the injection time that too short or spiky (5msec over 200msec). This condition made the flow time of the simulation become unstable and the next time injection became zero velocity that made the prediction of temperature distribution become undesirable. In real condition of engine, the 100msec is important based on

the rotational of the engine especially at start condition. Therefore in this simulation 0.1sec is considered to evaluate the distribution of field temperature during heating by microwave heating.

Figure 3.12 shows the output of incident and reflected wave power based on direct measurement using coupler detector. The reflected wave of fuel injection unit were recorded immediately after passing the microwave incident wave inside LMI injector. From measurement it was defined that the ratio between reflected power and incident power was around 40% and this model is same as the model square with inner part diameter of 1.6mm [23]. This size is the real size of injected using in experimental study. Comparing the simulation result with power reflected around 50% from the incident wave power, the different can be coming from the simulation properties or model that simplified from the complex geometry of real LMI injector. However, the important think of microwave heating system can be explained during simulation study. Temperature distribution is important for ensuring the spray of fuel can evaporate properly during injected into combustion chamber. This heating is expected to improve thermal efficiency of the engine as well as exhaust gas emissions.

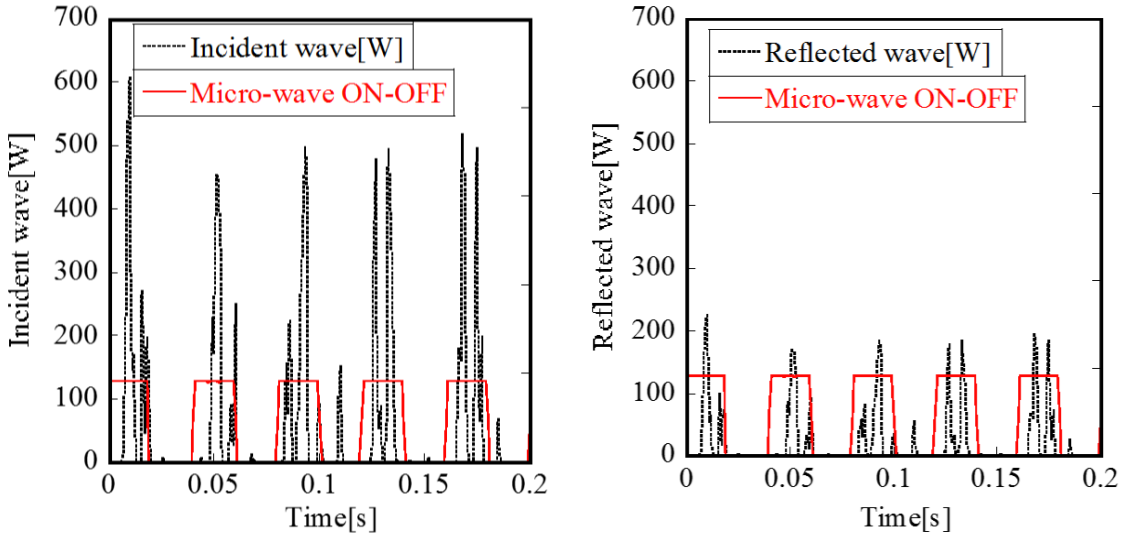

Figure 3.12. Incident and reflected power measured directly in the experimental study

3.7. Conclusions

Numerical model was developed to simulate microwave heating of ethanol fuel inside heating area of LMI system. The effect of geometry and shape of the inner part material on temperature distribution of the microwave heating is also studied. Simulation results were validated with the direct measurement data. The results of studies can be concluded as follow:

- Volumetric heating in microwave heating offers the advantages for ethanol fuel heat. Temperature of fuel increased shortly after imposing microwave into the system. Trend of temperature distribution at injector tip in the microwave heating simulation result agrees with the experimental data.
- Geometry of the heating zone has significant effect on the temperature characteristics of fuel heated. It is noticeable that a slight change in the inner conductor can alter the electric field distribution and leads to change the temperature distribution of the fuel.
- In additional, simulation result of microwave heating can show the flexibility of the shape and geometry of heating zone for optimal development of LMI system.

Nomenclature

c : Speed of the light in vacuum [m/sec]

$c_{p.}$: Specific heat of fuel [J/kg/K]

CO : Carbon monoxide [-]

CFL : Courant number [-]

E : Electric field [V/m]

F : External momentum force [N/m2]

f : Frequency [Hz]

H : Magnetic field [A/m]

HC : Unburned hydrocarbon [-]

h : Coefficient convection [W/m^{2}K]

k : Thermal conductivity [W/mK]

k_0 : Wave factor [-]

NOx : Natrium oxide [-]

P : Power [W]

p : Pressure [Pa]

PTFE: Poly Tetra Fluoro Ethylene.

Q : Heat generation [J]

SMD : Sauter Mean Diameter [μm]

T : Temperature of surface [K]

T_a : Temperature of fluid flow [K]

u : Axial velocity of fuel [m/sec]

Symbols:

λ : Wave length [m]

ω : Angular velocity [rpm]

μ : Fluid viscosity [Pa.sec]

ρ : Density of fuel [kg/m3]

ε_r : Relative permittivity [-]

μ_r : Relative permeability [-]

ε_0 : Electric permittivity of free space (F/m)

ε' : Electric permittivity of material(F/m)

ε'' : Dielectric loss in the heated material.(F/m)

μ_0 : Dielectric permeability of free space (H/m)

μ' : Dielectric permeability of material (H/m)

μ'' : Magnetic loss (H/m).

σ : Electric conductivity [S/m]

υ : propagation of electromagnetic (m/s)

Δx : Cell size [m]

Δt : time step size [sec]

References

1) Padala, **S**., Le, M.K., Kook, S. and Hawkes, E.R., : Imaging Diagnostics of Ethanol Port Fuel Injection Sprays for Automobile Engine Applications, Applied Thermal Engineering, 52, (2013), 24-37.
2) Gumus, M., Reducing Cold-Start Emission from Internal Combustion Engines by Means of Thermal Energy Storage System, Applied Thermal Engineering, 29, 2009, pp. 652-660.
3) Sales, L.C.M. and Sodre, J R., : Cold Start Characteristics of an Ethanol-Fuelled Engine with Heated Intake Air and Fuel, Applied Thermal Engineering 40, (2012), 198-201.
4) Kabasin, D., Hoyer, K., Kazour, J., Lamers, R. and Hurter, T., : Heated Injector for Ethanol Cold Starts, SAE International, 2009-01-0615, (2009).
5) Aleiferis, P.G. and van Romunde, Z.R., : An Analysis of Spray Development with Iso-

octane, n-pentane, Gasoline, Ethanol and n-butanol from a Multi-hole Injector under Hot Fuel Conditions, Fuel **105**, (2013), 143-168.

6) Enomoto, H. and Iida, T., : Development of Fuel Injector using Local Contact Microwave Heating, , JSDE Paper 43**,** 6, (2008), 339 – 344.
7) Mangalla, L.K. and Enomoto, H., : Spray Characteristics of Local-contact Microwave-heating Injector Fuelled with Ethanol, SAE Technical Paper 2013-32-9126, (2013).
8) Zhu J., Kuznetsov A.V. and Sandeep, K.P. : Mathematical Modeling of Continuous Flow Microwave Heating of Liquids (Effect of Dielectric Properties and Design Parameters), International Journal of Thermal Science, 46, (2007), 328-341.
9) Chandrasekaran, S., Ramanathan, S, and Basak, T., : Microwave Food Processing- A Review. Food Research International 52, (2013), 243-261.
10) Ayappa, K.G. Davis, H.T. Crapiste, G. Davis, E.A. and Gordon, J., : Microwave heating: an evaluation of power formulations, Chemical Engineering Science 46 ,(1991), 1005–1016.
11) Funawatashi, Y., and Suzuki, T., : Numerical Analysis of Microwave Heating of a Dielectric, Heat Transfer-Asian Research, 32, 3, (2003), 227-236.
12) Salvi, D., Boldor, D., Aita, G.M. and Sabliov, C.M., : Comsol Multiphysics Model for Continuous Flow Microwave Heating of Liquid, Journal of Food Engineering, 104, 3, (2011), 422-429.
13) Denecker, B., Knockaert, L., Olyslager, F., and Zutter, D.D., : A New State-space-based Algorithm to Asses the Stability of the Finite-difference Time-domain Method for 3D Finite Inhomogeneous Problem. International Journal of Electronics and Communication, 58, (2004), 339-348.
14) Pithcai,K., Birla, S.L., Jones D., and Thippareddi, H., : Coupled Electromagnetic and Heat Transfer Model for Microwave Heating in Domestic Ovens,Journal of Food Engineering, 112, (2012),100-111.
15) Kakuta, Y., Watanabe, S., and Hashimoto,O., : Examination of the Wave Propagation Characteristics of a Rectangle Wave using FDTD, CIP, and R-CIP Methods, The Institute of Electronics, Information and Communication engineers (IEICE) Technical Report, ED2005-221, MW2005-175, (2006)-1).
16) Knoerzer, K., Regier, M., and Scubert, H., : A computational Model for Calculating Temperature Distribution in Microwave Food Application, Innovative Food Science and Engineering Technologies, 9, (2008), 374-384.

17) Wyman, J., : Dielectric Constants of Ethanol- Ether and Urea-Water, Journal of The American Chemical Society, 55, 10, (1933), 4116-4121.
18) Papanastasiou, E. G. and Ziogas, I.I., : Physical Behavior of Some Reaction Media. Density, Viscosity, Dielectric Constant, and Refractive Index Changes of Ethanol -Cyclohexane Mixtures at Several Temperatures, Journal of Chemical & Engineering Data, 36 (1), (1991), 45-51.
19) Xiang, F., Wang, H. and Yao, X., : Preparation and Dielectric Properties of Bismuth-Based Dielectric/PTFE Microwave Composites, Journal of the European Society 26, 10-11, (2006), 1999-2002.
20) Hossan, M.R., Byun D.Y. and Dutta P., : Analysis of Microwave Heating for Cylindrical Shaped Objects, International Journal of Heat and Mass Transfer, 53, (2010), 5129-5138.
21) Oliveira, M.E.C. and Franca A.S., : Microwave Heating of Foodstuff, Journal of Food Engineering 53, (2002), 347-359.
22) Du, Q. and Wang, D., Tetrahedral Mesh Generation and Optimization Based on centroidal Voronoi Tessellations, Int. Journal for Numerical Method in Engineering, 56, 2003, pp 1355-1373.
23) Ishumi, K. Effect of Fuel Temperature on Atomization and Evaporation of ethanol in Local-contact Microwave-heating Injector, Thesis, 2013.

Chapter 4

An Optical Measurement Analysis of Spray Formation from Local-contact Microwave-heating Injector.

4.1. Abstract

Injection strategy on the application of bio-ethanol fuel in internal combustion engine is expected to meet the increasingly stringent on emission regulation. Heating system is the potential solution for improving atomization and vaporization of ethanol fuel that has some limitation properties compare with gasoline. The influence of heating system from LMI injector on spray characteristics of ethanol fuel is the main focus of this study. Ethanol fuel flow was experienced microwave heating inside heating area before injected. An optical measurement of fuel injection was conducted using high speed camera. The stability of injected fuel was first observed in order to easily recognize the spray formation and then images captured were analyzed. Analysis of spray characteristic such us droplet size, droplet velocity and droplet quality was processed using images post processing software. Results show the indication of finer droplets size and faster droplet movement on the heating fuel injected from LMI system. These characteristics are supposed to improve atomization and vaporization of the fuel especially for cold start conditions.

Key Words: Spray characteristics, droplet size, heating fuel, microwave heating, and LMI system.

4.2. Introduction

Fuel spray characteristics plays an important role in the performance and emission reduction of internal combustion (IC) engine. Poor performances and high exhaust emission of the engine are the major problems related to the lack spray atomization and vaporization of fuel. This phenomena is more critical particularly when uses bio-component fuel for IC engine. The fuel has been widely recognized as an alternative for gasoline due to the higher octane

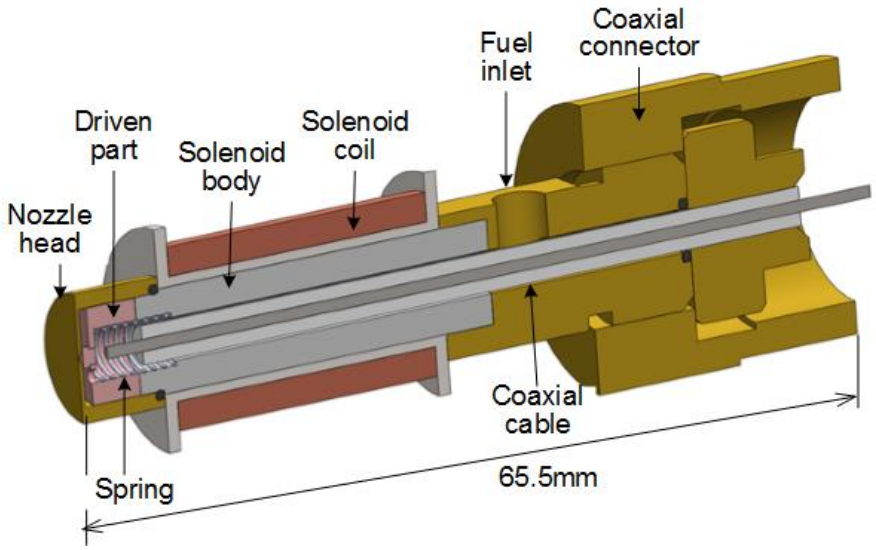

Figure 4.1 Schematic of LMI system.

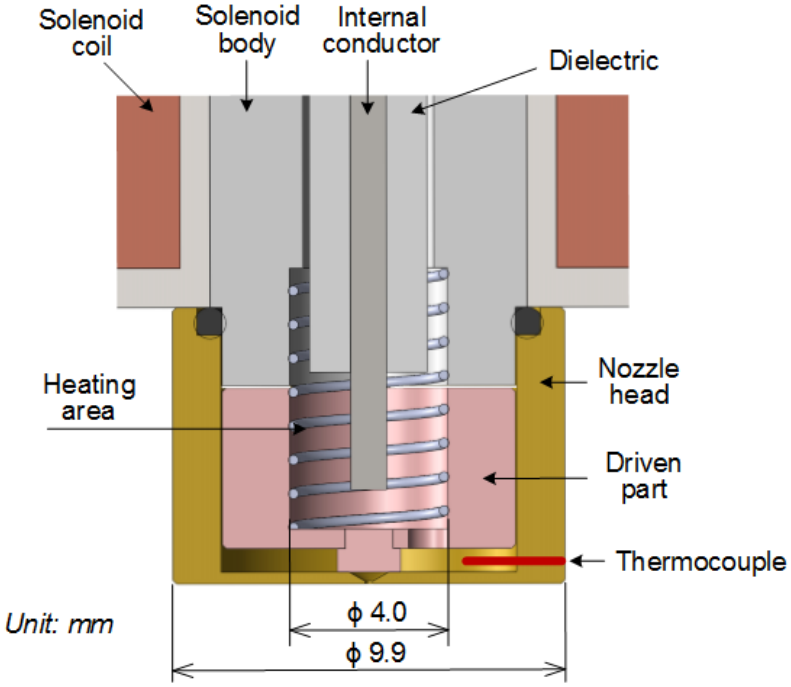

Figure 4. 2 Detail view of LMI injector head.

number, an oxygenated fuel and high latent heat of vaporization that can possibly run the engine with higher power output, better thermal efficiency and lower emissions [1], [2]. However, some properties of the fuel such as lower volumetric energy density, higher latent heat of vaporization and boiling point as well as high viscosity could be the main source problem especially for the cold start condition [3]. The vaporization of fuel must be good enough to ignite and burning faster in the combustion chamber for higher thermal efficiency and clean emissions of combustion engine.

Atomization, evaporation and combustion of the ethanol fuel are still remaining challenging for using its in engine applications. According to Anand et.al, [4] atomization process is complex and involves formation of multiple liquid jets especially in the low operating pressure spray. Injection strategies are necessary for ethanol fuel that has lower volumetric energy density 33% than in gasoline fuel [5]. Zhang, et.al., [6] investigated spray characteristics of gasoline, methanol and ethanol fuel using Mie scattering and Laser Induced Fluorescence. They analyzed effect of ambient pressure and fuel temperature on the distribution of liquid spray and found that high temperature of the fuel can improve spray atomization and distribution. However, atomization process of ethanol was a slightly slower due to the higher viscosity and lower vapor pressure. The raid vapor pressure of ethanol is 17kPa, whereas gasoline is 53.7kPa as in [2]. Therefore, the injection scheme should be improved to optimize the spray atomization and evaporation process.

Heating fuel flow inside the fuel injection system is one of the possible solution to improve the spray characteristics under engine cold-start conditions [7]. The temperature of the fuel or surrounding gas of the fuel sprayed should be increased to accelerate fuel distribution and vaporization. Pre-heating of fuel can reduce emission from internal combustion engine [8-9]. Several studies have been performed technical solution to increase temperature of fuel. Zajdel and Skorek [10] conducted experiment on heating the cylinder block engine and found the significant reduced on fuel consumption (up to 30%). Gumus [9] tryied to reduce cold-start emissions by heat the block engine, however, it was found that the physical challenging due to losses heating to several components and the efficiency was become lower. Another challenging way is directly heating fuel flow inside injector. Electrical heating was the popular heating way that aim to increase the temperature of injected fuel [11-12]. Aleiferis and Van-Romunde, [7] conducted experiment to investigate the spray characteristic of several bio-component fuels by heating fuel in injector and found that spray formation was sensitive to the fuel temperature.

More recently study, Enomoto and Iida [13] developed new model of heating fuel flow, mainly ethanol or ethanol-gasoline blended, inside injector. An in-house injector development was used to heat fuel flow using microwave heating. The main aim of this system is to add some energy equivalent to the fluid flow and this called Local-contact Microwave-heating Injector (LMI) system. Heating area was created inside head injector of LMI and connected to magnetron of microwave heating. Microwave energy can penetrate into material and produces volumetrically heat distribution due to molecular friction [14]. Polarization of electromagnetic wave in this system can increase fuel temperature rapidly and lead to reduce SMD of droplet sprayed even in the early injection starting [15]. This advantageous can offer the potential used of bio-ethanol fuel for cold start conditions.

The sensitivity of fuel temperature on the pray characteristic of fuel injection such as spray cone angle, droplet size, and spray tip penetration is the important phenomena and become main analysis in this study. Many researches have been discussed the fuel temperature effect on the atomization characteristic of fuel sprayed, however, there is no information so far regarding the spray analysis of fuel sprayed from LMI system. Spray characteristics of ethanol heated in LMI system was investigated and we focused on the effects of fuel temperature on the sprays structure and droplet behavior during injection. Temperature effect on the spray characteristic is supposed to be significant influencing the atomization and evaporation of ethanol fuel. It needs to be more accurate analysis and understanding about this phenomena between heated spray fuel and droplet distribution and dispersion.

In this study, analysis is focus on the images sprayed fuel captured by using high speed camera. High-magnification of images was produced with proper illuminating of incident light background from Halide Lamp. Images photos of the spray were processed and analyzed using post-processing images. The results of this analysis is expected to clearly describe the relationship between temperature and the spray distribution of ethanol fuel during injection.

4.3. Spray analysis

Spray of ethanol fuel was injected using single hole pressure nozzle of LMI injector with orifice diameter 0.3mm. The solid view of this injector can be seen in Fig.1. This injector, an in-house injector designed for special purposes, was operated at constant pressure 0.3MPa, a typical operating pressure for port fuel injection system. Fuel flow inside the injector was subjected to the microwave heating in the heating zone before injected into the room temperature. The

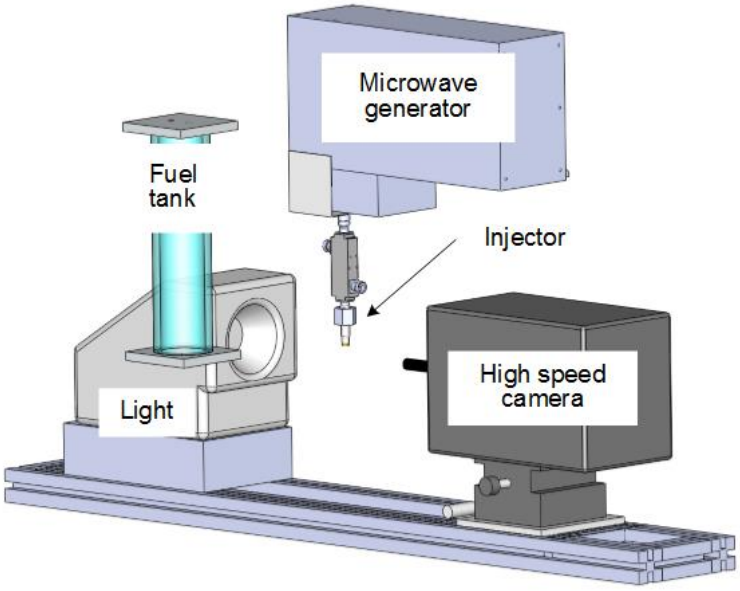

Figure 4. 3 Direct observation with high speed camera.

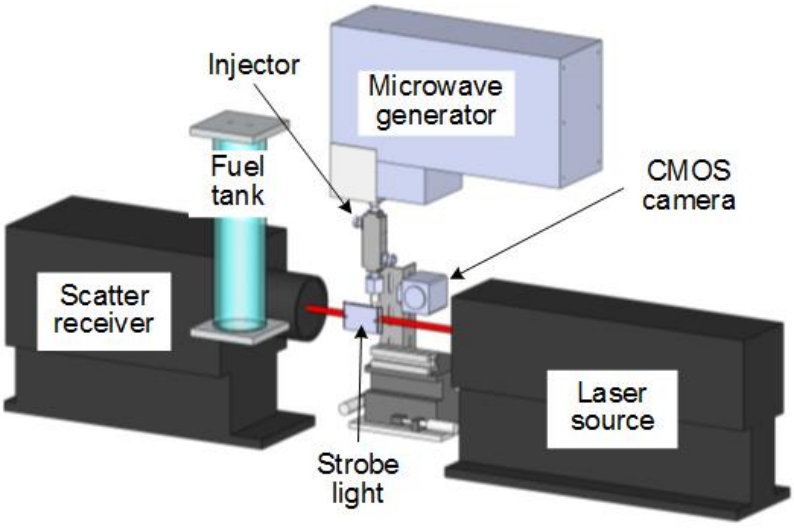

Figure 4. 4 Droplet size (SMD) measurement system.

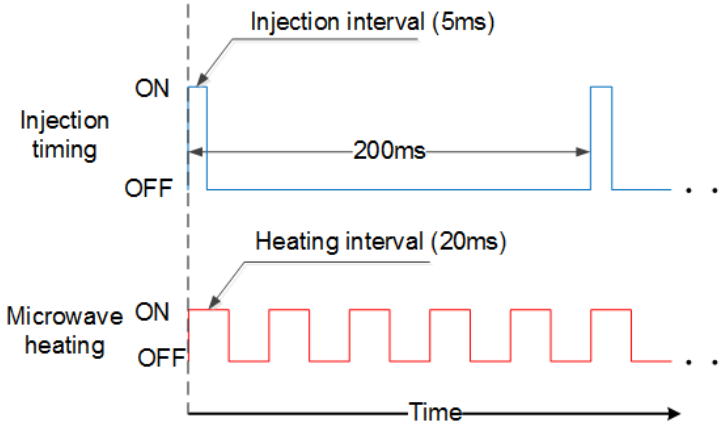

Figure 4. 5 Input signal controlling for injection and heating process.

Experimental study was conducted in a state of the art of measurement devices. Injector was mounted vertical to magnetron of the microwave generator and the schematic of this arrangement devices with imaging system and droplet size measurement can be seen in Fig. 3 and Fig. 4.

4.3.1. Fuel properties

The commercial grade of anhydrous ethanol (99.5% Ethanol) was used as the liquid fuel for the current study. Temperature of the fuel was around 293K, thermal condition of fuel during experiment. Table 4. 1 shows the typical properties of ethanol fuel compare with gasoline fuel. Composition of 100% ethanol was used in this study.

Table 4.1. Properties of ethanol compare with gasoline [22]

Property	**Ethanol**	**Gasoline**
Chemical formula	C_2H_5OH	Various
Oxygen content by mass (%)	34.8	0
Density (kg/L)	0.79	0.74
Research Octane Number	109	95
Stoichiometric Air-Fuel ratio	9	14.7
LHV (MJ/kg)	26.95	42.9
Boiling point(^{o}C)*)	78.4	25-215
Latent heat (kJ/kg)*)	904	380-500

*) Matsumoto et.al.[5]

4.3.2. Injector and heating zone geometries

A single hole of injector was developed for special purposes of studying the effect of microwave heating system on the vaporization of fuel. Schematic system of LMI system can be seen in Fig.1. The injector has orifice diameter D = 0.3mm and the heating zone has diameter around 4mm and 4mm in length. Heating created inside the tip injector aims to generated heating of fuel flow by using microwave heating scheme. This area is connected to the magnetron via coaxial cable as the passage of the electromagnetic wave. Cover of heating zone consists of metallic material that function as insulator for electromagnetic wave. Fuel flow inside the system experiences heating that generated by polarization of electromagnetic wave in ethanol fuel.

4.3.3. Experimental conditions.

The injector was designed special to operate at lower injection pressure (0.3MPa), the typical injection pressure for port fuel injection (PFI) engine. Electric power of 60Watt was imposing into the microwave heating generator that operated at constant frequency of 2.45GHz. By this frequency the electromagnetic wave can generate heating for ethanol flow. Control of

Table 4.2 Experimental condition

Conditions	Description
Fluid (Material)	Ethanol
Injection Pressure	0.3MPa
Fuel temperature	293K
Injection interval	5ms over 200ms (as 600rpm in engine speed)
Heating duration	20ms over 40ms
Power Input	60Watt

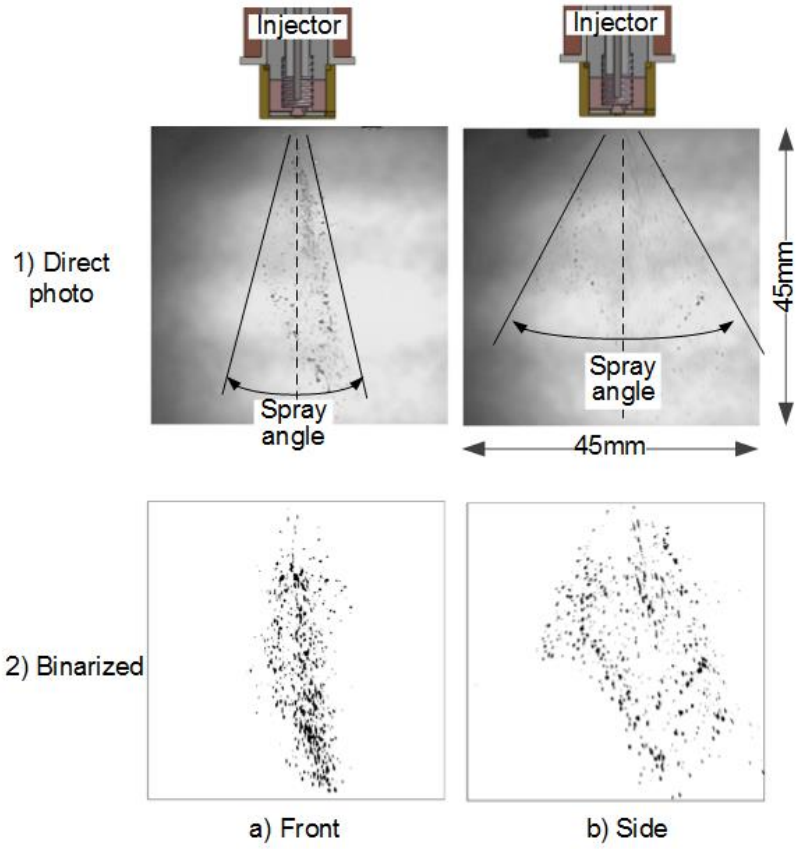

Figure 4. 6 Angle of view of the imaging system of fuel spray; a) is the front view of sprayed fuel and b) is the side view of spray, 90 degree from the front view.

heating and injection system was formulated in function generator to provide the proper temperature distribution of fuel flow inside heating area. The schematic of control system can be seen in Fig. 5. The injection control system was arranged based on the engine rotation of 600rpm at the normal operation. Heating control was adjusted for obtaining the proper temperature of the fuel generated inside heating area.

4.3.4. An imaging procedure and droplet sizing mechanism

In this paper, the results of spray distribution from both of measurement devices and images analysis were explored. Droplet size distribution of the sprayed fuel can be one of important characteristic between heated and non-heated fuel. Figure 6 shows the photograph of fuel sprayed at different view angle. Imaging system was assembled to show the spray characteristic of fuel under different heating scheme: heated spray and non-heated spray. Droplet distribution was measured using Laser Diffraction of Spray Analyzer (LDSA) at each injection duration. Laser scattering from He-Ne was used as an illuminating system for high quality images purposes. The centerline of measurement position was placed at 20mm from the tip of injector (Fig. 4). The device can measure the SMD and droplet size distribution of sprayed fuel. Droplet size is one of the most important characteristic of the spray [16].

Optical system of fuel spray was carried out using high speed camera (PHOTORON FASTCAM SA5). For the appropriate analyzing system, the high speed camera and a source light were synchronized at 1/30000 fps to produce imaging quality at 512x512 pixels. In order to optimize the imaging system the source light from metal halide lamp is coupled with the camera. The images captured in this system were analyzed in image processing software such as Image-J, Memrecam HXLink and Photoshop.

For the purposes of determining spray angle and droplet size analyzed, the threshold value was adjusted to distinguish between background noise and fuel spray. Two angle view of imaging recorded, front and side view, were taken in to account. The different spray angle on the different view is due to the small deformation of injector orifice during injection. Binarization of droplet sprayed was performed in Image-J to define area of circularity edges of the images thresholded. Droplet size of the spray was analyze base on the basic concept of Sauter Mean Diameter (SMD).

4.4. Result and analysis.

Spray characteristics of LMI Injector were investigated in order to understand the effect of fuel temperature on the spray structure. Direct measurement and images analysis results are presented in this paper. During injection of fuel, particle size and distribution formation of droplet sprayed was measured by LDSA. Spray characteristics were analyzed from the images captured with the high speed camera.

Direct measurement results of droplet distribution and droplet size can be seen in Fig. 7 and Fig. 8. It clearly shows that particle distribution of non heating fuel is bigger than that of heating fuel. In the Fig. 7 it can be seen that peak frequency of droplets distribution of non-heating fuel moves to the left side of heating fuel. This trend imply that particles size of heating fuel is smaller in heating than in non-heating fuel. In the preview study [15] the droplet size of

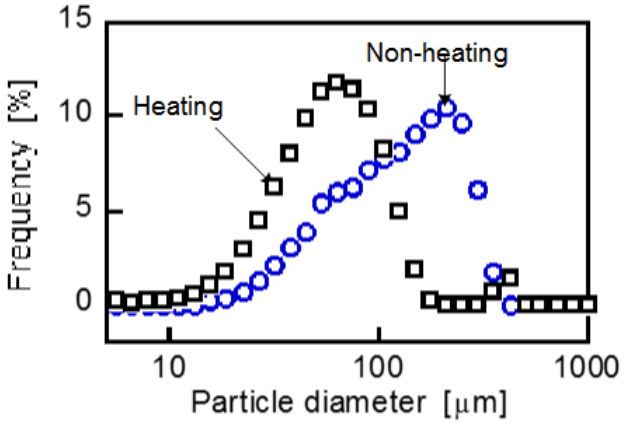

Figure 4. 7 Particle distribution of sprayed fuel.

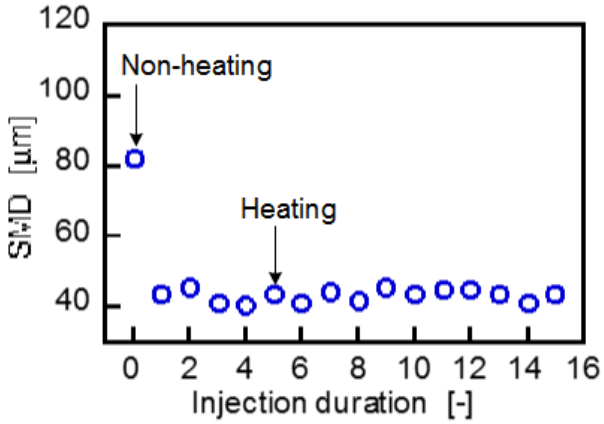

Figure 4. 8 Droplet size (SMD) of injection.

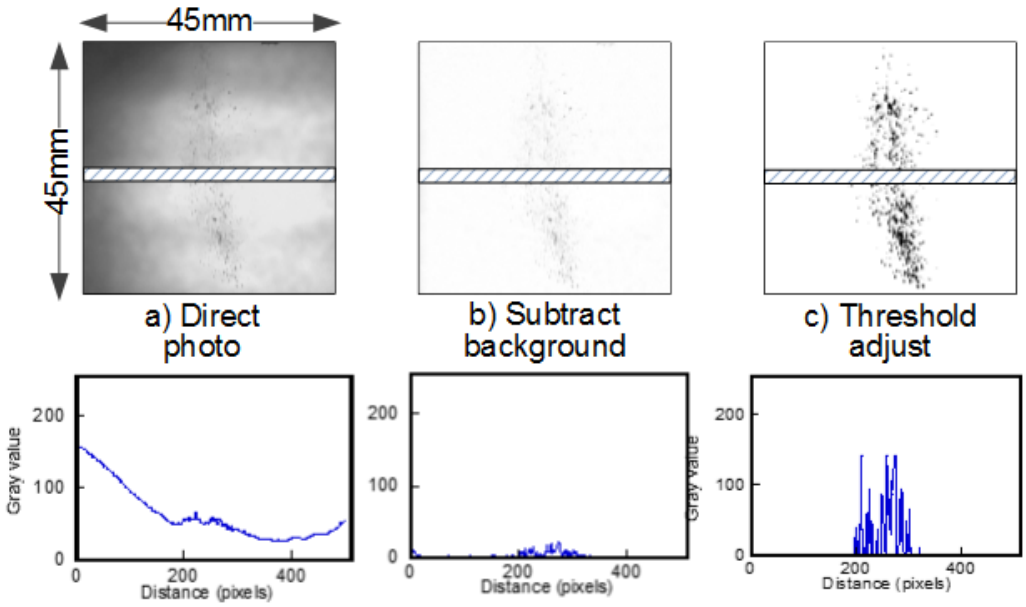

Figure 4. 9 Imaging analysis process steps

spray, expressed as SMD, was also reduced significantly in the heating fuel. The reduction of SMD in the early injection is due to the rapid increasing of fuel temperature after applying microwave heating into the fuel flow and this phenomena is expected to enhance vaporization rate of injected fuel into combustion chamber.

Instead of direct measurement analysis, the image analysis of fuel sprayed was also performed. Figure 9 show the description of binarization steps, an image processing, performed in the post image processing. Background noise of the images can be eliminated by subtracted the background and later the threshold value would be adjusted based on the mean of background pixels to leave a binary image. Subtracted background also makes the distance of background pixel become plate, thus, it can easily perform binarization of spray photos. Adjusting threshold number is critical for the droplet size analysis since it is related to the spatial area and diameter of droplets in the spray images.

Figure 10 compares the number of droplets and number of pixel in the black area of the three different threshold number. Black images of the thresholded pictures can show the liquid area where the droplets supposed to be existed. The differences in the spray formation between heating and non-heating fuel were quantified from the calculation of droplet number and droplet diameter (SMD). In all threshold adjustment it seems that heated spray of the fuel has significantly affected by temperature of fuel. However, it is not clear between injection timing and temperature effect. The images of spray cannot compare the spray pattern as same timing

injection. The penetration of the sprays is totally different between heating and non-heating spray.

SMD is the common parameter for expressing the fineness of spray in terms of surface area of the spray [17]. The sizing information is presented in form of Sauter mean diameters (SMD) and calculated using expression [17-18]:

$$SMD = \frac{\sum_{0}^{n} d_i^3}{\sum_{0}^{n} d_i^2} \quad (1)$$

Where d_i is the droplet diameter of fuel sprayed, n is the number of particle inside the spray. Figure 10 shows the distribution of SMD of injected fuel of the two different views. In the heating fuel spray, the frequency of smaller size droplets is higher than that in the non-heating spray. This indicates the finer droplet size can be produced by heating the fuel sprayed. High temperature fuel will reduce the surface tension and viscosity and leads to reduce the droplets size of the spray [19]. The quantitative measurement of liquid spray is based on the edge detection on the images. The size of edges detection in this analysis was later convert to the droplet size of the spray.

On this experimental study, the images was captured with high speed camera, however the quality of images produced still remain the unclear droplets structure due to the high speed moving of droplet. As the result, the edges of each droplet in the picture are unclear and the SMD of droplet became bigger Fig. 12. Further analysis on the imaging process is necessary. In image processing of injection, watersheld can help to divide areas of droplet spray. Watershed on the image processing is a way of automatically separation or cut the particles that are touched. This step is important to convert object overlapping in the images.

In order to deeply understand the watershelf effect on the images analysis, the waterseld steps on the images of several sprays was considered. Figure 13 can show the effect of watersheld process on the image structure of fuel spray. Fig. 14 shows the characteristic of this treatment in terms of SMD distributions. The bigger size of droplet in the image can be separated by waterseld into small droplet size and leads to reduce SMD of the spray.

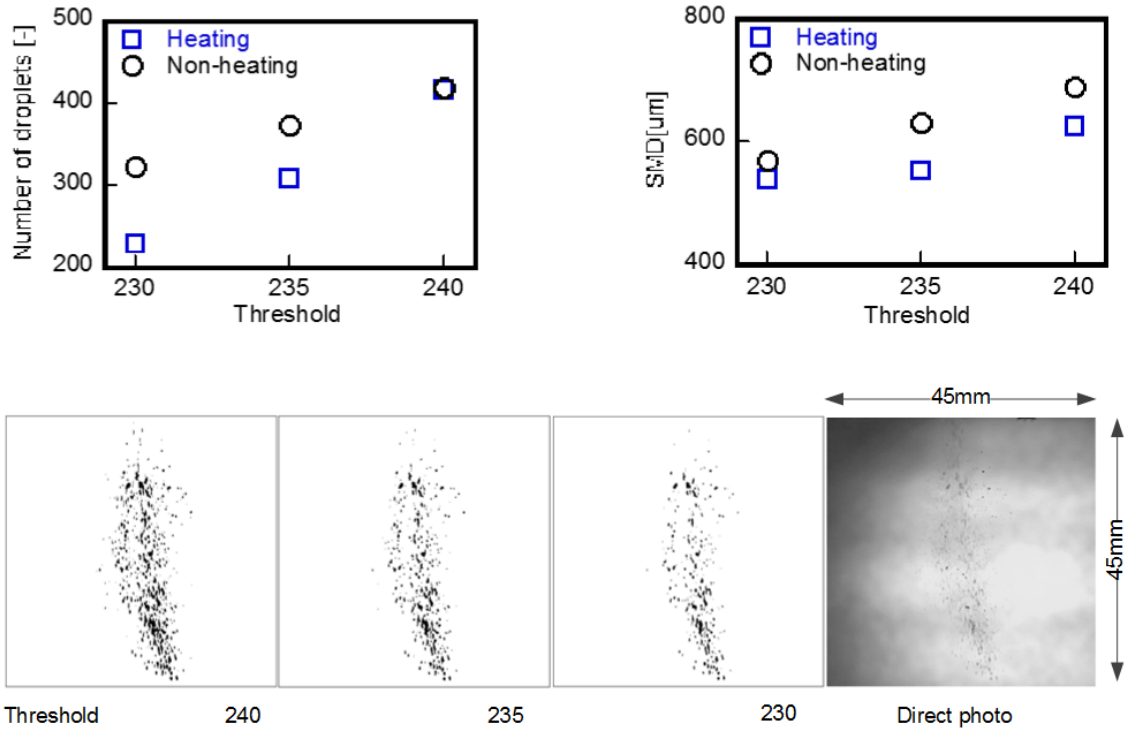

Figure 4. 10 Difference view of droplet images in the different threshold number.

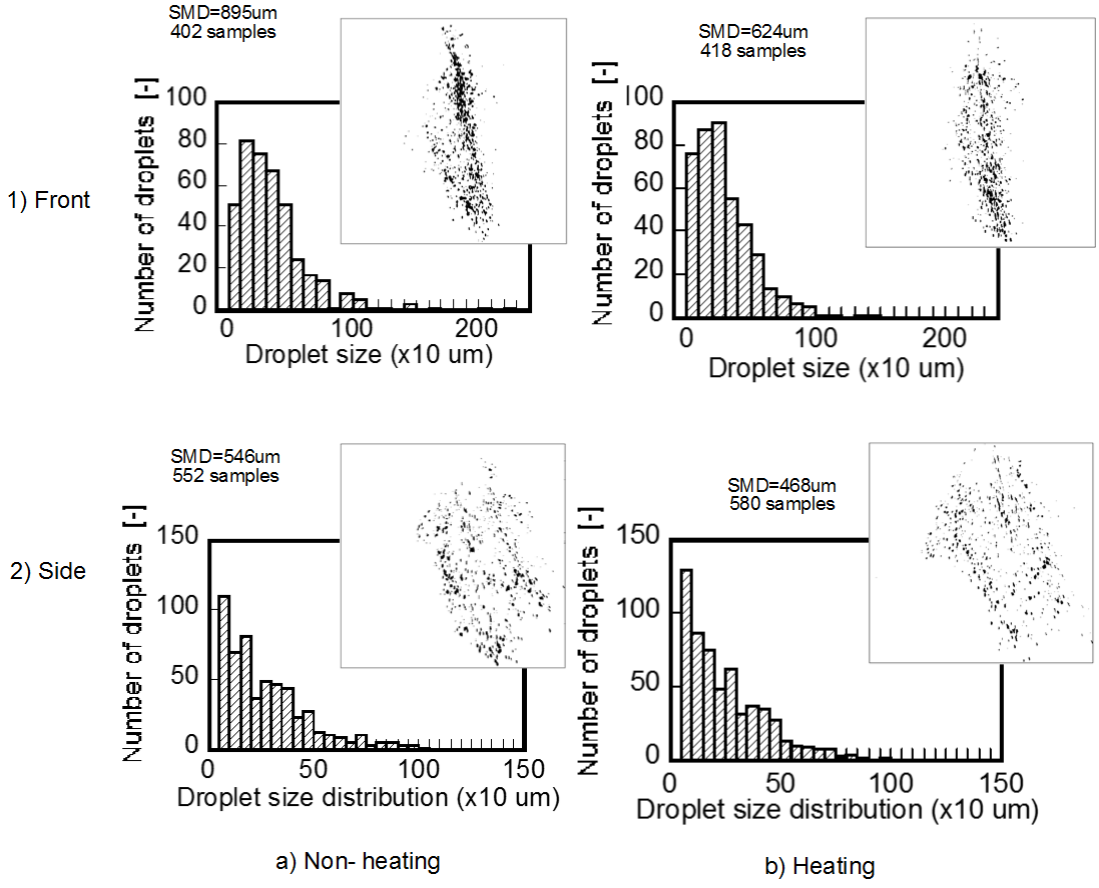

Figure 4. 11 Droplet size analysis of heating and non-heating spray.

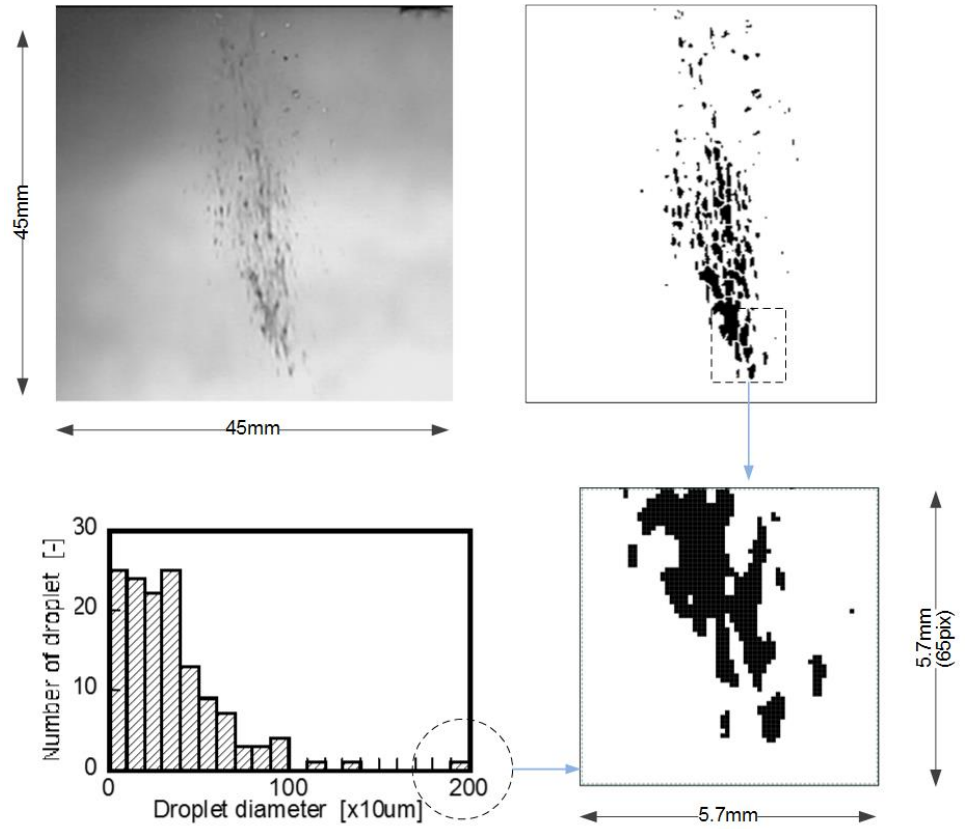

Figure 4. 12. Overlapping droplets in the images and the effect on the droplets size and distribution.

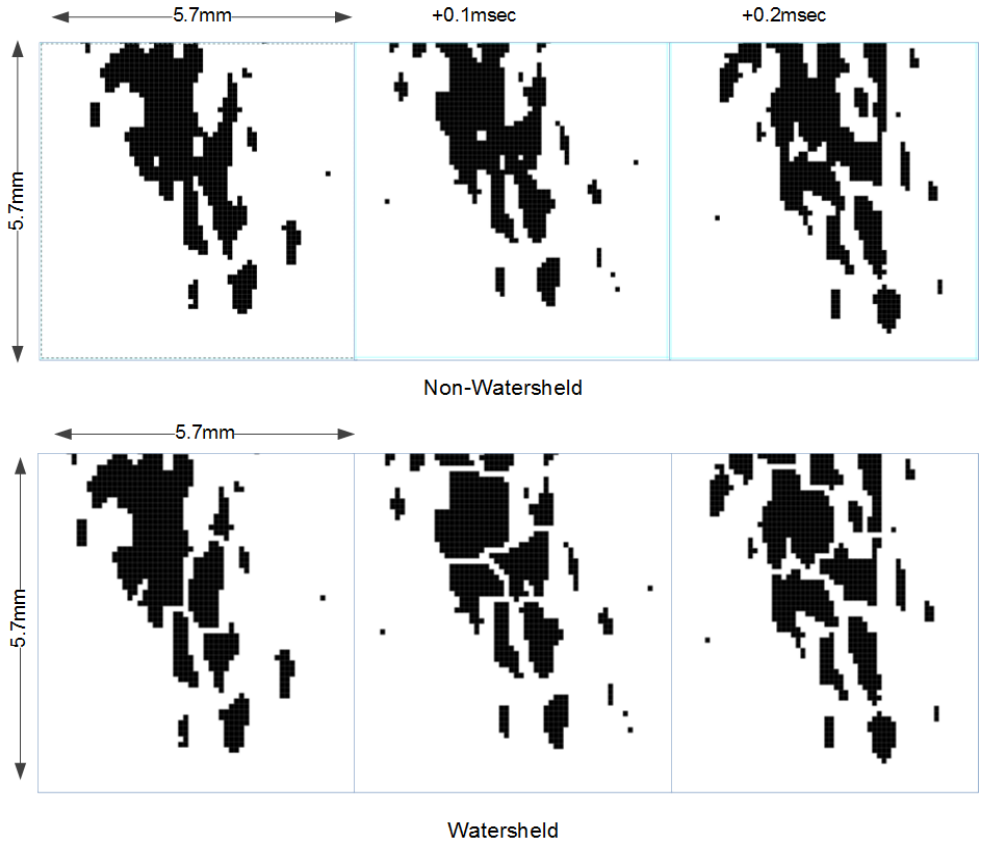

Figure 4. 13 Watersheld effect on the images structure of spray.

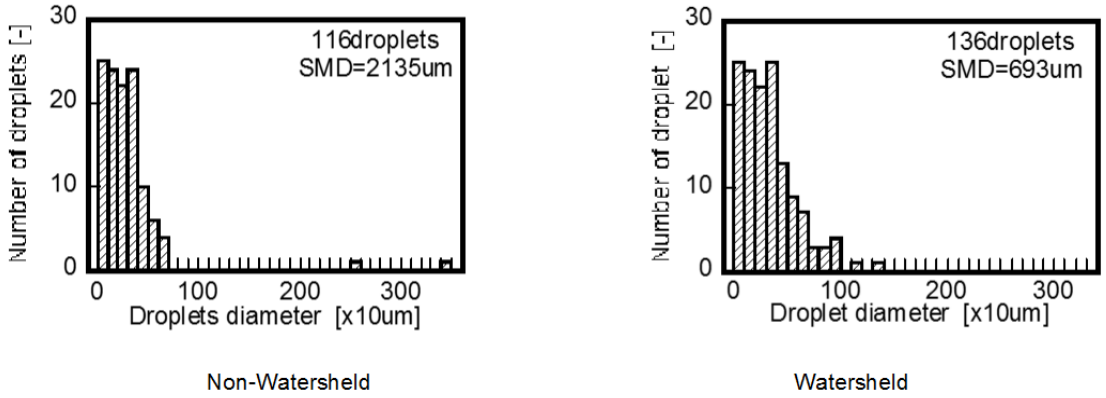

Figure4. 14 Watersheld effect on the droplet size of fuel spray.

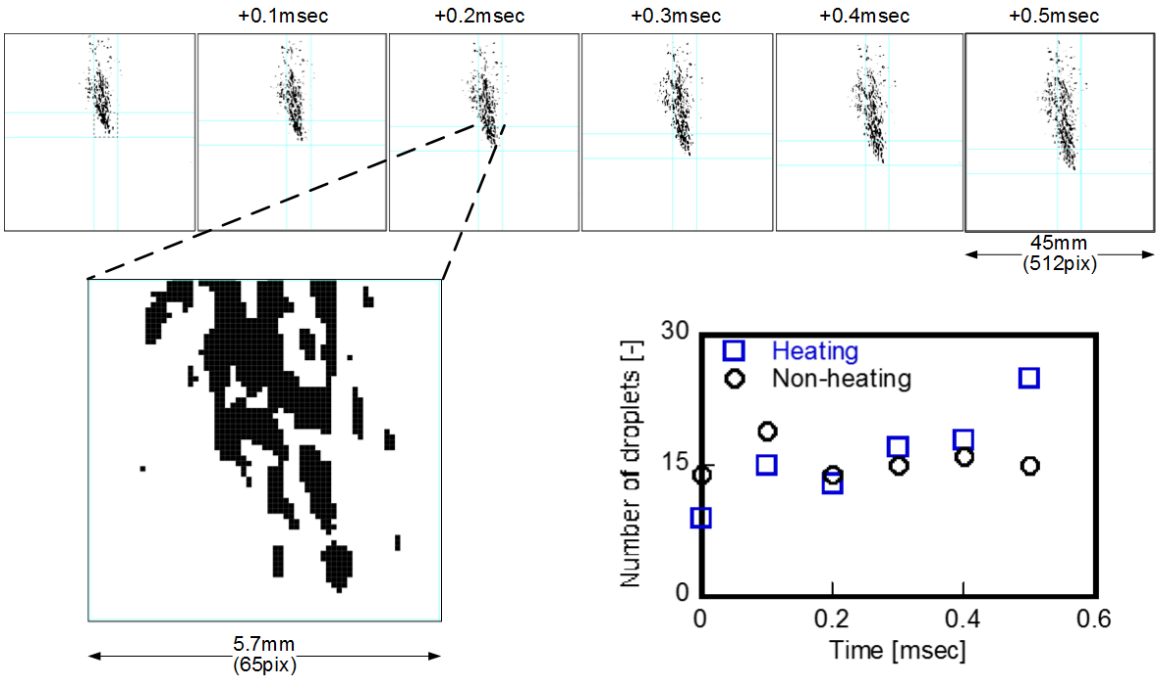

Figure 4. 15 Characteristic of sprayed droplets during the time of injection.

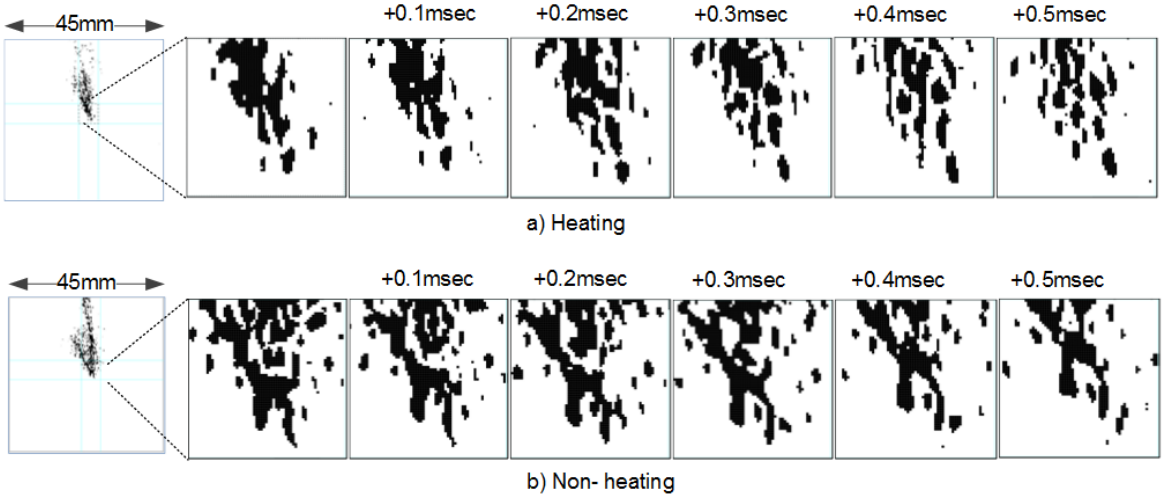

Figure 4. 16 Two different view of droplet structure in different time.

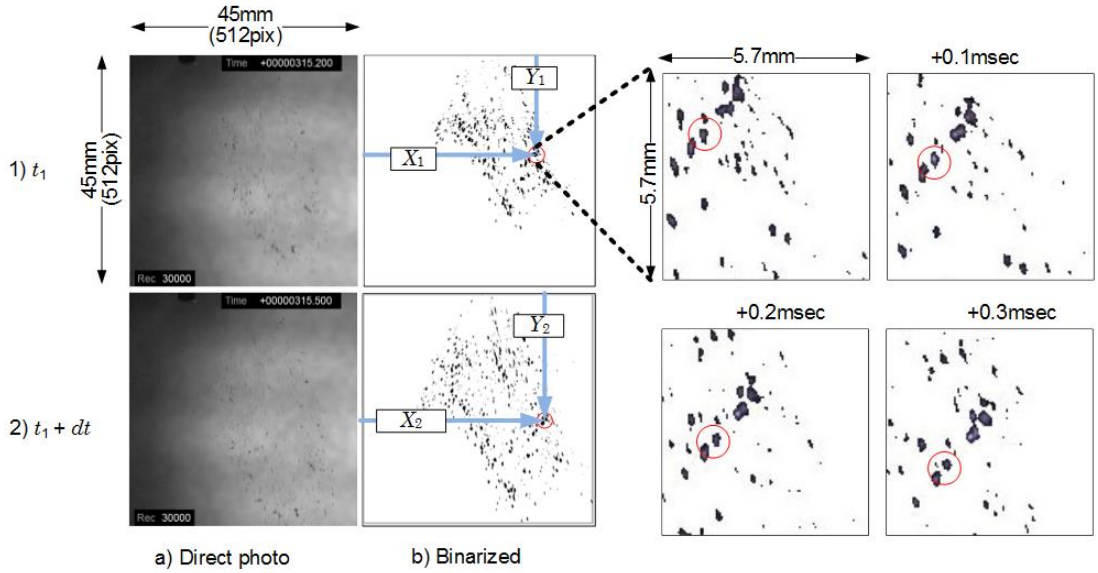

Figure 4. 17 Spatial and temporal of droplet position in the images.

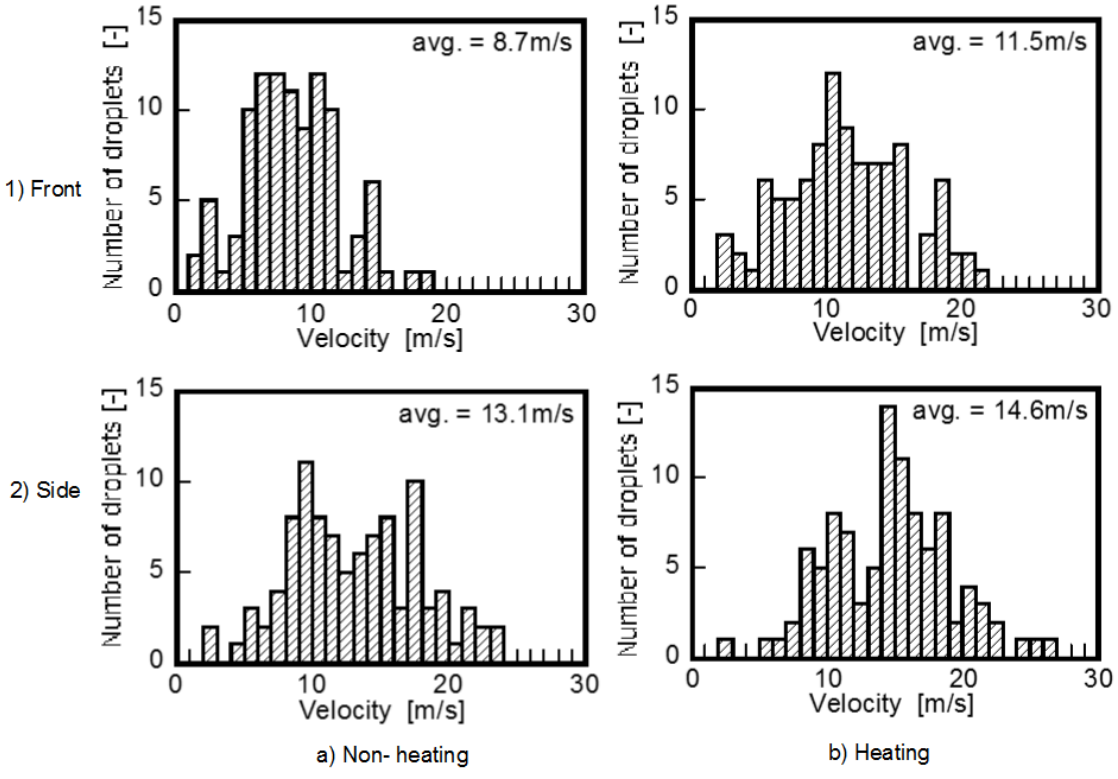

Figure 4.18 Velocity analysis of droplets.

Figure 15. and Fig. 16 show a series of zooming (puffing) photograph in the tip of ethanol fuel spray. This analysis is proposed to evaluate the liquid component in the spray dispersed into the small droplets. Thresholded images spray provide clear information of spray structure between heated and non-heated fuel during injection. In the heated spray, the liquid spray changes into the finer droplet in the short time which means the surface volume area became dispersion in to several parts. The liquid fuel of heated spray at the specific location was completely changed into small droplets component in around 0.5msec. Different characteristic of spray structure is showed in non-heated fuel. In the histogram analysis of droplets size in Fig.15, it clearly shows the trend of droplets distribution between heating and non-heating fuel. In the 0.5msec the number of droplets in the heating spray become higher than non-heating spray.

Spray characteristics of the fuel injection can also be affected by the jet inertia force, viscous force, air drag force and surface tension force [20]. Reynolds number and Weber number are the non-dimensional parameter that usually influence the spray structure. Changing of temperature of fuel sprayed can influence the Reynolds and Weber number parameters. Correlation between the fluid properties and velocity distribution of the spray is also considered in this study. This analysis aim to differentiate between droplet velocity of the heating and non-heating fuel flow. Figure 17 describes the droplet position in each time exposure of droplets spray. In this analysis the speed of droplets can be calculated from the images capture based on the frame information of the photos. Velocity of droplet was calculated using formula:

$$V = \sqrt{\frac{(Y_2 - Y_1)^2}{(X_2 - X_1)^2}} \frac{dis\tan ce}{pixel} pfs \qquad (2)$$

The images of spray consists of 512 pixel size with *pfs* is frame size of imaging system (1/30.000). X and Y are the spatial position of droplet analyzed in the spray image. Real distance of photos frame during experimental is 45 mm. In each image spray analyzed, we were chosen 100 droplets to be considered and analyzed. The same process analysis was performed in the two different views, front and side view.

Figure 18 shows the velocity distribution between heating and non- heating fuel at two different view of spray. The averages velocity of droplets indicate the different droplet velocity under heated and non-heated fuel. In the front view the average speed of non-heating droplets is 8.7m/sec whereas in the heating fuel is 11.5m/sec. Similar trend appears in the side view where the velocity of heating fuel is higher than that of non-heating fuel. In heating fuel the average velocity is 14.6m/sec whereas in non-heating fuel, the average velocity is 13.1m/sec.

This trends can explain the effect of temperature fuel on the droplet velocity. In the heated fuel the properties such as density and viscosity become changing and lead to change droplet velocity. The bigger the density the faster the droplets moves.

Fuel heating process is sensitive to the droplets position and size distributions [21]. For all images analyzed, strong correlation between heated fuel and number of droplets in the spray images is observed, which describes the important of heating effect on the atomization and vaporization of injected fuel. An increasing of fuel temperature can increase the droplets number in the sprayed structure. The increasing of temperature is also influence the droplets movement that is expected to improve atomization and evaporation of fuel during injected into combustion chamber of IC engine.

4.5. Conclusion

An optical analysis on the images of fuel sprayed from injector of LMI system was investigated. Heating effect on the droplet characteristics such as droplets size distribution and droplet velocity is the main focus in this study. According to the analysis results the following conclusion can be obtained:

- Heating system on LMI influenced the spray structure of bio-ethanol. Finer droplets was found in heated fuel sprayed which is expected to improve evaporation during injection.
- The average velocity of fuel droplets was also affected by the temperature of the fuel. Heated droplets fuel move faster than non-heated droplets.
- Image analysis results imply the important of heating system on the droplet dispersion and velocity of ethanol fuel.

References

(1) Zervas, E., Montagne, X. and Lahaye, J., The Influence of Gasoline Formulation on Specific Pollutant Emissions, Journal of the Air Management Association, 49:11, 1999, pp.1304-1314.

(2) Chen, R.H., Chiang, L.B., Chen, C.N., and Lin, T.H., Cold-start Emissions of An SI Engine Using Ethanol-Gasoline Blended Fuel, Applied Thermal Engineering, 31, 2011, pp. 1463- 1467.

(3) Aleiferis, P.G., Pereira, J.S., van Romunde, Z., Caine, J., and Wirth, M., Mechanisms of spray formation and combustion from a multi-hole injector with E-85 and Gasoline, Combustion and Flame, 157, 2010, pp.735-756.

(4) Anand, T.N.C., Mohan, A.M., Ravikhrisna, R.V., Spray Characteristic of Gasoline-Ethanol Blends from a Multihole Port Fuel Injector, Fuel, 102, 2012, pp. 613-623.

(5) Matsumoto, A., Moore, W.R., Lai, M., Sheng, Y., Foster, M., Xie, X, Yen, D., Confer, K., and Hopkins, E., Spray Characterization of Ethanol Gasoline Blends and Comparison to a CFD Model for a Gasoline Direct Injector, SAE International 2010-01-0601, 2010.

(6) Zhang, M., Xu, M., Zeng, W., Zhang, G., Zhang, Y., Cleary, D.J., Characterization of Methanol and Ethanol Sprays Using Mie-Scattering and Laser Induced Fluorescence Under Engine Cold-start Conditions, The 13th Annual Conference on Liquid Atomization and Spray System-Asia, 2009.

(7) Aleiferis, P.G., and van Romunde, Z.R.,: An Analysis of Spray Development with Iso-octane, n-pentane, Gasoline, Ethanol and n-butanol from a Multi-hole Injector under Hot Fuel Conditions, *Fuel* ,**105**, 2013, pp. 143-168.

(8) Vasiliev, L.L., Burak, V.S., Kulakov, A.G., Mishkinis, D.A. and Bohan, P.V., Heat Storage Device for Pre-heating Internal Combustion Engines at Start-up, International Journal of Thermal Science, 38, 1999, pp. 98–104.

(9) Gumus, M., Reducing Cold-Start Emission from Internal Combustion Engines by Means of Thermal Energy Storage System, Applied Thermal Engineering, 29, 2000, pp. 652-660.

(10) Zajdel. A., and Skorek, J., Evaluation of The Influence of Liquid Fuel Atomization on Fuel Consumption During Heating of Solids in A Furnace, Energy, 26, 2001, pp. 1135-1144.

(11) Kabasin, D. , Hoyer, K., Kazour, J., Lamers, R. and Hurter, T., Heated Injector for Ethanol Cold Starts, SAE International, 2009-01-0615, 2009.

(12) Aleiferis, P.G., Pereira, J.S., Augoye, A., Davies, T.J., Cracknell R.F. and Richardson, D., Effect of fuel Temperature on In-nozzle Cavitation and Spray Formation of Liquid Hydrocarbons and Alcohols from a Real-size Optical Injector for Direct Injection Spark Ignition Engine, Int. Journal of Heat and Mass Transfer, 53, 2010, pp.4588-4608.

(13) Enomoto H. and Iida T., Effect of Microwave Heating on the Spray Droplet Size Distribution by Using Local -contact Microwave-hating Injectors, JSAE Paper 40**,** 3, 2009, pp.769 – 774.

(14) Oliveira M.E. and Franca A.S., Microwave Heating of Food Stuffs, Journal of Food Engineering, 53, 2002. Pp.347–359.

(15) Mangalla, L.K. and Enomoto, H., Spray Characteristics of Local-contact Microwave-heating Injector Fuelled with Ethanol," SAE Technical Paper 2013-32-9126, 2013.

(16) Padala, S., Le, M.K., Kook S., and Hawkes, E.R., Imaging Diagnostics of Ethanol Port Fuel Injection Sprays for Automobile Engine Applications, Applied Thermal Engineering, 52, 2013, pp. 24-37.

(17) Li, G., Cao, J., Li M., Quan, Y. and Chen, Z., Experimental Study on The Size Distribution Characteristics of Spray Droplets of DME/Diesel Blended Fuel, Fuel Processing Technology, 104, 2012, pp. 352-355.

(18) Mishra, Y.N., Kristensson E. and Berrocal, E., Reliable LIF/Mie Droplet Sizing in Spray Using Structure Laser Illumination Planar Imaging, Journal of Optics Express, 22: 4, 2014, pp.4480-4492.

(19) Vicente, J. Pinto, J., Menezes J. and Gaspar, F., Fundamental Analysis of Particle Formation in Spray Drying, Powder Technology, 247, 2013, pp.1-7.

(20) Zeng, W., Xu, M., Zhang, M., Zhang, Y., and Cleary, D.J., Macroscopic Characteristics for Direct-Injection Multi-hole Sprays Using Dimensionless Analysis, Experimental Thermal and Fluid Science, 40, 2012, pp. 81-92.

(21) Sazhin, S.S., Kristyadi, T., Abdelghaffa, W.A. and Heikal, M.R., Models for Fuel Droplet Heating and Evaporation: Comparative Analysis, Fuel, 85, 2006, pp.1613–30.

(22) Vancoillie J., Demuynck J., Sileghen L., Van De Ginste M., Verhelst S., Brabant L, and Van Hoorebeke L. The Potential of Methanol as a Fuel for Flex-Fuel and Spark-Ignition Engine, Applied Energy 2013; 102; 140-49.

Chapter 5

Spray Characteristics of Local-contact Microwave-heating Injector Fueled with Ethanol.

5.1. Abstract

A microwave-heating system is integrated inside port-injector to minimize the cold-start problems and exhaust emissions of engine. A novel system called local-contact microwave-heating injector (LMI) is developed to add electromagnetic energy into the fuel flow inside injector for enhancing atomization and evaporation of fuel. This paper reported the experimental investigations of spray characteristics and numerical simulation of fuel temperature inside tip of injector. Experimental investigation showed that LMI can increase temperature of ethanol near boiling point (351.5K) before injected. Characteristics of fuel spray were observed using high speed camera, CMOS camera and LDSA. Numerical simulation was conducted to verify fuel temperature and its effect on spray distribution. 2-D geometry of domain simulation with finer quadrilateral mesh (56,000 meshes) was solved in ANSYS Fluent. Conservation equations of mass, momentum and energy were modelled on time dependent using Pressure-Implicit with Splitting of Operation (PISO) algorithm in pressure based solver. The result shows good agreement between numerical and experimental measurement of temperature distribution at tip injector. An increasing of fuel temperature inside port injector is considerably reducing Sauter Mean Diameter (SMD) of ethanol spray. Pre-heating fuel system by LMI can improve spray quality and leads to possibly being used at port injection engine.

Key words: LMI system, Spray characteristics, SMD and Evaporation

5.2. Introduction

An increasing global concern on air pollution and limited of oil reserves have been turned intentions on the environmentally friendly fuels. Internal combustion engines mainly use fossil fuel to generate power for many applications. However, combustion system of this fuel produce several gas emissions that are extremely harmful for environment and human health. Aiming at improving combustion efficiency and exhaust emissions, the development of new highly efficient combustion system especially for alternative fuel is very important.

Energy alternative like ethanol has tremendous popularity recently in several countries in respect to the clean combustion system and sustainability of this fuel. Comparing the properties with gasoline, ethanol has high octane number which makes excellent gasoline blending component in several combustion applications. The high octane number helps to run vehicles more smooth, knocking resistance and high compression ratio. However, ethanol has higher heat of vaporization and lower calorific value. Those properties lead to not only poor vaporization in intake manifold but also wall-wetting problem during operation [1]. Advance research on this fuel have to develop to exploring bio-ethanol fuel for combustion system.

The new concept of fuel supply system have to optimize the constituent of the fuel-air mixing inside cylinder for automobile engine. Fuel injection system plays a significant role on atomization and vaporization of injected fuel especially for ethanol application in gasoline port injection (GPI) engine which has very low injection pressure (typically 0.25-0.45Mpa) [2]. Injection development should be consider for fuel that has high boiling temperature, lower energy density and lack of volatility. In spark ignition engine, atomization and vaporization quality influences the mixture of fuel and air. Improving on vaporization rate has directly affected combustion performances and engine-out emissions. Therefore, an ideal fuel distribution is required to accelerate the mixing preparation in combustion chamber [3].

An increasing temperature of fuel before injected is critical for improving spray characteristic especially for bio-fuels which mainly have high viscosity and low calorific value. Preheating of fuel flow is expected to change the fuel properties and enhances mixing quality of fuel and air. This treatment leads to improve thermal efficiency of combustion and reduce exhaust emission. The increasing of fuel temperature can also help to accelerate fuel vaporization during start injection at cold start condition [4]. Physical and chemical properties of the fuel are important characteristic related to atomization and evaporation during injection. Improving thermal properties of fuel can be done throughout heating process that can make the fuel easily evaporated.

Several studies tried to improve fuel vaporization by heated block cylinder of engine or directly heated fuel inside injector [5-7] , however, the efficiency was not significant due to several losses and many others challenging conditions. However, research and development on this field are interested for several researchers in engine advancement. In contrast with electric heating, Enomoto and Iida [8] were developed fuel injection system that using microwave heating as heating source and this system called Local-contact Microwave-heating Injector (LMI). In this system, fuel flow in the port injector is heated by microwave heating generator

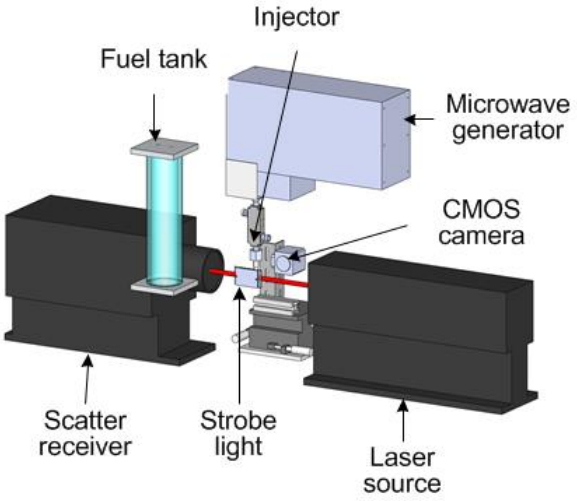

(a) SMD measurement with Laser scattering and direct photo with strobe.

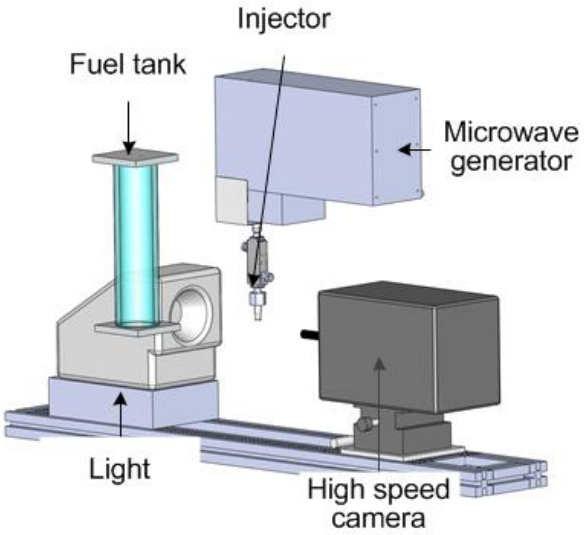

(b) Direct observation with high speed camera.

Figure 5.1. Unit measurement system.

that connected to the coaxial cable inside injector. More recently study, Tran et al. [9] developed a new model on predicting the droplet diameter of gasoline-ethanol fuel blended using LMI system. Their analysis was focus on the effect of fuel heating short time before injected on the spray characteristics and the performance of the LMI system on generate heating

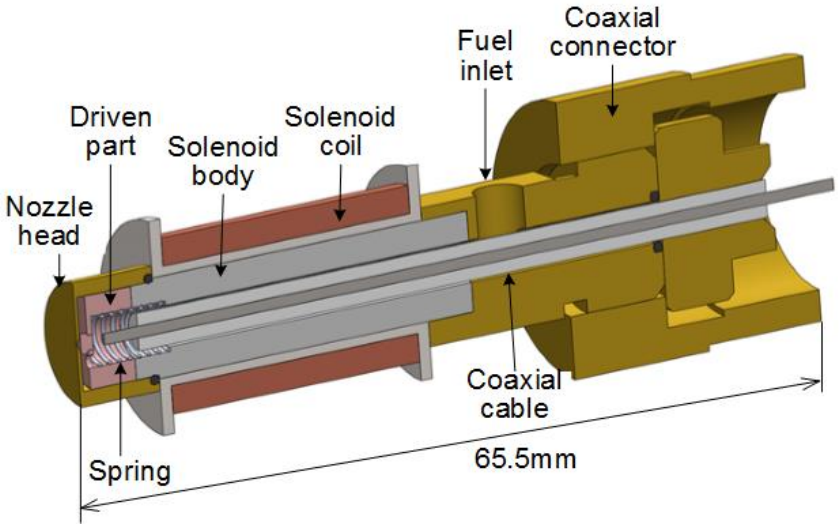

Figure 5. 2. LMI structure.

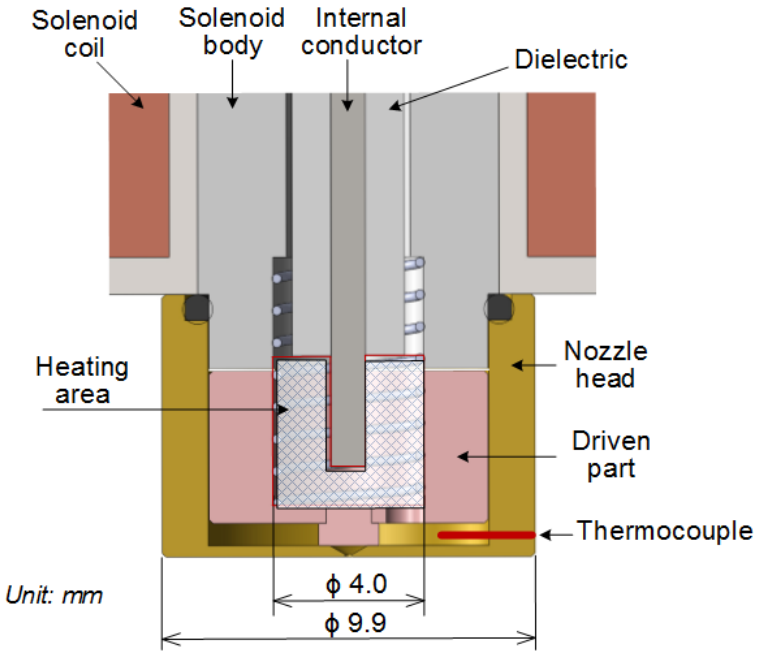

Figure 5. 3. Details of LMI head.

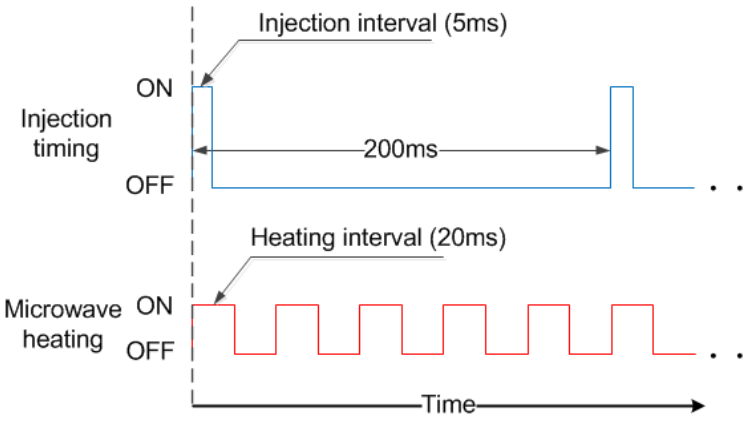

Figure 5.4. Control schematic for heating and injection.

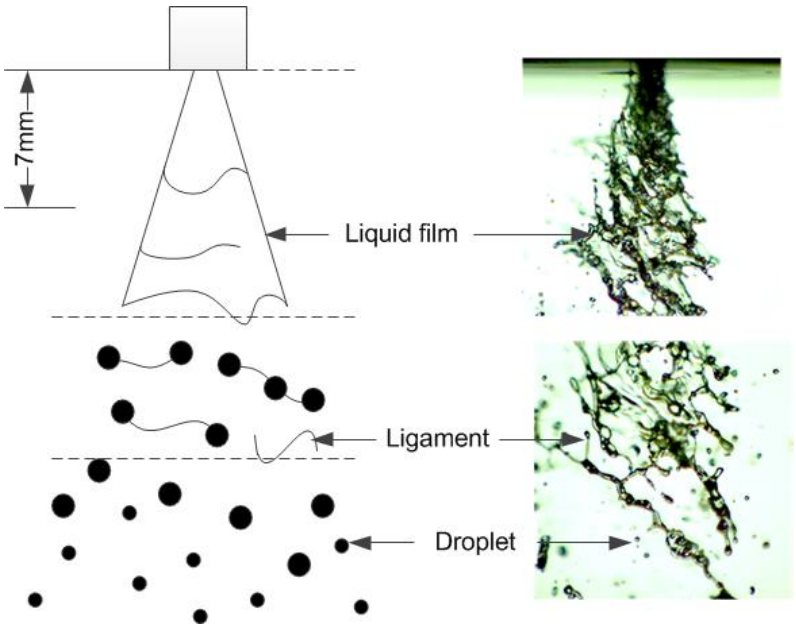

Figure 5.5. Measurement position.

for fuel flow inside injector. Spray characteristics such as droplet diameter SMD, spray angle and spray length from injector were analyzed and concluded that the droplets diameter decreased with the increased of the local temperature of fuel inside the injector.

It is generally understand that atomization quality of fuel spray can be affected by fuel properties, as well as injector geometry, angular velocity inside the injector and injection pressure. Perfect quality of fuel spray is recently expected for high performance combustion and low exhaust emissions of internal combustion engine especially for bio-fuel that become most attractive fuel in the recent year. This paper describes the effect of fuel pre-heating inside port-injector on the spray characteristics of ethanol fuel.

Parallel to experimental investigations, simulation study was used to simulate heat transfer phenomena inside heating area of injector. Conservation of mass, momentum and energy was solved using finite volume method in ANSYS Fluent. Result of this simulation would be validated with direct measurement of fuel temperature at tip of injector.

5.3. Methodology

The effect of an increasing fuel temperature in port-injector on the spray characteristic of ethanol fuel was examined in this study. Microwave heating was used to generate heating of fuel flow inside heating area of injector. LMI system has been develop in-house to investigate the effect of pre-heating fuel inside injector on spray characteristics. Heating supply from microwave-heating aims to add energy equivalent on fuel flow for easily evaporation during injection. Microwave heating contains a magnetron to produce wavelength radiation at the frequency of 2450MHz. The magnetron is connected to the coaxial cable inside injector to generate microwave radiation that convert magnetic and electrical current into heat inside heating area of LMI. In this way the fluid flow inside injector undergoes heat exchange before injected. Heating area of LMI is located inside the injector head with volume size around 200mm^3 (Fig.5.3). This heating process is expected to influence the atomization process short time after injected into combustion chamber. The working fluid is ethanol fuel with 99.9% ethanol (anhydrous ethanol).

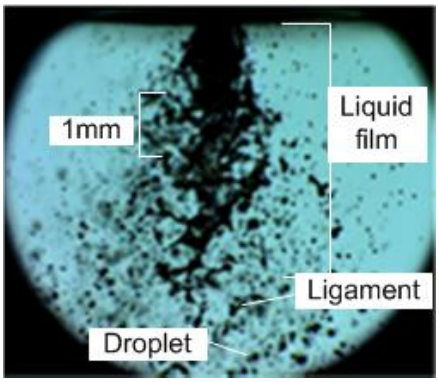

Figure 5.6. Spray components.

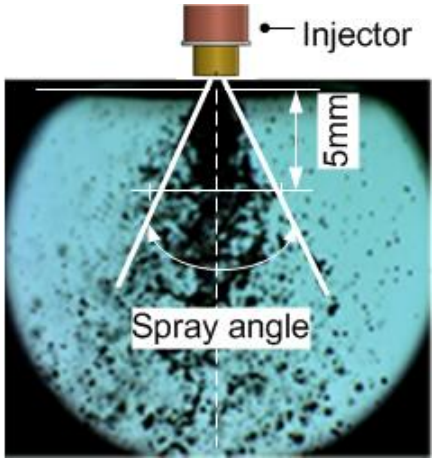

Figure 5.7. Definition of spray angle.

Most of the measurement components were controlled simultaneously for the appropriate injection and heating system. Unit measurements also organized in function generator for optimum result of spray imaging and measurement. Figure 5. 1 shows the experimental apparatus of the system. The element of measurement consists of adjustable injector, control unit and unit measurements. Unit measurements consist of Laser Diffraction Spray Analyzer (LDSA) and CMOS camera (Fig. 5. 1a) and high speed camera (Fig. 5. 1b). Spray characteristics of SMD was measured by LDSA. Spray components such as ligaments, droplets and spray angle were measured by high speed camera while the photographs of fuel spray with high speed of movement were determined by CMOS camera. In order to provide the illuminating system for high quality images, strobe light from He-Ne was used for LDSA and metal halide lamp was used for high speed camera and CMOS camera.

Figure 5. 2 displays the structure of injector using for this experiment. The injector is produce for experimental purpose with dimension 65.5mm in length and 0.3mm of nozzle hole. Fuel flow inside port injector was transported from fuel tank by means of high pressure of fuel pump. Experimental condition of this study can be seen in Table 1. Operating pressure of fluid flow was fixed at 0.3MPa and it is same as the well-known of operating pressure for fuel port injection (FPI) engine. Figure 5. 3 shows the components of injector head and the size of heating area of LMI system. Heating area is located near the tip of injector to minimize the heating loss through the injector body. The amount of fuel sprayed from nozzle is regulated by the movement of driven part which controlled by magnetic force from solenoid coil.

Injection duration of fuel as well as heating interval time were controlled simultaneously for this level of testing. Function generator was installed as a control system for appropriate condition fuel heating and spray (Fig. 5. 4). Heating time was fixed at 20ms per 40ms while injection cycle was setting 200ms. Injection interval in each cycle was setting at 5ms. The electric power impose to the microwave heating is constant at 60W. Respond of signal used the LMI system for heating and injection is easily controlled during experiment.

Droplet size from ethanol spraying was recorded and measured at some specific locations along the axis of injector (Fig. 5. 5). The imaging photos of fuel spray characteristic were recorded at certain location (in each 7mm from the injector tip) by CMOS camera and high speed camera for spray components. The images of the spray were later analyzed to observe the spray component of fluid fuel. Spray distribution of droplets was recorded by LDSA at specific location from injector tip. All photos imaging were processed using post-processing image software.

The macroscopic behaviors of the injector spray, such as spray image, spray penetration, and spray cone angle, were determined from the image obtained at various time after start of injection. Figure 6 shows the component of liquid spray from injector such as liquid film, ligaments, and droplets. Figure 5. 7 demonstrates the measurement position of spray angle of injection which measured at 5mm under the tip injector using CMOS camera.

Temperature of fuel flow inside the nozzle hole was measured at injector tip using K-Type thermocouple. This device was connected to data logger for recording and analyzing of temperature effect on fuel spray during experiment.

Table 3.1. Experimental conditions

Description	Unit value
Injection pressure	0.3MPa
Injection interval	5ms
Injection cycle	200msec (as 600 rpm in engine speed
Heating duration	20ms per 40ms
Fuel temperature	280K
Ambient Temperature	280K

5.4.Numerical simulation

Modeling of fuel flow characteristics concerning the heating process inside the port-injector is finalized to obtain data base result. The operating conditions applied in this simulation are based on experimental conditions with respect to the optimal result in spray characteristics. The injector model was simplified to obtain cost-effective solution in CFD simulation. Two dimensional (2D) geometry of injector tip is using as the computational domain for this study (Fig.5. 8).

5.4.1. Governing equations.

In this simulation the following Navier-Stokes equations of fluid flow were used.

- Mass conservation

$$\frac{\partial \rho}{\partial t} + \nabla \cdot (\rho V) = S_m \tag{1}$$

Where S_m is the mass added to the continuous phase from dispersed phase and any other user defined sources. However in this simulation this mass is negligible.

For 2D axisymmetric geometry, the continue equation become.

$$\frac{\partial \rho}{\partial t} + \frac{\partial}{\partial x}(\rho V_x) + \frac{\partial}{\partial r}(\rho V_r) + \frac{\rho V_r}{r} = S_m \tag{2}$$

Where x is the axial coordinate, r is the radial coordinate, Vx is the axial velocity and Vr is the radial velocity.

- Momentum conservation

$$\frac{\partial}{\partial t}(\rho V) + \nabla \cdot (\rho V V) = -\nabla p + \nabla \cdot (\tau) + \rho g + F \tag{3}$$

Where p is the static pressure, τ is the stress tensor, ρg is gravitational force, and F is the external body force that contain dependent source term such as porous media and user defined sources.

The stress tensor (τ) is given by

$$\tau = \mu \left[\left(\nabla V + \nabla V^T \right) - \frac{2}{3} \nabla \cdot V I \right] \tag{4}$$

Where μ is the molecular viscosity, I is the unit tensor.

For 2D axisymmetric geometry, the axial and radial momentum conservation equation are given by the following equations.

$$\frac{\partial}{\partial t}(\rho V_x)+\frac{1}{r}\frac{\partial}{\partial x}(r\rho V_x V_x)+\frac{1}{r}\frac{\partial}{\partial r}(r\rho V_r V_x)=-\frac{\partial p}{\partial x}+\frac{1}{r}\frac{\partial}{\partial x}\left[r\mu\left(2\frac{\partial V_x}{\partial x}-\frac{2}{3}(\nabla\cdot V)\right)\right]$$
$$+\frac{1}{r}\frac{\partial}{\partial r}\left[r\mu\left(\frac{\partial V_x}{\partial r}+\frac{\partial V_r}{\partial x}\right)\right]+F_x \quad (5)$$

and

$$\frac{\partial}{\partial t}(\rho V_r)+\frac{1}{r}\frac{\partial}{\partial x}(r\rho V_x V_r)+\frac{1}{r}\frac{\partial}{\partial r}(r\rho V_r V_r)=-\frac{\partial p}{\partial r}+\frac{1}{r}\frac{\partial}{\partial x}\left[r\mu\left(\frac{\partial V_r}{\partial x}+\frac{\partial V_x}{\partial r}\right)\right]$$
$$+\frac{1}{r}\frac{\partial}{\partial r}\left[r\mu\left(2\frac{\partial V_r}{\partial r}-\frac{2}{3}(\nabla\cdot V)\right)\right]-2\mu\frac{V_r}{r^2}+\frac{2}{3}\frac{\mu}{r}(\nabla\cdot V)+\rho\frac{V_z^2}{r}+F_r \quad (6)$$

Where $$\nabla\cdot V=\frac{\partial V_x}{\partial x}+\frac{\partial V_r}{\partial r}+\frac{V_r}{r} \quad (7)$$

- Energy conservation can be expressed as following equation.

$$\frac{\partial}{\partial t}(\rho E)+\nabla\cdot(V(\rho E+p))=-\nabla(\sum h_j J_j)+S_h \quad (8)$$

5.4.2. Initial and boundary conditions.

In the simulation study, the initial temperature of ethanol is assumed same condition as the environment temperature at the experimental condition. Temperature of ambient is 280K. Inlet velocity of 0.1m/s is applied in the inlet boundary condition to supply fuel into the heating area. In the outlet flow outlet pressure boundary was used with the default of pressure. This boundary imply that the outlet condition is depend on the condition generated inside the system. In the wall of fluid the wall boundary condition was used with assumed that there is no fluid absorbed by the solid wall and the velocity at the wall is zero.

In the heating source wall the thermal boundary condition was applied with input heat flux in the boundary. Heat flux applied in that wall boundary is derived from the power imposed into the system divided by the area of the heat source. Area of heat source can be counted from outer and inner of coaxial cable, inner diameter is 1.6mm and outer diameter is 5mm. Electric power imposed into this system is 60Watt, hence the heat flux in the heating source is $1.76154\text{x}10^{-5}$ W/m^2.

In the outside of the wall convective boundary was applied with assumed free convection to the environment during heating. Some of heat generated inside the system will transfer out to the ambient temperature of air at 280K. Coefficient of free convection of the air chosen at 5.0W/m^{2}K was applied in the boundary to consider heat transfer outside the system.

5.4.3. Meshing.

Domain of simulation consist of 5.2 mm x 3.9 mm in size. The geometry was discretized using uniform finer quadrilateral meshing (mesh size 0.025mm) in all domain simulations. Ethanol liquid is used as fluid flow inside injector which has properties of density 790kg/m3, specific heat 2470kJ/kg-K, thermal conductivity 0.182W/m-K and viscosity 1.2g/m-s. Conservation equations of mass, momentum and energy of fluid flow were solved using pressure based solver. The computation of time dependent solution was modelled by Pressure-Implicit with Splitting of Operation (PISO) algorithm. Standard k-ε model is used to simulate the turbulence of fluid flow.

Fluid flow in the inlet domain was setting on initial velocity 0.1m/s and initial temperature 280K. Heat flux flowing in the heating area was arisen from electric power,

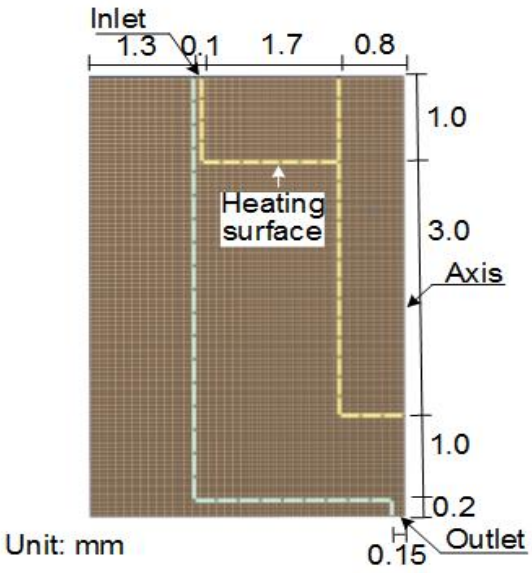

Figure 5.8. Boundary condition and grid.

60Watt, imposed into the microwave heating. The wall temperature was setting as coupled for conjugate heat transfer while the outer wall was setting as insulated wall. In outlet boundary fluid flow was also controlled to determine the appropriate mass flow rate discharged from the nozzle. The fuel flow rate in the simulation set as the same as in the experiment. Fuel mass

flow rate of 8e-05kg/s (0.10mL/sec) was applied in the outlet boundary to control fuel flow injected from nozzle. Contour of temperature and flow line of fluid flow were analyzed to predict fuel properties and characteristic inside the injector due to heating effect from microwave-heating.

Table 2. Simulation properties

Parameter	**Value**
Working fluid	Ethanol
Injection pressure	0.3MPa
Input power	60Watt
Fuel Temperature	280K
Ambient temperature	280K

5.5. Result and analysis

Experimental studies were carried out to investigate the effect of fuel heating on the spray characteristics. Figure 5. 9 exhibits the time histories of fuel temperature at injector tip during experimental injection. It can be seen that the temperature of fuel increases significantly in the short time after heating. In the first injection time the temperature of fuel was 280K and increased markedly to the peak temperature around 350K at around 1.25sec after heating. This temperature tends to constant during the next injection period which is very close to the boiling temperature of ethanol fuel (351.4K).

Figure 5. 10 displays the temperature distribution of fuel flowing out the injector in the simulation result. The temperature was recorded at injector tip same position as done in experiment. Temperature of ethanol was also increased rapidly during heating and it was quite similar characteristic of the experimental result. In the first 2 second after heating the temperature was increased rapidly but in the next time flow the temperature became stable around 360K. It is appearing that in the heating area the process of heat transfer is critical and markedly influence the spray from injector.

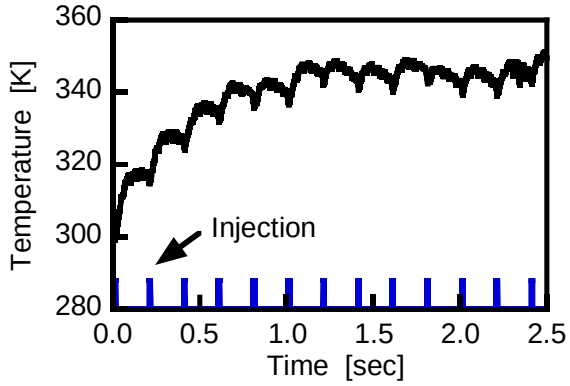

Figure 5. 9. Time history of injector tip temperature (Experimental).

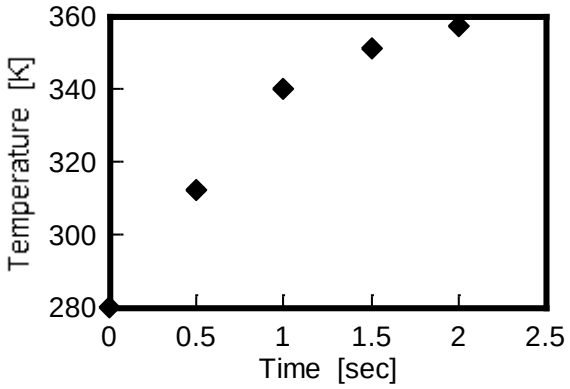

Figure 5. 10. Time history of injector tip temperature (Simulation).

Droplet distribution was measured by LDSA at each injection duration. Measurement position of LDSA was positioned at 20mm from the tip of injector. Comparison of the fuel droplet size distribution before and after heating can be seen in Figure 5. 11. It clearly shows the critical effect of fuel temperature on droplet size distribution of ethanol. Particle size (SMD) of droplets decreases significantly, around 50%, after experienced heating. In the process of heating, temperature of fuel increases rapidly and leads the changing of droplet diameter. The different trend in Figure 5. 9 can possibly due to the position measurement of thermocouple.

Figure 5. 12 explains the trend of droplet distribution frequency of injected fuel before and after-heating experienced heating. Particle size of droplets injected was significantly affected by heating. As the temperature increasing, the frequency of small droplets become

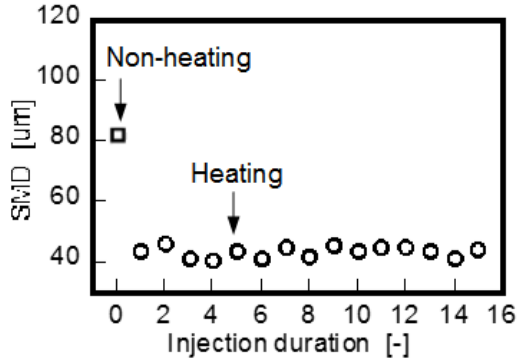

Figure 5. 11. SMD at each injection.

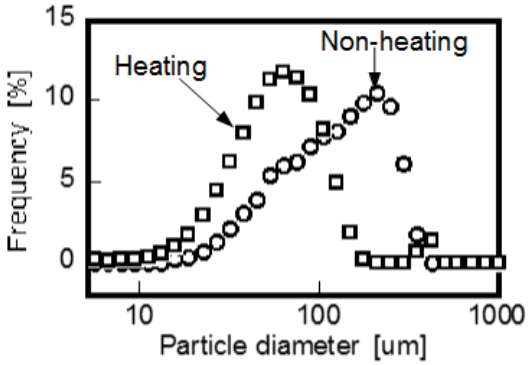

Figure 5. 12. Droplet size distribution.

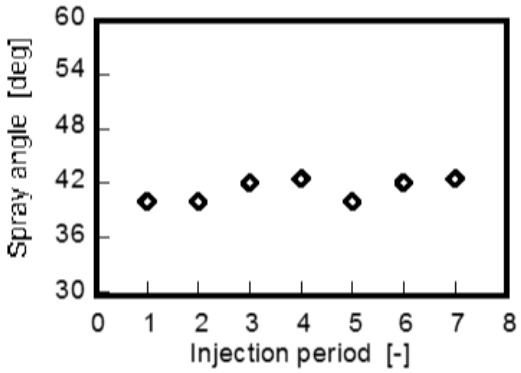

Figure 5. 13. Spray angle at each injection

increasing compared with of non-heating fuel. It seems that viscosity and surface tension of heated fuel are changed and leads to reduce particle size of droplets.

In LMI system, signal control was highly responsive that can easily adjust the signal for appropriate heating time and injection interval. However, LMI system has slightly sensitive on clearance adjustment (0-10μm) between driven part and nozzle head of injector which affect the volume flow and spray characteristic of injected fuel.

Fig.5. 13 shows the spray cone angles of the fuel in various injection period. Spray angle was slightly increased with the increased of injection period as a representative of the increase fuel temperature. The increasing in temperature tends to reduce droplet diameter and increases the spray angle. The increase of fuel temperature can also affect the atomization quality of the fuel spray and accelerates the mixing of air and fuel before ignited.

Spray distribution of droplet fuel injection under various injection time and temperature is considered in Figure 5.14. The first four figures were shown the longer distance penetration of liquid film of the spray along the axis. It is also shows that there is a bent penetration occurred from the axis of injector at the beginning of injection. Fuel ligaments were also seen dominant in the spray at initial injection especially in the first four injection. However, the rest injections period were shown reducing the fuel ligaments and at the same time increasing the droplet quantities. Ligaments of fuel was immediately changed into small droplet even in the early injection. This may indicate that the higher temperature of fuel can reduce the spray penetration and droplet size. Heating time is needed to increase the fuel temperature at around boiling point before injected in order to improve evaporation of fuel.

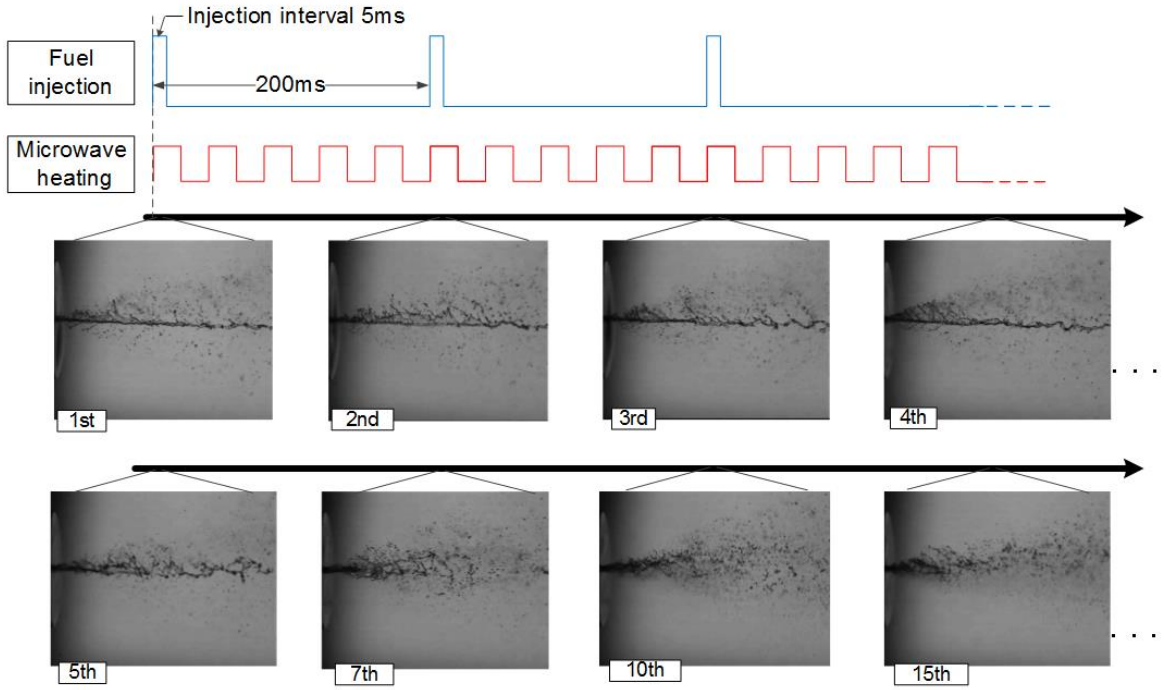

Figure 5. 14. Spray photos at different injection

5.6. Conclusions

The present study considered the performance of spray characteristic of ethanol fuel heated by microwave heating in port-injector. Spray characteristics such as droplet diameter and droplet distribution size were measured and analyzed. The following conclusions are drawn from the above analyzed:

1) Local heating of fuel has the significant impact on droplet diameter of ethanol fuel. Droplets size were smaller when the temperature of fuel increased at around boiling point.
2) Pre-heating treatment by LMI system can significantly improve the spray characteristics of ethanol. The increasing of fuel temperature leads to change in properties which makes the droplet fuel easily breakup in to small droplets.
3) Pre-heating system of LMI seems offering advantageous used for bio-ethanol fuel on port fuel injection engine. Heat is generated immediately after dissipated power into LMI system and improve fuel vaporization.

REFERENCES

1. Ahn K. , Stefanopoulou A.G., and Jankovic M., IEEE Trans. *Control System Technology* Vol. 18, 2010, pp. 1241-1253.
2. Rotondi R., and Bella G., *Int.Journal of Thermal Science* Vol. 45, 2006, pp. 168-179.
3. Spegar T.D., Chang S., Das S., Norkin E. and Lucas R., *SAE International*, 2009-01-1504.
4. Pandey R.K., Rahmen A., and Sarviya R.M., *Renewable and Sustainable Energy Review* Vol. 16, 2012, pp.1762-1778.
5. Gumus R., *Applied Thermal Engineering*, Vol. 29,2009, pp. 652-660.
6. Zajdel A., and Skorek J., *Energy*, Vol. 26 ,2001, pp. 1135-1144.
7. Kabasin D., Hoyer K., Kazour J., Lamers R, and Hurter T., *SAE International* , 2009-01-0615, 2009.
8. Enomoto H. and Iida T., *JSAE paper*, Vol. 40, No. 3, 2009, pp. 769 – 774.
9. Tran T.H.T., Enomoto H., Nishioka K., Kushita M., Sakitzu T., and Ebisawa N., SAE technical paper 2011-32-0582, 2011.

Chapter 6

Summary and Future Woks

6.1. Brief Introduction

The aim of this study is to investigate the spray performances of LMI system that used electromagnetic energy to increase the temperature of fuel flow inside injector. Numerical simulation was conducted in order to develop heating area of LMI for better heating generation. Model developed in this study was based on the existing LMI model with dimension of heating area is 4mm of length and 7.8mm of diameter. Model of simulation for microwave heating was generated in COMSOL Multiphysics to predict temperature profile inside heating zone. We also conducted simulation of fluid flow and heat transfer in the heating domain using ANSYS Fluent. Temperature characteristic from simulation study was validated with direct measurement of tip temperature of injector. An investigation on temperature profile and spray characteristic of LMI was conducted at Combustion Applied Laboratory of Kanazawa University. Ethanol fuel produced from Kanto Chemical Company in Japan was used as working fluid. Direct investigation was completed with compact measurement devices for achieving the main goal on this study. Measurement devices consist of Laser Diffraction Spray Analyzer (LDSA), High Speed Camera (PHOTRHON), CMOS camera and K-Type Thermocouple. The use of optical measurement techniques allowed for measurements with very high accuracies compared to other techniques found in many papers. For fuel spray with long tip penetration, an optical setup using CMOS camera was used at different position from the tip of injector. LDSA was used to measure the droplet size and size distribution of the spray. High Speed camera was used to record the spray fuel during injection. The image captured at this device can be used to identify the droplets size and velocity. CMOS camera was used to characterize the spray component of injected fuel. In addition, all data gained from measurement devices were collected in data logger for further analyzed.

6.2. General Conclusion

Several conclusions can be made as follow:

- Temperature of ethanol increases very fast since the imposed of electromagnetic wave into the heating zone. Volumetric heating from microwave heating offers the advantageous in generated heat inside ethanol material. Temperature profile in the tip injector was in good agreement with temperature measurement in experimental study. Furthermore, the simulation result showed that shape and geometry of heating area is essential for microwave heating system. The model is allowed for further development and design for high performance heating of LMI system.
- Direct measurement shows that temperature of ethanol was increased to around its boiling point temperature in around 1 sec after imposed electromagnetic wave into the system. The increasing of fuel temperature leads to change in properties which makes the droplet fuel easily breakup in to small droplets. Pre-heating system seems suitable used for bio-ethanol fuel on port fuel injection engine.
- Local heating of fuel has the significant impact on droplet diameter. The investigation on spray performances such as droplets size and distribution were performed during injection. Results of size histories showed that in the early injection the droplets size became reduced significantly from around 83 to 42 um of diameter droplets. Moreover, the distribution characteristic of droplet size also showed a strong effect of fuel heating on the droplet size. The liquid sheets changed rapidly into droplets as the temperature of fuel increased. It was expected that the properties of heated fuel became changed and lead to improve atomization and evaporation of fuel spray.
- Temperature of fuel also affects the distribution of spray components. The spray angle cone and the spray component such as liquid sheet, ligaments, and droplets were investigated from the image captured. The images captured from CMOS camera were used in these analyzed. Results of showed that the spray cone angle almost constant. The spray components were clearly changed in the short time after heating applied to the system. This is because the heating fuel can change the properties of fuel such viscosity, surface tension and density that lead to improve atomization and evaporation during injection.

6.3. Recommendations for the future works

The result of this study can show the temperature distribution inside heating area of LMI system. The simulation result can also predict the model for more uniform distribution of temperature. For further development of LMI system, it is need to advance research and development on the heating area that can allow for rapid heating and evaporation of fuel. Injection control is also important for heating resident time inside heating zone, and therefore it is needed to further develop for high precisions of heating and injection system. Mechanical adjustment on heating zone size and shape as well as injector holes are also important to be considered and developed for LMI system.

As development results, it is need to further research and application of this system for high pressure fuel injection application such using in direct injection engine. However the injector design is the most challenging one for this application especially for modern engine that operates at very high injection pressure.

REFERENCES

[1] US Environmental Protection Agency (US EPA); 2011, Inventory of US Greenhouse Gas Emissions and Sinks: 1990–2009.

[2] OECD/IEA 2011, World Energy Outlook 2011, Accessed from www.worldenergyoutlook.org

[3] Murya R. and Agarwal A., Experimental study of combustion and emission characteristics of ethanol fuelled port injected homogeneous charge compression ignition (HCCI) combustion engine, *Applied Energy* 88, 2011, pp 1169–1180.

[4] Park S.H., Kim H.J., Suh H K. and Lee C.S, Experimental and Numerical Analysis of Spray-atomization Characteristics of Biodiesel Fuel in Various Fuel and Ambient, *International Journal of Heat and Mass Transfer*, 30, 2009, pp 960-970.

[5] Joshi S., Lave L., Lester M., Lankey R., A life Cycle Comparison of Alternative Transportation Fuels. *SAE paper* 2000-01-1516.

[6] Balat M., Balat H., and Oz C., Progress in Bioethanol Processing, *Progress in Energy and Combustion Scienc*e, 34, 2008, pp. 551-573.

[7] Zervas E., Montagne X., and Lahaye J., The influence of Gasoline Formulation on Specific Pollutant Emissions, Journal of the Air Management Association, 49:11, 1999, pp.1304-1314.

[8] Ishida M., Yamamoto S., Ueki H. and Sakaguchi D., Remarkable Improvement of NOx-PM Trade-of in a Diesel Engine by Means of Bio-ethanol and EGR, *Energy*,35(12), 2010, pp.4572-4581.

[9] Henein N.A. and Tagomori M.K., Cold Start Hydrocarbon Emissions in Port-Injected Gasoline Engines, *Progress in Energy and Combustion Science* 25, 1999, pp. 563-593.

[10] Aleiferis P.G. and van Romunde Z.R, "An Analysis of Spray Development with Iso-octane, n-pentane, Gasoline, Ethanol and n-Butanol from a Multi-hole Injector under Hot Fuel Conditions," *Fuel* 105, 2012, pp.143-168.

[11] Anand T.N.C., Mohan A.M. and Ravkrisna R.V., Spray Characteristics of Gasoline-Ethanol Blends from a Multi-hole Port Fuel Injector, Fuel 102, 2012, pp.613-623.

[12] Padala S., Le M.K., Kook S. and Hawkes E.R., "Imaging Diagnostics of Ethanol Port Fuel Injection Sprays for Automobile Engine Applications, Applied Thermal Engineering 52, 2013, pp.24-37.

[13] Jia L.W., Shen M.Q., Wang J., Lin M.Q., Influence of Ethanol Gasoline Blended Fuel on Emission Characteristics from a Four-Stroke Motorcycle Engine, *J. Hazardous Mater*. 123 (2005) pp. 29-34

[14] Bayraktar H., Experimental and theoretical investigation of using gasoline ethanol blends in spark-ignition engines, *Renewable Energy* 30, (2005), pp 1733-1747.

[15] Chen R.H., Chiang L.B., Chen C.N. and Lin T.H, 2011, Cold start emissions of an SI Engine Using Ethanol-gasoline blended fuel, *Applied Thermal Engineering* 31, 2011, pp.1463-1467.

[16] Al-Hasan, M, 2002, Effect of ethanol–unleaded gasoline blends, Journal of Energy Conversion and Management 44 (2003) 1547–1561

[17] Gumus R., Reducing Cold-Start Emission from Internal Combustion Engines by Means of Thermal Energy Storage System, *Applied Thermal Engineering*, 29, 2009, pp. 652-660.

[18] Zajdel A., and Skorek J., Evaluation of the Influence of Liquid Fuel Atomization on Fuel Consumption During Heating of Solids in A Furnace, *Energy*, 26, 2001, pp. 1135-1144.

[19] Kabasin D., Hoyer K., Kazour J., Lamers R, and Hurter T., Heated Injector for Ethanol Cold Starts, *SAE International* , 2009, 2009-01-0615.

[20] Belanger J.M.R ., Pare J.R.J., Poon O., Fairbridge C., Mutyala Ng.S., "Remark on various application of microwave energy", *Micro power electromagnetic energy* 4 , 2008, pp. 24-44.

[21] Hagerty D.J., Ullrich C.R., and Denton MM., "Microwave drying of soil", *Journal of Geotech Test* 13, 1990, pp. 138-141.

[22] Yousefi T., Mousavi S.A., Saghir M.Z., Farahbaksh B., An Investigation on the Microwave Heating of Flowing Water: A Numerical Study, *International Journal of Thermal Science* 71, 2013, pp.118-127.

[23] Oliveira M.E.C., Franca A.S., Microwave heating of foodstuff, *Food Engineering* 53, 2002, pp.347–359.

[24] Chandrasekaran S., Ramanathan S., and Basak T., Microwave food processing- *A Review. Food Research International* 52, (2013), 243-261.

[25] Enomoto H. and Iida T.., Effect of microwave heating on the spray droplet size distribution by using local contact microwave hating injectors, *JSAE paper*, Vol. 40, No. 3, 2009, pp. 769 – 774.

[26] Tran T.H.T., Enomoto H., Nishioka K., Kushita M., Sakitzu T. and Ebisawa N., Effect of Ethanol Ratio and Temperature on Gasoline Atomizing using Local-contact Microwave-heating Injector, *SAE paper* 2011-32-0582.

[27] Mangalla L.K. and Enomoto H., Spray Characteristics of Local-contact Microwave-heating Injector Fuelled with Ethanol, *SAE Technical paper* 2013-32-9126, 2013.

[28] Ayappa K.G., Davis H.T., Davis E.A., and Gordon J., Analysis of microwave heating of materials with temperature-dependent properties, *AIChE Journal* 37 (1991) pp. 313–322.

[29] Ayappa K.G., Davis H.T., Crapiste G., Davis E.A., Gordon J., Microwave heating: an evaluation of power formulations, *Chemical Engineering Sci*ence 46, 1991, pp.1005–1016.

[30] Zhu J., Kuznetsov A.V. and Sandeep K,P., Mathematical modeling of continuous flow microwave heating of liquids (effects of dielectric properties and design parameters), *Int. Journal of Thermal Science* 46, 2007, pp328-341.

[31] Hossan M.R., Byun D.Y. and Dutta P., Analysis of Microwave Heating for Cylindrical Shaped Objects, *International Journal of Heat and Mass Transfer* 53, 2010, pp. 5129-5138.

[32] Hossan M.R. and Dutta P., Effect of temperature dependent properties in electromagnetic heating, Int Journal of Heat and Mass transfer 55, 2012, pp 3412-3422.

[33] Zhang Q., Jackson T.H., and Ungan A., Numerical modeling of microwave induced natural convection, *International Journal of Heat and Mass Transfer* 43 (2000) pp. 2141–2154.

[34] Salvi D., Boldor D., Aita G.M., and Sabliov C.M., Comsol Multiphysics Model for Continuous Flow Microwave Heating of Liquid, *Journal of Food Engineering*, 104, 3, (2011), 422-429.

[35] Funawatashi Y. and Suzuki T., Numerical Analysis of Microwave Heating of a Dielectric, *Heat Transfer-Asian Research*, 32, 3, (2003), 227-236.

[36] Pozar D.M. , *Microwave engineering*, John Wiley& Sons, Inc. 4th edition

[37] Chen H., Tang J. and Liu F., Simulation model for moving food Packages in Microwave Heating Process using Conformal FDTD Method, *Journal of Food Engineering* 88, 2008, pp.294-305.

[38] Geedipalli, S.S.R., Rakesh, V., and Datta, A. Modeling the heating uniformity contributed by a rotating turntable in microwave ovens., *Journal of Food Engineering* 82, 2007, pp.359-368

[39] Popovic Z., and Popovic B.D., *Introductory Electromagnetics*, Prentice Hall, Inc., 2000, Version 12 April 2012.

[40] Roussy G., and Pearce J.A., *Foundations and Industrial Applications of Microwaves and Radio Frequency Fields: Physical and Chemical Processes*, Wiley, Chichester, 1995. pp. 7-14.

[41] Cherbanski R. and Rudniak L., Modelling of Microwave heating of Water in a Monomode Applicator- Influence of Operating Conditions, *International Journal of Thermal Science* 74, 2013, pp.214-229.

[42] Chatterjee S., Basak T. and Das S.K., Microwave Driven Convection in a Rotating Cylindrical Cavity: A Numerical Study, *Journal of Food Engineering* 79, 2007, pp. 1269-1279.

[43] Jordan E.D., and Balman K.G., *Electromagnetic waves and Radiating System*, Prenticel-Hall, Inc, New Jersey, Second Edition, 1968.

[44] Knoerzer, K., Regier, M., and Scubert, H., A Computational Model for Calculating Temperature Distribution in Microwave Food Application, Innovative Food Science and Engineering Technologies, 9, 2008,pp. 374-384.

Appendix 1

List of published papers

Journal Papers

1. L.K. Mangalla, H. Enomoto, H. Nozue, and S. Sawasaki, Numerical Analysis of Local-contact Microwave-heating Injectorp Heating Part with Ethanol, Japan Society of Design Engineering (JSDE) paper (Submitted-in progress).
2. L.K. Mangalla and H. Enomoto; Spray Characteristics of Local-contact Microwave-heating Injector Fueled with Ethanol, SAE International Paper, 2013-32-9126, 2013.
3. H Enomoto; S. Sawasaki, K. Nishioka and L.K. Mangalla, Observation of Kerosene Droplet Evaporation under High Pressure and High Temperature Environment, SAE International Paper, 2013-32-9117, 2013.
4. H Enomoto; S. Kunioka, L.K. Mangalla, and N. Hieda, Small Kerosene Droplet Evaporation Near Butane Diffusion Flame, SAE Tinternational Paper, 2013-32-9116, 2013.

Conference Paper.

1. L.K. Mangalla, H. Enomoto, H. Nozue, Y. Teraoka and N. Hieda, Numerical Simulation of Heating Zone Detailed Structure in the Local-contact Microwave-heating Injector, International Conference on Grand Renewable Energy 2014, Tokyo, July 27th – August 1st , 2014.

Appendix 2. Structure of COMSOL and ANSYS Fluent

A.6.1. Structure of COMSOL simulation

COMSOL Multiphysics is a simulation software for various physics and engineering applications, specially coupled phenomena or multi-physics.

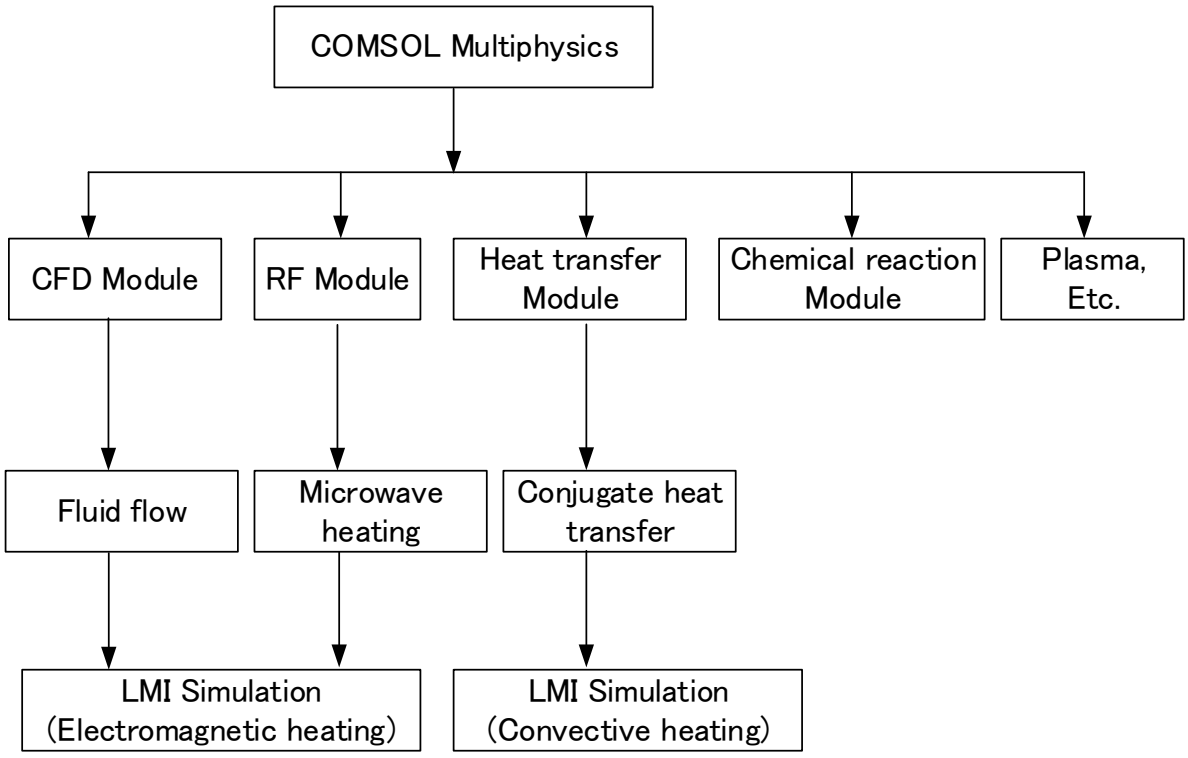

The main structure of COMSOL can be seen as follow:

1. Global definitions: In this section, we can define several parameters, variables, and functions.
2. Model: This section consist of several parts such as definition, geometry, material, physic study and mesh.
   - Definitions is the section to define parameter, variable and function for using in this boundary condition of this model.
   - Geometry is the section to create geometry or import geometry from other software.
   - Material is the section to define material for domain simulation.
   - Physic that going to simulate such as microwave heating, conjugate heat transfer, laminar or turbulence flow, etc.
   - Mesh is the section to discretize the geometry into small parts or elements.
3. Study: this section can define the sort of simulation study going to be solved. Study steps and solver used can be define in this part. In study step we can choose transient or steady state, frequency domain, eigenvalue, etc.
4. Results: Simulation result can be explore in this section such us temperature, velocity, pressure, density, etc. We can also export the data of result simulation and get the report of the simulation completely.

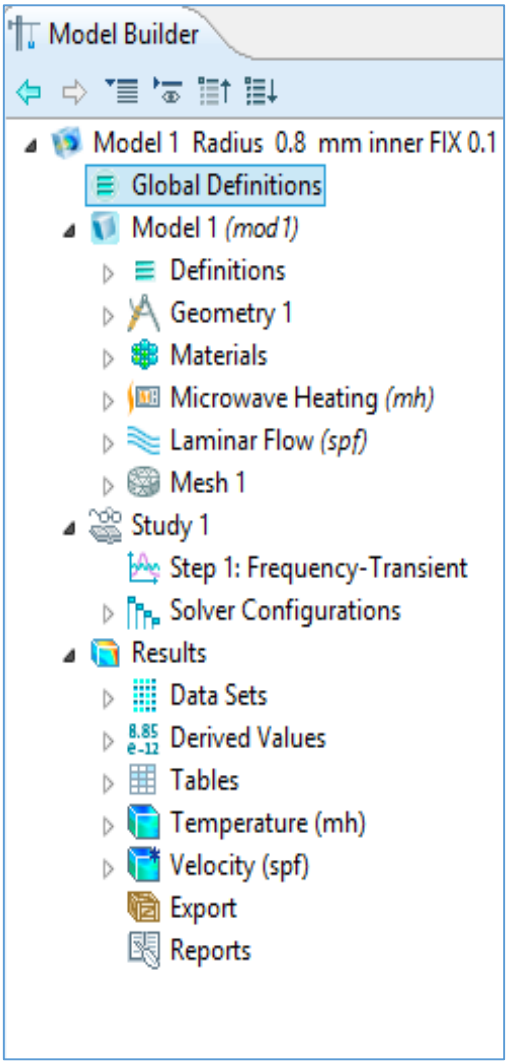

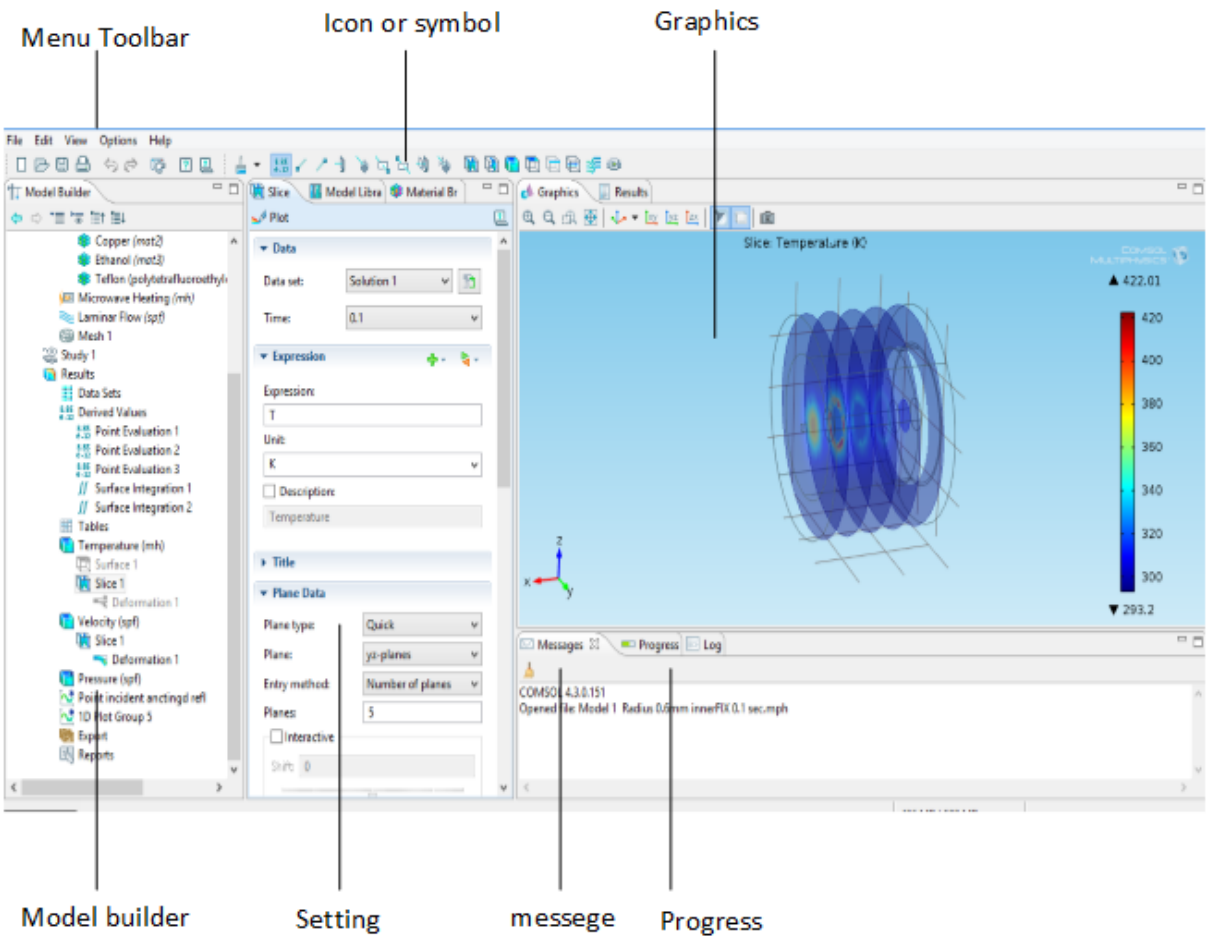

Figure A.2.1. Main windows of COMSOL Multiphysics.

Main steps in COMSOL:

1. Define the geometry for the domain simulation (3D, 2D, 1 D or 0D)

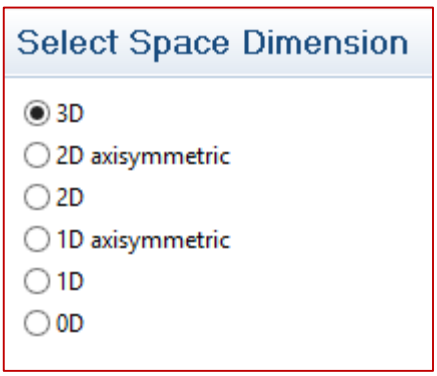

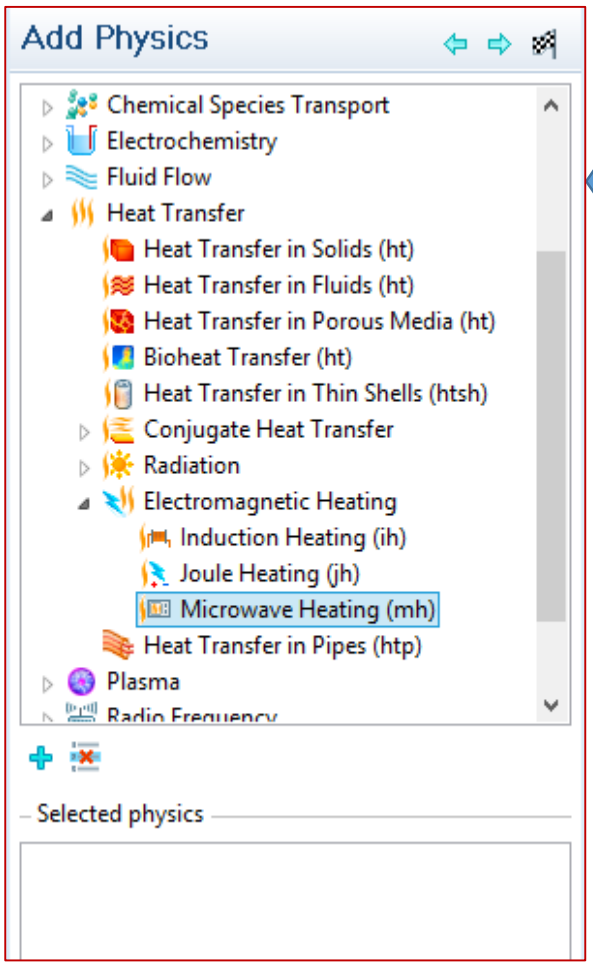

2. Add physics to be simulated

- One or more physics can be chosen to be considered.

- Initial and boundary condition are defined and setting in this pat

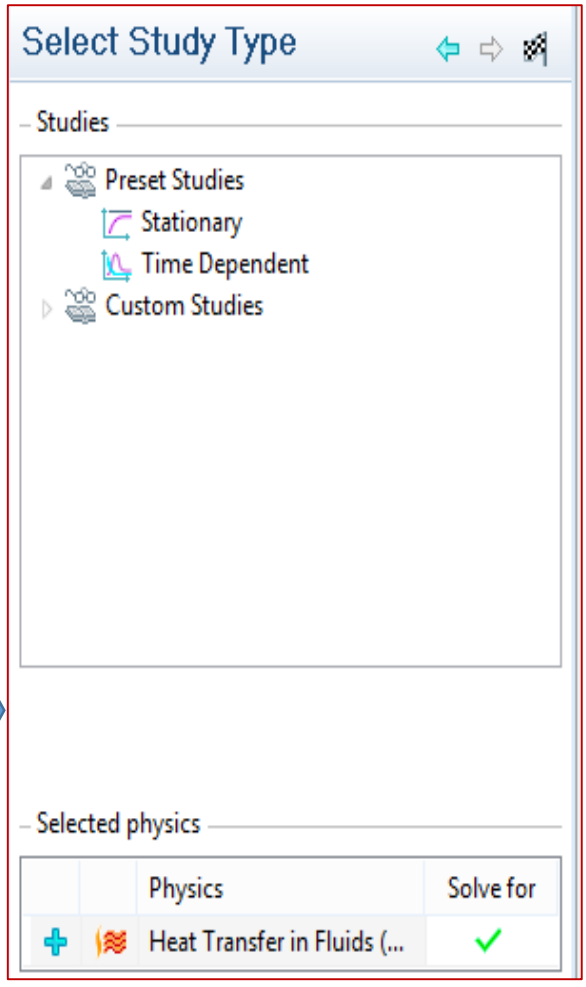

3. Selected type of study

We can choose type of study to be simulated such as stationary, transient, frequency time dependent, frequency stationary, etc.

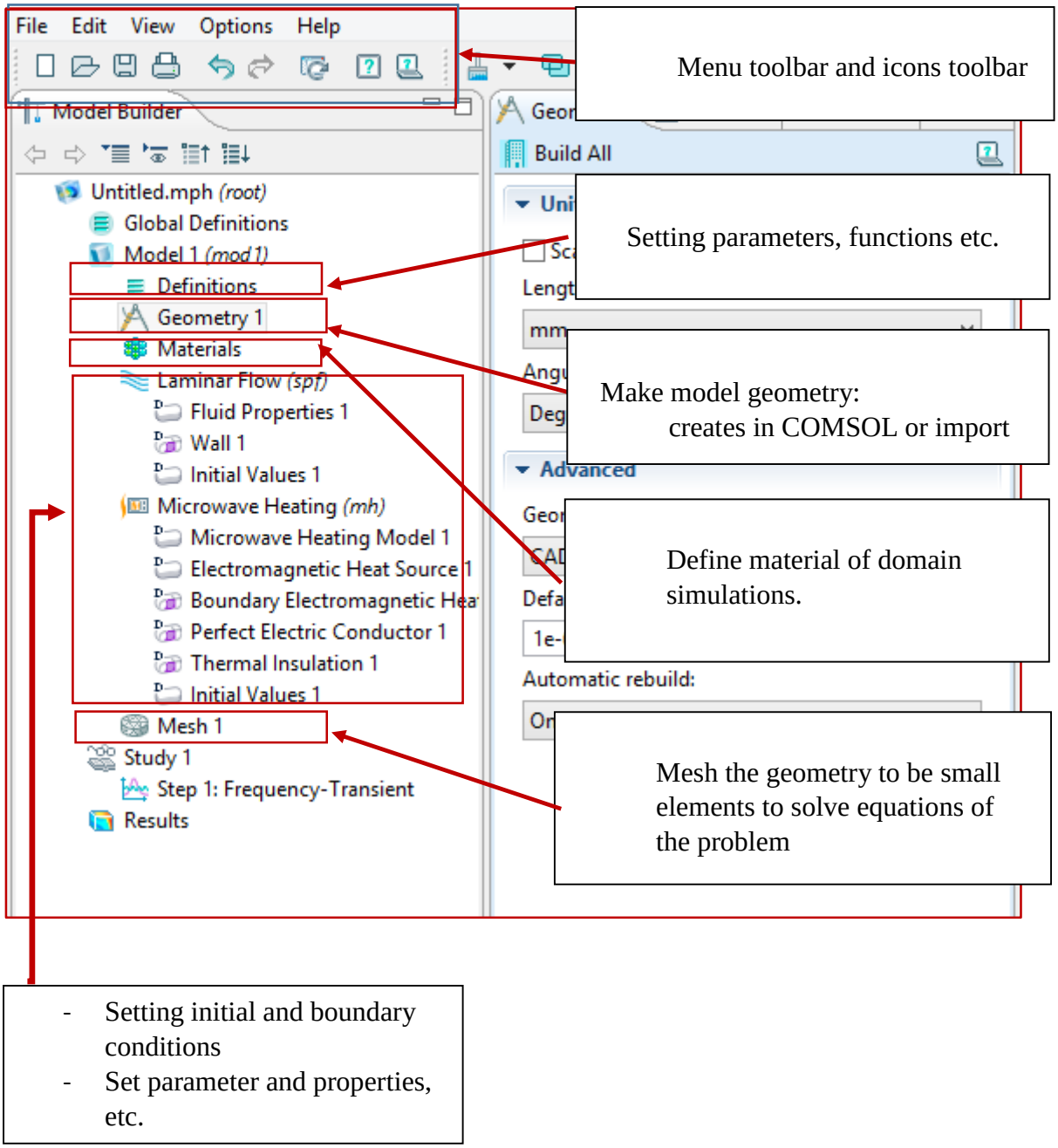
File Edit View Options Help
Model Builder
Build All
Untitled.mph (root)
Global Definitions
Model 1 (mod 1)
Definitions
Geometry 1
Materials
Laminar Flow (spf)
Fluid Properties 1
Wall 1
Initial Values 1
Microwave Heating (mh)
Microwave Heating Model 1
Electromagnetic Heat Source 1
Perfect Electric Conductor 1
Thermal Insulation 1
Initial Values 1
Mesh 1
Study 1
Step 1: Frequency-Transient
Results
Advanced
Automatic rebuild:
Menu toolbar and icons toolbar
Setting parameters, functions etc.
Make model geometry:
creates in COMSOL or import
Define material of domain simulations.
Mesh the geometry to be small elements to solve equations of the problem
- Setting initial and boundary conditions
- Set parameter and properties, etc.

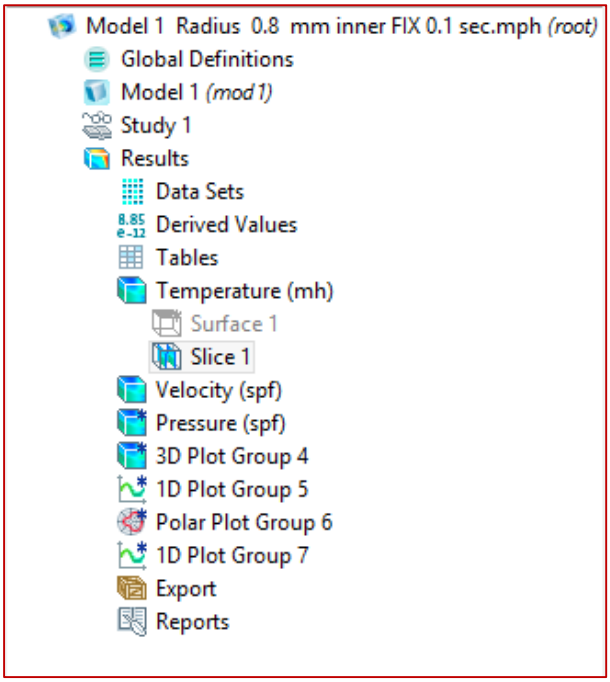

4. Result post processing

- to show simulation result we can do with several way, types, color, etc.
- We can export result simulation.
- we can also show reports of setting and results of simulation.

5. Graphics of simulation results

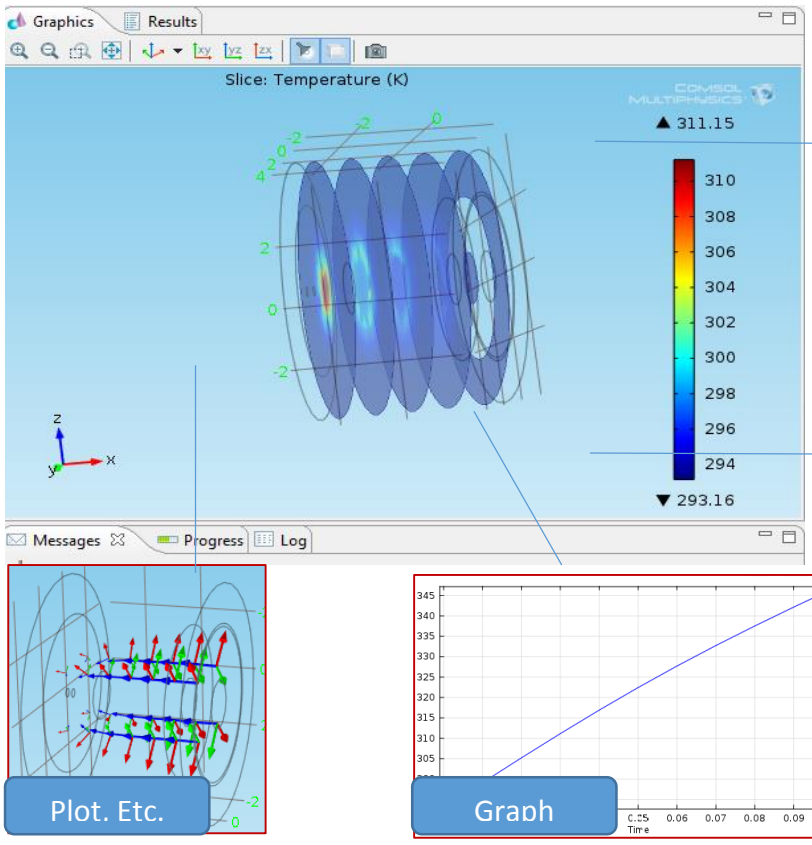

A.6.2. Structure of ANSYS Fluent simulation

ANSYS Fluent is a computational fluid dynamic (CFD) simulation software for various application. This software usually used to model flow, turbulence, heat transfer and reaction system for academic research and industrial application.

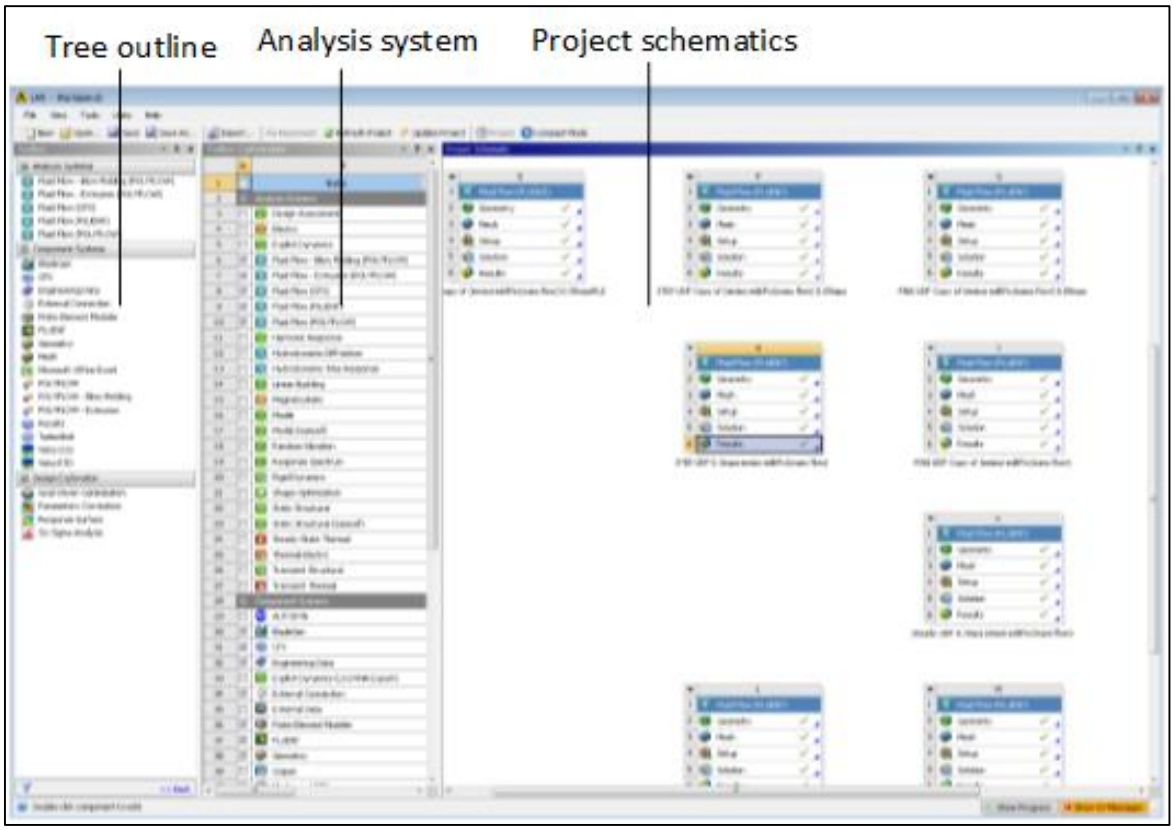

Figure A.2.2. Main windows of ANSYS Fluent workbench

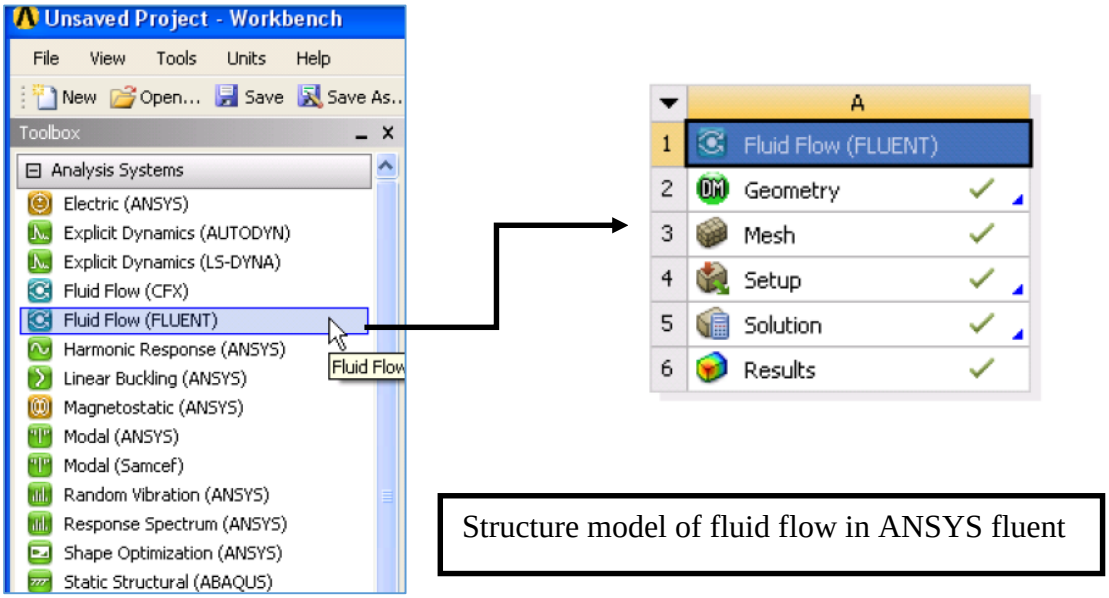

Structure model of fluid flow in ANSYS fluent

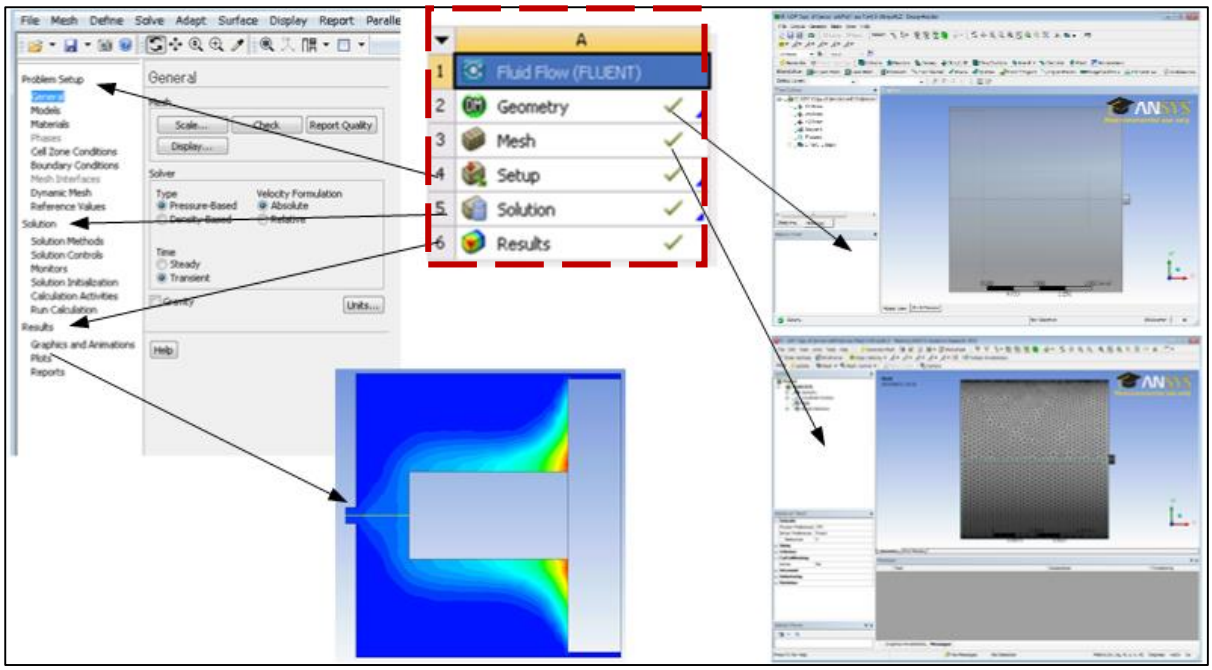

Figure A.2.3. Main structure of ANSYS Fluent simulation

SOLUTION STEPS

1. Create geometry

Geometry of domain simulation can be created in ANSYS workbench or import from other software such as Solidworks, Go engineer, etc.

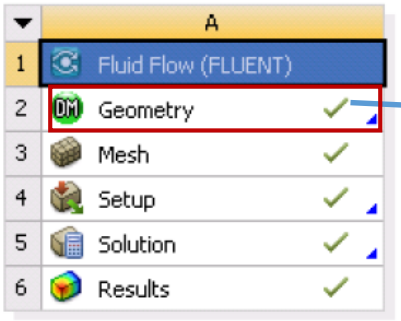

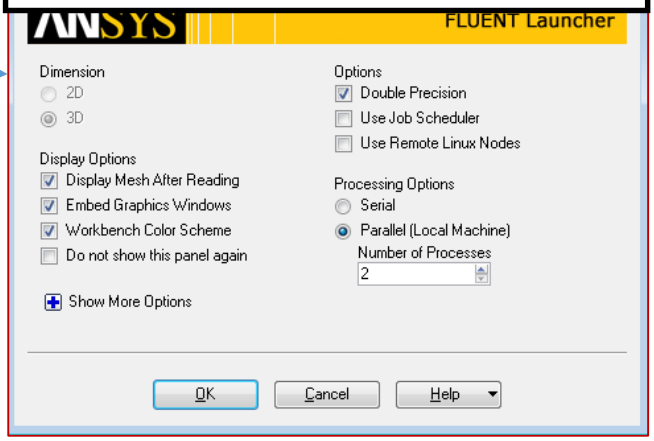

2. Meshing geometry

In order to solve problem inside the domain simulation the geometry is discretized into small grid or element

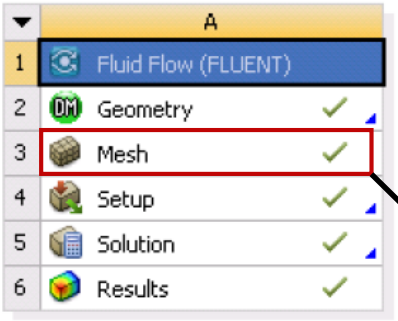

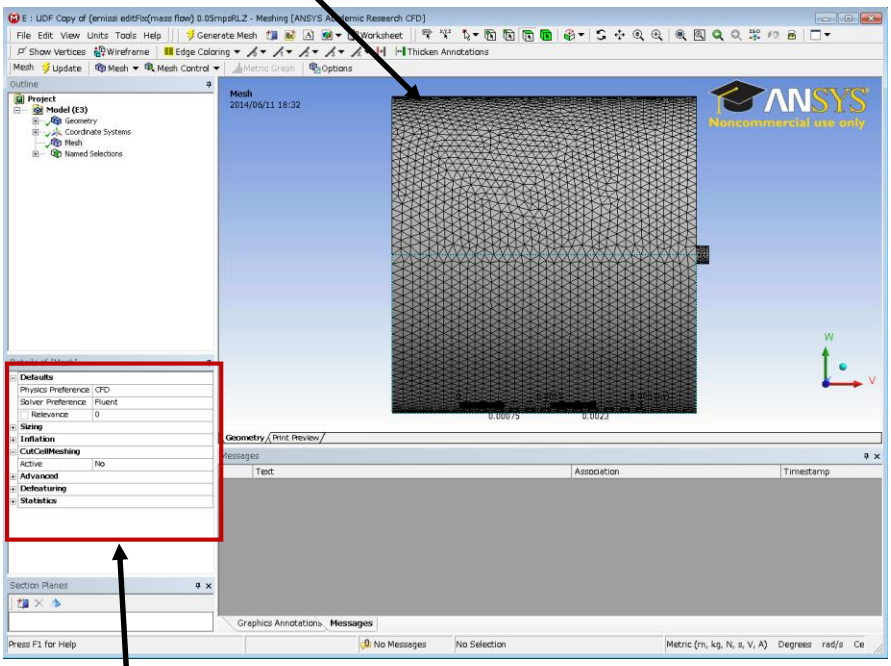

- Mesh size can be controlled in this section.
- Quality of mesh also can be evaluated in this section.

3. Setup

- In this section we can define type and time in solver simulation.
- Set the model to be considered (e.g. energy, laminar or turbulence, multiphase, heat exchange, etc.)
- Define material of domain simulation
- Set the boundary conditions, etc.

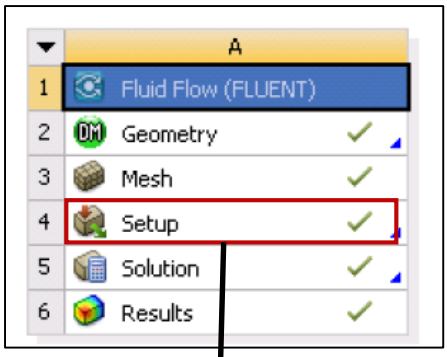

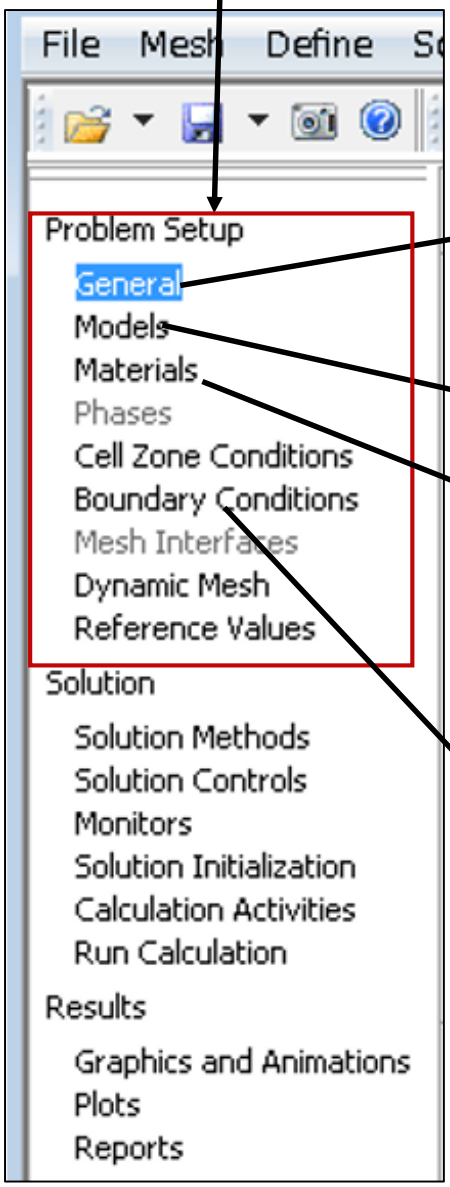

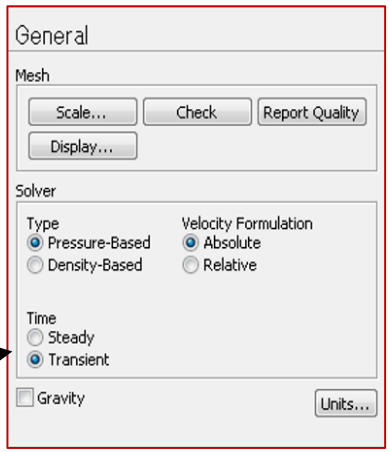

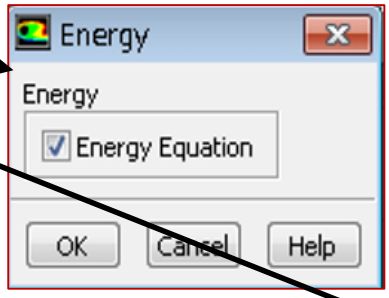

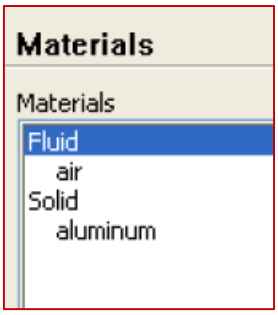

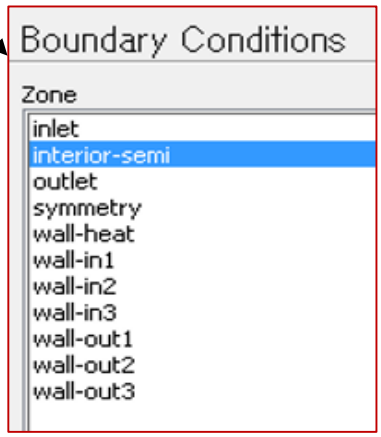

4. Solution

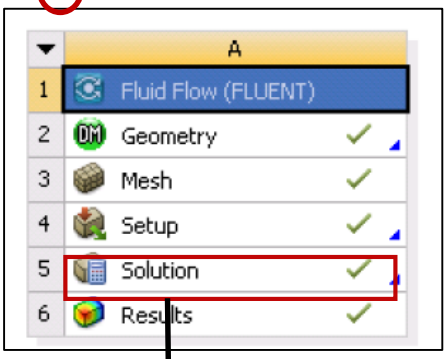

- In this section we can define the solution solver such SIMPLE, SIMPLEX and PISO scheme
- Solution control and initialization.
- Set the time step and number of time to be solved.

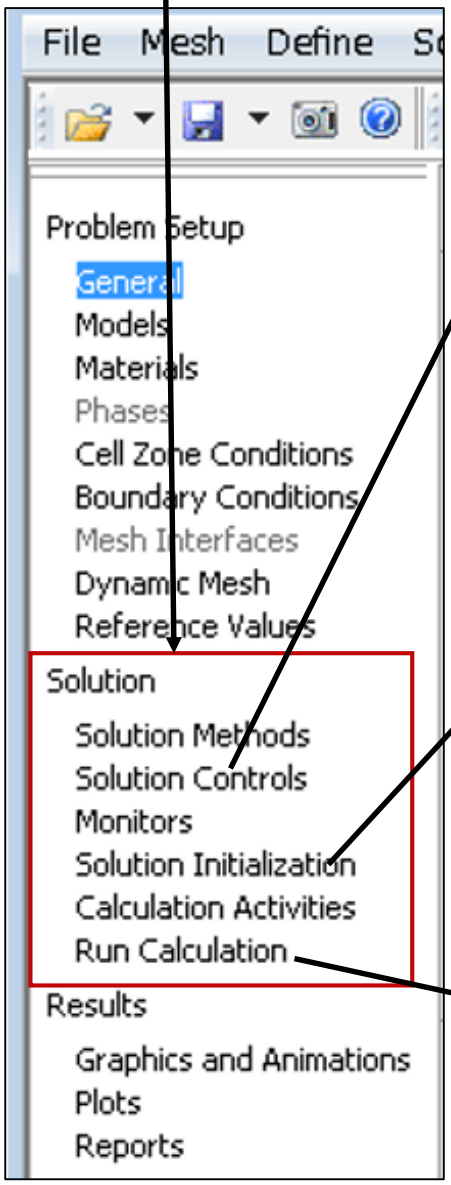

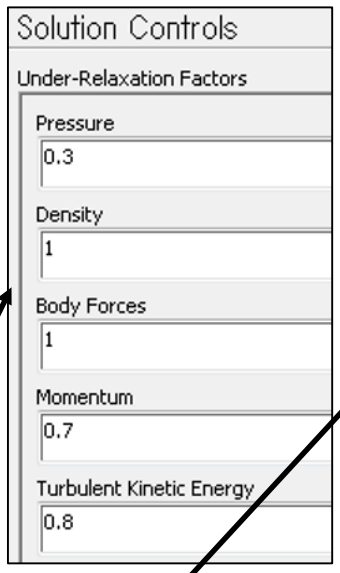

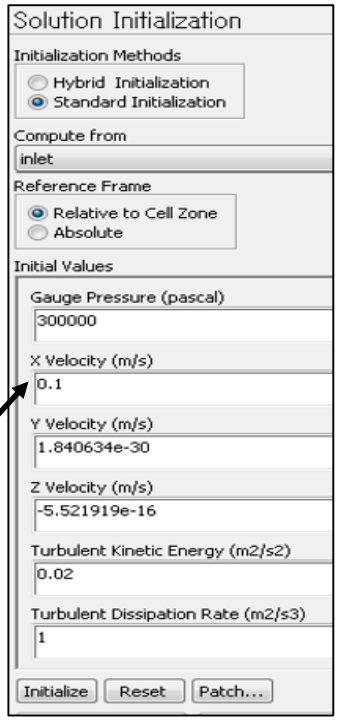

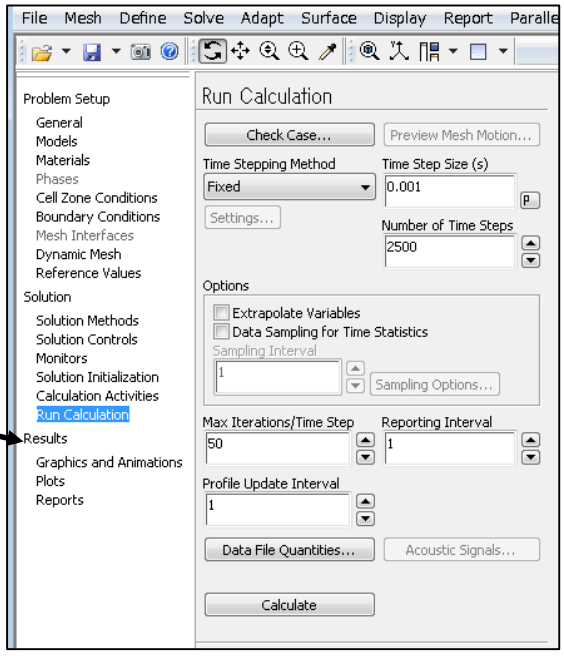

5. Post processing of result

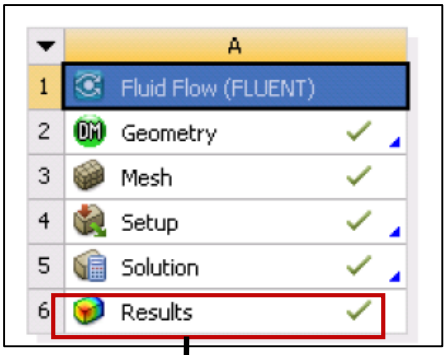

- To show the result we can make in this section or double click result to show the dialogue box of result.
- We can also show the video animation of result simulation
- Data simulation can be plot in this part

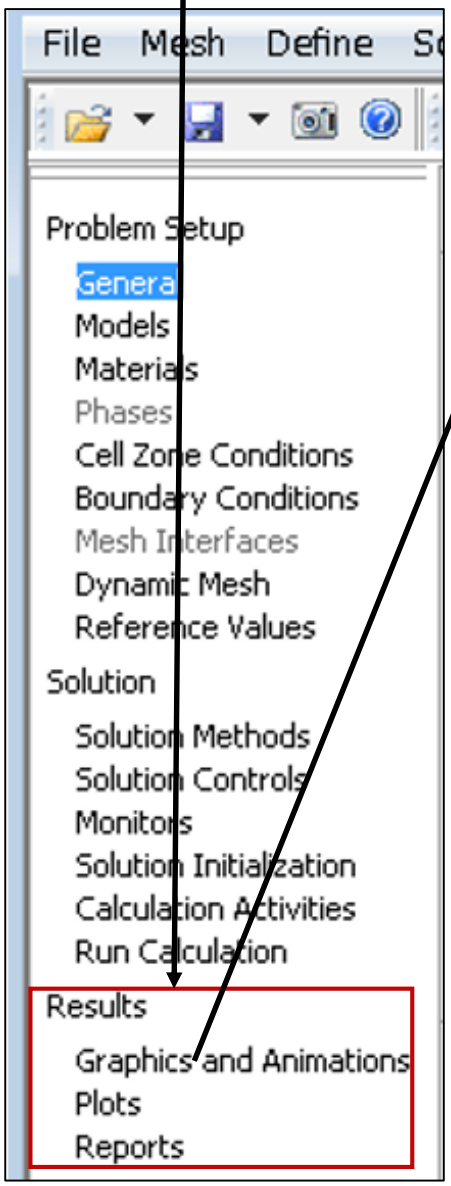

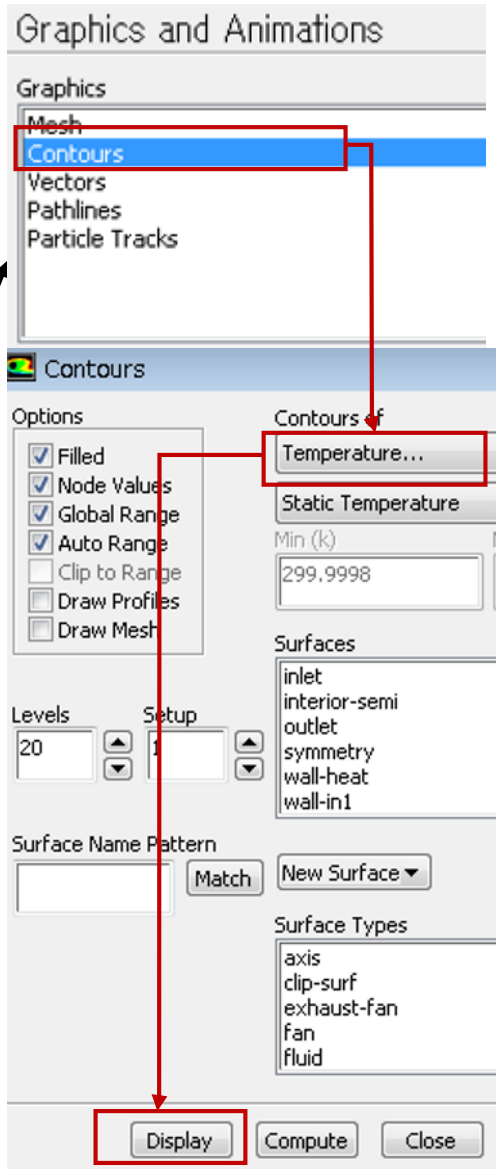

Appendix 3

A.3. Governing equations

A.3.1. Electromagnetic wave equations.

Electromagnetic wave equations that solved in this simulation study to determine electric field distribution can be expressed from Maxwell's law as follow:

$$\nabla \times \mu_r^{-1}(\nabla \times E) - k_o^2(\varepsilon_r - \frac{j\sigma}{\omega\varepsilon_o})E = 0 \quad \text{(a)}$$

The scattering magnetic field is calculated from Faraday's law as follow:

$$H = -\frac{1}{j\omega\mu}\nabla \cdot E \quad \text{(b)}$$

Where ε_r is relative permittivity and μ_r is the relative permeability of material. E is electric field (V/m) and H is the magnetic field. ε is permittivity of material (F/m) and μ is permeability of material (H/m), ω is angular wave frequency (2πf, rad/sec), k_o is the wave factor.

$$ko = \omega\sqrt{\varepsilon_0\mu_0} \quad \text{(c)}$$

Relative permeability and relative permeability can be expressed as:

$$\varepsilon_r = \frac{\varepsilon}{\varepsilon_o} \quad \text{and} \quad \mu_r = \frac{\mu}{\mu_o} \quad \text{(d)}$$

Permittivity of material consist of real and imaginary part and can be written as follow:

$$\varepsilon = \varepsilon' - j\varepsilon'' \quad \text{and} \quad \mu = \mu' - j\mu'' \quad \text{(e)}$$

The ratio of imaginary part to real part of complex permittivity is called loss tangent. Loss tangent provides a measure of how much power is lost in material versus how much is stored. Loss tangent in material can be expressed as follow:

$$\tan\delta = \frac{\varepsilon''}{\varepsilon'} \quad \text{and} \quad \tan\delta = \frac{\mu''}{\mu'} \quad \text{(f)}$$

Where ε'' is the imaginary part of dielectric permittivity, ε_0 is permittivity of vacuum and ε' is the real part of dielectric permittivity. μ" is the imaginary part of dielectric permeability μ_o is the permeability of vacuum and μ' is the real part of dielectric permeability.

A.3.2. Heat transfer equations.

Temperature distribution generated inside material can be derived from heat transfer equation:

$$\rho c_p \frac{\partial T}{\partial t} + \rho c_p u \cdot \nabla T = \nabla \cdot (k \nabla T) + Q \quad \text{(g)}$$

Where ρ is density of material (kg/m^3) and c_p is the specific heat of material (J/kgK). T is temperature (K) and u is vector velocity (m/s). k is thermal conductivity of material (W/mK), Q is heat generated (J).

A.2.3. Conservation of mass and momentum equations.

Mass conservation and momentum of liquid flow can be derived from the Navier-Stokes equation as follow:

- *Mass conservations:*

$$\frac{\partial \rho}{\partial t} + \nabla \cdot (\rho u) = 0 \quad \text{(h)}$$

- *Momentum equation:*

$$\rho \frac{\partial u}{\partial t} + \rho (u \cdot \nabla) u = -\nabla p + \nabla \cdot \left[\mu (\nabla u + (\nabla u)^T) - \frac{2}{3} \mu (\nabla \cdot u) \mathrm{I} \right] + F \quad \text{(i)}$$

Where ρ is the density of the liquid (kg/m3), p is the pressure (Pa), f is the momentum force u is the velocity (m/s), μ is the dynamic viscosity of the fluid (Pa.s) and I is the unit tensor that is represent the normal stress in fluid due to the gradient velocity. F is the external forces that exist in the system (N).

- *Energy equation:*

Energy equation can be expressed in integral form as follow.

$$\rho c_p\left(\frac{\partial T}{\partial t}+(u\cdot\nabla)T\right)=-(\nabla\cdot q)+\tau:S$$
$$-\frac{T\partial\rho}{\rho\partial T}\left(\frac{\partial p}{\partial t}+(u\cdot\nabla)p\right)+Q \qquad \text{(j)}$$

The first left equation is the rate change of kinetic and internal energy. In the right the first equation is the net inflow of kinetic and internal energy, the second is work done by body force, the third is net work done by the stress tensor and the last is the net heat flow.

Appendix 4

A.4. Explicit and Implicit method

Differential equations are usually involved the unknown function and derivatives. In order to solve these problem, the accurate approximation should be used. Exact solution of partial differential equation is sometimes difficult. Therefore, the numerical solution become necessary to get accurate approximation of the actual solutions. Two different methods are popular to solve the partial differential equations, explicit method and implicit method.

A.4.1. Explicit method

Explicit method calculate the state of the system at a later time from the state of the system at the current time. Explicit method or the forward Euler's method begins with choosing a step size or Δt**.** This step size will effect on the accuracy of approximation and number of computations. This method produce a series of line segment to solve the problem.

Let t_k, k= 0,1,2,…is the order of time and

$$t_{k+1} = t_k + \Delta t \tag{a}$$

For the partial differential equation of

$$y_t = f(t, y), \quad y(t_0) = y_0 \tag{b}$$

The approximate solution will be Y_k at $t = t_k$ and exact solution become y_k. We can get Y_{k+1} from (t_k, Y_k) from the differential equation. The Euler method determine the poit (t_{k+1}, Y_{k+1}) by assuming that this point is exist on the line through (t_k,Y_k) with slope f(t_k,Y_k). We can determine the formula of slope of this line by

$$\frac{Y_{k+1} - Y_k}{\Delta t} = f(t_k, Y_k) \tag{c}$$

From equation (b) we can get the value of next state by:

$$Y_{k+1} = Y_k + f(t_k, Y_k)\Delta t \tag{d}$$

If the time step decreased, the error between actual and approximation is reduce. But the reducing the time size will increase time of computation.

A.4.2. Implicit method

Implicit method sometimes called backward Euler method. This method is solving the equation by finding the solution of current state and next step one. For the same case of equation (b) we can get the formula of slope:

$$\frac{Y_{k+1} - Y_k}{\Delta t} = f(t_k, Y_{k+1}) \quad \text{(e)}$$

And

$$Y_{k+1} = Y_k + f(t_k, Y_{k+1})\Delta t \quad \text{(f)}$$

From this equation we can see that it needs longer time to solve the problem or equations. And the advantageous of this scheme is more stable in solving equations.

Summary:

Method	**Advantageous**	**Disadvantageous**
Explicit	Simple and faster	- Sensitive to stability - Need very small mesh to be stable
Implicit	- More stable (unconditionally stable) - More accurate result - Allow larger time step	Time and memory consuming

Appendix 5

A.5.1 COMSOL Schemes

In Comsol Multyphysics there are two schemes of solver for solution of equations:

1. Direct method.
2. Iterative method.

A.5.1.1. Direct method

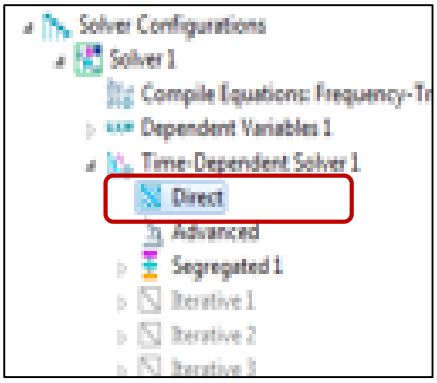

In order to solve partial differential equation applied in the system the appropriate method should be chosen correctly for stabilization and converge of the solution. In achieving the convergence for multiphysics problem the direct solver method is useful.

Direct solver consist of three specific schemes with each characteristics as follow:

1. MUltifrontal Massively Parallel sparse direct Solver (MUMPS). MUMPS has some characteristics as :
   - Robust and faster
   - Multi-core capable
   - Use complex arithmetic for solving problem
   - Arising from finite element method
   - Parallel factorization
2. PARallel DIrect linear SOlver (PARDISO) with characteristic as:
   - Memory efficient
   - Robust and high performances
   - Faster
   - Multi-core
   - Useful for very large three-dimensional system

3. SParse Object Oriented Linear Equation Solver (SPOOLES) with several characteristic as follow:
    - Solve equations using multifrontal factorization
    - Slow
    - Multi-core and cluster capable
    - Use the least memory.

A.5.1.2. Iterative method

Iterative schemes include a variety approaches but simple. Iterative scheme approaches the solution gradually. Several characteristic of this scheme are given as:

- Automatically choose iterative setting. Different physics require different iterative setting depend on equation being used.
- Slower convergence but it is depend on the input conditions. For well-conditioned problem the convergence should be monotonic (constant), but for ill-conditioned the convergence become a little bit slower.
- Less memory usage.

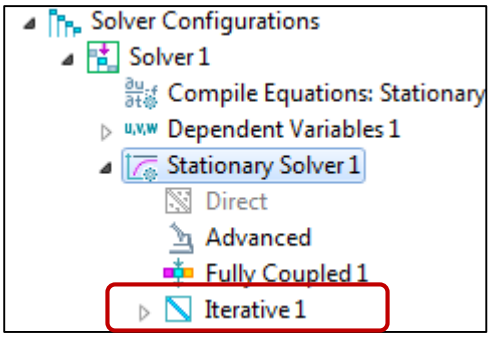

Fortunately, In COMSOL we can just go to solve (Compute) because the solver already has built-in default scheme solver for all physics interface. It means that the software will automatically detect the physics being solved and choose the scheme solver- direct or iterative - for that case. It will choose the highest degree of robustness and accuracy to set them up.

However, for specific reason on the problem we can set the solver scheme based on the purposes and characteristic solver.

In this simulation case, the MUMPS scheme solver was used for microwave heating simulation. This method was stable to solve the coupled equations of electromagnetic wave, heat transfer and mas and momentum of fluid flow.

A.5.2 ANSYS Fluent Schemes

In order to stabilize the numerical solution of equation, the appropriate scheme is important. In ANSYS Fluent, The discretization value of scalar ϕ transport equation will be store at cell centers for solving the non-linear system. For solving this problem, the set of algebraic equation will be linear using Implicit Gauss-Seidel method. This method require convection terms to interpolate the value at the cell center. This scheme called an upwind scheme.

Upwind scheme discretizes the partial differential equation using finite difference to simulate the direction of propagation of information in flow field. This scheme derived value at specific location from cell upstream relatively to normal velocity.

Several upwind scheme available for solving the problem:

1. First order upwind scheme.
   - This scheme is stable and provide accuracy for hyperbolic partial differential equations.
   - This scheme is also more stable if CFL condition less than or equal to 1.
   - Often the best scheme to start calculations.
2. Second order upwind scheme.
   - This scheme is more accurate than first-order upwind scheme.
   - The numerical diffusion become reduced to converge the solution. Basically, converge the solution first with first-order upwind and then switch to second order scheme and converge again.
3. Power law scheme.
   - This scheme solve problem numerically using the exact solution.
   - Convergent is faster and sometime better then second upwind scheme.
   - It is usually used for hydrodynamic flow.
4. QUICK scheme.
   - This scheme usually provide for quadrilateral and hexahedral meshes.
   - Working based on the second-upwind and central interpolations of variable.
   - This scheme is more accurate and stable on many types of mesh structure.